NAVAL POSTGRADUATE SCHOOL

MONTEREY, CALIFORNIA

THESIS

DETERMINING ROUTE SURVEY PERIODICITY FOR MINE WARFARE: INVESTIGATION OF BEDFORMS, WAVES, TIDES, AND CURRENTS

by

Nicola S. Wheatley

September 2009

Thesis Advisor:	Peter Chu
Second Reader:	Thomas H. C. Herbers

Approved for public release; distribution is unlimited

REPORT DOCUMENTATION PAGE			Form Approved OMB No. 0704-0188
Public reporting burden for this collection of information is estimated to average 1 hour per response, including the time for reviewing instruction, searching existing data sources, gathering and maintaining the data needed, and completing and reviewing the collection of information. Send comments regarding this burden estimate or any other aspect of this collection of information, including suggestions for reducing this burden, to Washington headquarters Services, Directorate for Information Operations and Reports, 1215 Jefferson Davis Highway, Suite 1204, Arlington, VA 22202-4302, and to the Office of Management and Budget, Paperwork Reduction Project (0704-0188) Washington DC 20503.			
1. AGENCY USE ONLY ***(Leave blank)***	**2. REPORT DATE** September 2009	**3. REPORT TYPE AND DATES COVERED** Master's Thesis	
4. TITLE AND SUBTITLE Determining Route Survey Periodicity for Mine Warfare: Investigation of Bedforms, Waves, Tides, and Currents		**5. FUNDING NUMBERS**	
6. AUTHOR(S) Nicola S. Wheatley			
7. PERFORMING ORGANIZATION NAME(S) AND ADDRESS(ES) Naval Postgraduate School Monterey, CA 93943-5000		**8. PERFORMING ORGANIZATION REPORT NUMBER**	
9. SPONSORING /MONITORING AGENCY NAME(S) AND ADDRESS(ES) Ronald E. Betsch, Naval Oceanographic Office 1002 Balch Blvd, Stennis Space Center, MS 39529		**10. SPONSORING/MONITORING AGENCY REPORT NUMBER**	
11. SUPPLEMENTARY NOTES The views expressed in this thesis are those of the author and do not reflect the official policy or position of the Department of Defense or the U.S. Government.			
12a. DISTRIBUTION / AVAILABILITY STATEMENT Approved for public release; distribution is unlimited		**12b. DISTRIBUTION CODE**	

13. ABSTRACT (maximum 200 words)

To retain maritime security, an up-to-date database of mine countermeasures route surveys is essential. In 2005, the United Kingdom Hydrographic Office (UKHO) developed a GIS weighted suitability model to determine survey periodicity; allowing optimization of survey resources, increasing time and cost efficiency. The U.S. currently has no such model. Bedforms are an integral part of the survey periodicity problem. Sediment grain size, tides, currents, and wind-generated waves are influential in bedform formation. In this thesis, San Francisco Bay was chosen as a case study. To investigate if sediment properties change over time, localized grab samples for a three-year period were analyzed. The analysis showed little variability in sediment characteristics at a given location. A weighted suitability model based on the UKHO model was constructed. Three layers were developed including sediment grain size, interpolated from 174 grab samples, tidal and current data from over 50 current stations and ripple height inferred from wind generated wave height. A weighting for each layer was determined. Regions indicating the presence of bedforms were assigned a low survey periodicity, as bedforms reduced, survey periodicity was increased. High-resolution multi-beam survey data was used as a comparison and validation, this showed extremely good correlation with the model.

14. SUBJECT TERMS Mine Warfare, Route Survey, Bedforms, Waves, Tides, Currents, Survey Periodicity, Sediment Transport, Sediment Dynamics, Bathymetry, GIS, Weighted Suitability Model, San Francisco Bay			**15. NUMBER OF PAGES** 127
			16. PRICE CODE
17. SECURITY CLASSIFICATION OF REPORT Unclassified	**18. SECURITY CLASSIFICATION OF THIS PAGE** Unclassified	**19. SECURITY CLASSIFICATION OF ABSTRACT** Unclassified	**20. LIMITATION OF ABSTRACT** UU

NSN 7540-01-280-5500 Standard Form 298 (Rev. 8-98)
Prescribed by ANSI Std. Z39.18

THIS PAGE INTENTIONALLY LEFT BLANK

Approved for public release; distribution is unlimited

DETERMINING ROUTE SURVEY PERIODICITY FOR MINE WARFARE: INVESTIGATION OF BEDFORMS, WAVES, TIDES, AND CURRENTS

Nicola S. Wheatley
Lieutenant, Royal Navy
BSc (Hons), University of Plymouth, 2000

Submitted in partial fulfillment of the
requirements for the degree of

MASTER OF SCIENCE IN PHYSICAL OCEANOGRAPHY

from the

NAVAL POSTGRADUATE SCHOOL
September 2009

Author: Nicola S. Wheatley

Approved by: Peter Chu
Thesis Advisor

Thomas H. C. Herbers
Second Reader

Jeffrey D. Paduan
Chairman, Department of Oceanography

THIS PAGE INTENTIONALLY LEFT BLANK

ABSTRACT

To retain maritime security, an up-to-date database of mine countermeasures route surveys is essential. In 2005, the United Kingdom Hydrographic Office (UKHO) developed a GIS weighted suitability model to determine survey periodicity; allowing optimization of survey resources, increasing time and cost efficiency. The U.S. currently has no such model. Bedforms are an integral part of the survey periodicity problem. Sediment grain size, tides, currents, and wind-generated waves are influential in bedform formation. In this thesis, San Francisco Bay was chosen as a case study. To investigate if sediment properties change over time, localized grab samples for a three-year period were analyzed. The analysis showed little variability in sediment characteristics at a given location. A weighted suitability model based on the UKHO model was constructed. Three layers were developed including sediment grain size, interpolated from 174 grab samples, tidal and current data from over 50 current stations and ripple height inferred from wind generated wave height. A weighting for each layer was determined. Regions indicating the presence of bedforms were assigned a low survey periodicity, as bedforms reduced, survey periodicity was increased. High-resolution multi-beam survey data was used as a comparison and validation, this showed extremely good correlation with the model.

THIS PAGE INTENTIONALLY LEFT BLANK

TABLE OF CONTENTS

THIS PAGE INTENTIONALLY LEFT BLANK

LIST OF FIGURES

LIST OF TABLES

THIS PAGE INTENTIONALLY LEFT BLANK

LIST OF ACRONYMS AND ABBREVIATIONS

BGS	British Geological Survey
CEFAS	Centre for Environment, Fisheries and Aquaculture Sciences
DW	Deep Water
GEODB	Geological Database
GIS	Geographical Information Systems
HFEVA	High Frequency Environmental Acoustics
MCM	Mining and Mine Countermeasures
MODIS	Moderate-Resolution Imaging Spectroradiometer
MS	Microsoft
NASA	National Aeronautics and Space Administration
NOAA	National Oceanographic and Atmospheric Association
NAVOCEANO	Naval Oceanographic Office
NPS	Naval Postgraduate School
RSDB	Route Survey Database
SEAs	Strategic Environmental Assessments
UK	United Kingdom
UKHO	United Kingdom Hydrographic Office
U.S.	United States
USGS	United States Geological Survey
VSW	Very Shallow Water

THIS PAGE INTENTIONALLY LEFT BLANK

LIST OF SYMBOLS

ω	Angular frequency
τ_b	Bed shear stress
α	Coefficient to modify friction velocity
U_{*c}	Critical friction velocity
θ_c	Critical Shields parameter
C_D	Drag coefficient
d	Diameter of a sediment particle
ρ	Fluid density
F_D	Flow drag force
U_*	Friction velocity
X	Grain size in mm
φ	Grain size measurement
X_φ	Grain size mean
m_φ	Grain size mean multiplied by percentage of sub-sample
σ_φ	Grain size standard deviation
$\alpha_{3\varphi}$	Grain size skewness
g	Gravity
C_L	Lift coefficient
D	Mean grain diameter (mm)
d_0	Near bed orbital diameter
U_{orb}	Near bed orbital velocity
H_r	Ripple height
L_r	Ripple length

λ_{ano}	Ripple wavelength (anorbital)
λ_{orb}	Ripple wavelength (orbital)
λ_{sub}	Ripple wavelength (suborbital)
R_o	Rouse Number
ρ_s	Sediment density
w_s	Settling velocity
U_s	Shear velocity
θ	Shields parameter
V	Velocity
ν	Viscosity of a fluid
κ	Von Karman constant
h	Water depth
H	Wave height
k	Wave number
T	Wave period
c	Wave speed

ACKNOWLEDGMENTS

I would like to thank my advisor, Prof. Peter Chu, and second reader Prof. Thomas Herbers for their support, advice and patience throughout this project. For help during my practical work, thanks must go to Professor Curt Collins and the staff of the R/V Point Sur.

Many thanks to Dr. Julie Armishaw, from UKHO, for allowing me to investigate her model and answering the many questions I asked at the beginning of this project. Thanks also to Dr. Partrick Barnard, from USGS, for allowing me to use his data, ask questions, and provide comments and feedback throughout the modeling process.

Lastly and most importantly, I would like to thank my family and friends back in the UK and in Monterey for their continued support and encouragement throughout my time at NPS.

THIS PAGE INTENTIONALLY LEFT BLANK

I. INTRODUCTION

A. AIMS AND OBJECTIVES

In recent years, the Navy has undergone a shift in operational focus from the traditional 'blue water operations' in deep open ocean, to 'brown water operations in the littoral zone. The littoral, traditionally an unfamiliar area for Naval operations, brings with it different challenges. A significant threat when operating in the littoral are mines. Mine warfare is not a new concept; mines have been used since the American Revolution. They are inexpensive, simple to manufacture, and relatively easy to obtain and maintain. Mines have resulted in damage and have sunk more ships in the past century than all other weapons combined. More than 50 countries possess a mine-laying capability (National Research Council, 2001).

Mines are used to deny sea control, in order to maintain warfighting capability, and naval forces need the ability to open and maintain sea lines of communication in order to dominate the littoral battle space (Royal Navy, 2004). In order to retain maritime security, it is essential to maintain an up-to-date database of mine countermeasures route surveys, particularly for ports, harbors, and sea-lanes of strategic importance.

The littoral region is subject to many temporal and spatial variations, and it is therefore difficult to assess how often a region should be surveyed in order to maintain up-to-date data. The United Kingdom Hydrographic Office (UKHO) has developed a model to maintain the UK mine warfare route survey database, taking into account environmental and geospatial parameters. This enables survey periodicity to be calculated in order to optimize survey resources, thus making this task more time and cost effective. The U.S. Navy currently has no such model.

B. MINE WARFARE

1. The Threat

The first floating mine was designed by David Bushnell in 1776—'the Bushnell Keg'—it was used during the American Revolution. It was a primitive design that was comprised of a watertight keg filled with gunpowder and a flintlock detonator, which was suspended from a float. These mines were placed in the Delaware River so that they would float into British ships that were stationed down river (Royal Navy, 2009) (U.S. Navy and Marine Corp, 2005).

During the Second World War, many different types of mine were developed, and new ways to lay the mines were also developed. Aircraft dropped mines proved very successful; on average the Allies lost one mine-laying plane for every twenty enemy ships sunk (Royal Navy, 2009).

In the Korean War, a major U.S. amphibious operation was delayed by eight days due to a relatively primitive mine threat. The Admiral in charge of the operation, Real Admiral Allan Smith, was quoted as saying (Royal Navy, 2009):

> A backward nation with a fleet of sampans designed at the time of Christ has used mines designed during the United States Civil War to halt the mightiest naval power in the history of the world.

This remains true today. The most recent use of mines in combat was during the 1991 Gulf War. The Iraqi forces laid minefields, comprised of an estimated 1300 mines (Royal Navy, 2009) (U.S. Navy and Marine Corp, 2005). This resulted in two U.S. ships, the USS Princeton and the USS Tripoli, being badly damaged.

The mine has played an important role in all major naval campaigns. Although mines have become far more sophisticated, they remain relatively cheap to manufacture and deploy. The cost of producing and laying a mine is approximately 0.5% to 10% of the cost of removing it, and it can take up to two hundred times longer to clear a mine field than to lay one (Wikipedia, 2009).

Mine damage to a ship can include hull rupture, caused by the pressure wave created by detonation. Internal damage to equipment is caused by vibration and flooding and also structural damage to the ship. The magnitude and type of damage depends upon the size of the explosive force and the shock resistance of the target (U.S. Navy and Marine Corps, 2005).

2. Mine Classification

Mine warfare is defined as the strategic and tactical use of sea mines and their countermeasures (U.S. Navy and Marine Corps, 2005). Mines can be classified into the following three categories.

a. Bottom Mines

Bottom mines, also known as Ground mines, are designed to sink and rest on the seabed; they are most effective in comparatively shallow waters. In deep waters, surface vessels may pass over the mine without triggering it. A bottom mine planted in deep water is still effective against submarines. Acoustic, magnetic, or pressure sensors can activate bottom mines.

b. Moored Mines

Moored Mines are placed at a pre-determined depth under water, designed for deep-water, and are effective against submarines and surface ships. The explosive charge and firing mechanism in a moored mine floats, and a cable attached to an anchor on the bottom holds the case at the pre-determined depth below the surface.

c. Drifting Mines

Drifting mines, which were banned under the Hague Convention of 1907, move freely through the water at, or near, the surface; they have no anchoring devices. A moored mine that has lost its tether cable becomes a drifting mine.

3. Mine Warfare Operations

Mine Warfare operations can be divided into two categories, Mining and Mine Countermeasures (MCM).

a. Mining

Mining operations are used to establish or maintain control of sea areas that are deemed to have tactical or significant importance. Mining has the advantage of being able to inflict major damage on enemy shipping. A mine field is covert and passive. This makes it an effective weapon in the denial of a sea area to enemy forces. However, due to the passive nature of the mine, it cannot distinguish between friendly or enemy forces. Two important concepts are: Offensive Denial, which is the prevention of mining, and Defensive Protection, which is reducing the risk of mines that have already been laid (Royal Navy, 2004).

b. Mine Counter-Measures (MCM)

MCM operations can be sub-divided into two categories. Offensive MCM is the prevention of mines being laid in the first place. Strategic bombing of enemy mine factories, depots, airfields, harbors, etc., can achieve this. Sinking or shooting down of mine laying platforms, or excluding enemy mine layers from areas of operations, can also achieve this. If enemy mines have already been laid, then Defensive MCM operations must occur. These include active MCM such as Mine-sweeping, Mine-hunting, and Clearance Diving.

4. Environmental Factors for Mine Warfare

For successful MCM operations, a number of factors must be taken into account. The type, size, and aspect of the mine is important, as are the environmental factors that will influence the behavior of the mine, and the environmental factors that are present in the locality of the mine will influence operations.

Mining is most likely to occur in the littoral region, where choke points and shipping lanes are prime targets. In mine warfare the littoral region is divided into four zones, these are shown in Figure 1.

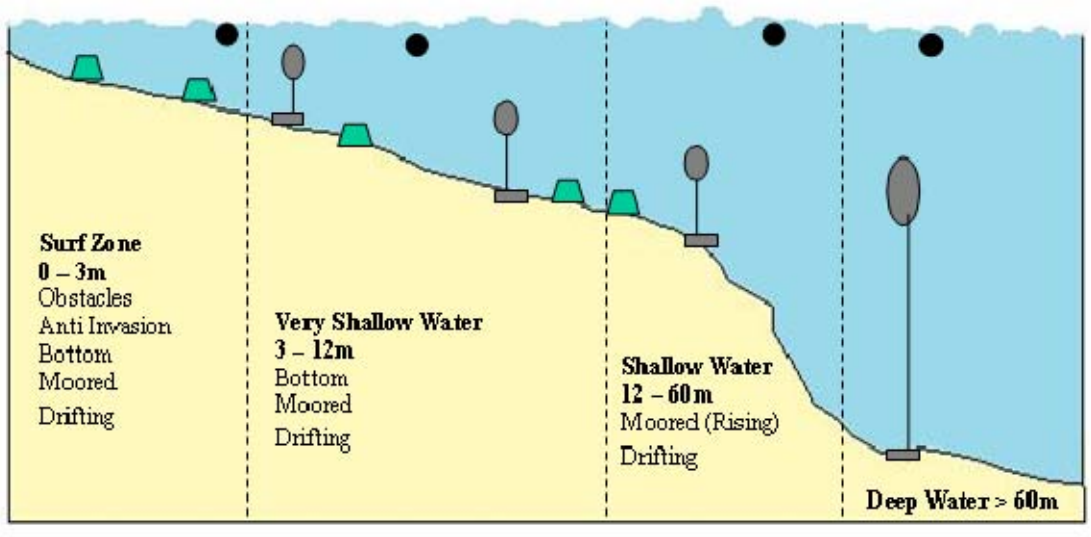

Figure 1. The Mine Warfare Environment (After National Research Council, 2000)

The Surf Zone: 0-3 m is where you find obstacles, anti invasion mines, bottom, moored, and drifting mines. Very Shallow Water (VSW): 3–12 m is a prime area for bottom, moored, and drifting mines. Shallow Water (SW): 12–60 m, likely mines include moored, drifting, and also rising mines, which are initially deployed on the sea bed, and will be activated by either a time delay, pressure, acoustic, or magnetic fluctuation that will cause the mine to rise. Bottom mines can also be found in this region, but are deemed less effective than if laid in VSW. Deep Water (DW): >60 m, moored, rising or drifting mines are likely, bottom mines are unlikely to be laid at this depth.

The different environmental parameters in each zone have varying levels of importance in MCM operations. They can be categorized by levels of importance (National Research Council, 2000), these are summarized in Table 1.

The oceanographic factors that are considered to be of high importance in a certain zone are assigned red, those of intermediate or moderate importance are yellow, and those considered less important are green.

	Surf Zone	VSW	SW	DW
Bathymetry				
Sediment Size				
Seafloor Clutter				
Bottom Roughness				
Mine Burial				
Currents/Waves				
Water Clarity				
Temperature and Salinity				
Acoustic Properties	N/A			

Table 1. Impact Matrix of Oceanographic Factors, red—high importance, yellow—moderate importance, green—low importance.

The factors deemed more important in relation to survey periodicity are discussed below.

a. Bathymetry

Bathymetry is an important factor when surveying the periodicity problem. Spatial and temporal variations in water depth and seafloor profile can influence the location and height of breaking waves, the position and strength of surface currents, and the propagation of the tide into very shallow waters.

In the surf zone, temporal changes in bathymetry can influence local dynamics in time periods as short as one day. In deeper waters, the fractional changes are smaller and slower, but can still easily be sufficient to cause mine burial. Prior knowledge of these conditions is an important aid to operational planning (National Research Council, 2000). Bathymetry is important

in mine hunting operations, due to scour or burial and bottom clutter characteristics. Bathymetry measurements are more complex in shallow water, the fluid dynamics mechanisms involved are increasingly sensitive to small-scale features (National Research Council, 2000). Temporal changes are important, and modern survey techniques, such as multi-beam surveys, are increasingly being used to study this area.

Burial potential varies strongly in the fluid environment, with activity generally increasing with decreasing depth (National Research Council, 2000). In the deep and shallow water zone, burial can occur either when the mine is laid, or soon afterwards. Bathymetry in very shallow waters changes rapidly due to a wide spectrum of bedforms; these are also found in shallow water. In this dynamic, morphology environment mines can quickly be susceptible to scour and be buried. Little is known about the climatology, variability, and importance of small-scale bedforms in shallow waters (National Research Council, 2000). It is thought that bedforms are likely to be an important mechanism for mine burial. Bedforms also affect the flow of the fluid through bottom dissipation. In bedform regions, mine detection is more difficult due to clutter. Knowledge of the presence and persistence of low-clutter regimes (no bedforms) would be useful (National Research Council, 2000).

b. Tides and Currents

Tidally driven changes of sea surface elevation vary globally from negligible to several meters in very shallow waters. In the shallow and deep-water zones, these elevation changes have little effect on mine hunting operations or effectiveness. Tidal effects primarily influence mine warfare operations in very shallow water and the surf zone, although in the surf zone, tidal currents are usually negligible compared to wave-driven flows (National Research Council, 2000).

Tidal currents can cause an increase in the scour of bottom mines, and can also cause significant transport of drifting mines. Outside the surf zone, tidal currents are often greater than 0.5 m/s, which has a detrimental effect on diver and marine mammal operations.

There is generally a decrease in magnitude of currents with depth. Deep and shallow water flows are geostrophic and low-frequency (and are likely to be predictable), while very shallow water and surf zone currents are more likely to be directly forced through wind, wave-driving forces, or buoyancy fluxes due to runoff or river outflow (National Research Council, 2000).

c. Seabed Sediment Type and Sedimentation

In the littoral zone, it is vital to have a good indication of sediment type and seafloor characteristics, if mine warfare operations are to be successful. The physical, chemical, and magnetic properties of the seabed can be important in all aspects of the mine warfare problem (National Research Council, 2000):

- Mine burial probability is a function of sediment properties; it is a key factor for mine sweeping or hunting tactical decisions.
- Seafloor conductivity and water depth are key factors for determining magnetic sweep paths.
- Bottom reflectivity is a factor in airborne LIDAR performance.
- Bottom sediment characteristics are a key factor in sediment transport, which affects water clarity and mine burial.

With increased understanding of sediment types and properties, many aspects of mine warfare operations can be improved and ultimately will become more efficient. Mine burial is an extremely important factor in mine warfare operations. There are four mechanisms by which mines will bury (U.S. Navy and Marine Corps, 2005):

- Scour (current-induced and wave-induced)
- Migrating sand ridges
- Burial by deposition
- Impact burial

In order to be more effective, we need to have an increased understanding of the forces that will cause mine burial (for example waves, currents, and sediment transport). In particular, we need to understand how these forces will interact with different mine types and the magnitude of these forces.

Mines have various shapes and sizes. For example, a common mine, called Manta, is a shallow seabed influence mine, which operates in depths from 2.5 m to 100 m. It is designed to rest on the seabed even in a region of strong flows. Typical dimensions of a Manta are: length 980 mm, width 980 mm, and height 470 mm. The dimensions are comparable to mines that operate in similar depths; the Rockan has a length of 1015 mm, width 800 mm and a height of just 385 mm. The Mk67 SLMM is 4090 mm in length, 485 mm in width and 485 mm height. If sediment transport causes a change of approximately 0.3 to 0.5 m in height of the seabed, it is significant in the possible burial of mines—this is before factors such as scour are taken into account.

Significant work has been done in sediment transport research, and a strong understanding of the physics involved has been developed, but these efforts have been generic, rather than mine warfare specific. For example; since 2001, strategic environmental assessments (SEAs) have been carried out in the UK. They are managed by the Department of Trade and Industry, primarily aimed at providing information for decisions that could affect the way large-scale commercial energy resources are developed. However, due to the nature of the research and the results obtained, this is an ideal source of data for the mine warfare problem.

C. THE UKHO MODEL

The UKHO developed a weighted suitability Geographical Information Systems (GIS) model in order to review the UK Mine Countermeasures Route Survey maintenance schedule. The objective of the model is to optimize resources, by determining which routes are susceptible to change, and should be surveyed at a higher frequency, than those that are unlikely to change frequently over time. This enables a more scientific approach to survey periodicity than that of frequently re-surveying routes of higher strategic importance and surveying lower priority routes on a less frequent basis.

1. The UKHO Model Concepts

There are three underlying concepts included in the UKHO model, which are detailed in the following sections.

a. The Mine Counter Measures Environment

The Mine Counter Measures Environment focuses on factors that are considered significant in mine burial, including burial mechanisms, burial probability, and burial rate. These factors were used to estimate how a mine could be buried, how likely this is, and the time period that these processes are likely to take.

b. The Maritime Environment

The Maritime environment is an extremely important factor in determining the survey periodicity for route surveys. The UKHO model included seabed sediment types, sediment deposition, bottom texture, gas presence, and vessel traffic. A summary of the data included is shown in Table 2. The data was obtained from many different sources, bottom texture and bottom contacts data was taken from the UKHO Route Survey Database (RSDB) and processed in Microsoft Excel, allowing it to be imported easily into ArcGIS. The British Geological Survey (BGS) supplied the seabed sediment type data in a digital

map. In order to determine total suspended matter, satellite data from the NASA MODIS satellites were used. The density of fishing vessels was obtained from the Centre for Environment, Fisheries and Aquaculture Sciences (CEFAS). Gas presence was taken from the UKHO Geological Database (GEODB) and vessel traffic was supplied by NAVOCEANO.

Data	Source	Brief Description of data and processing
Bottom Texture	UKHO RSDB	Bottom Texture information extracted from RSDB. Processed in MS Excel for input into ArcGIS.
Seabed Sediment Type	BGS	Digital 1:250 000 map of offshore seabed sediments obtained from BGS.
Total Suspended Matter	NASA MODIS sensor	Annual means for years 2001, 2002 and 2003 at 4km resolution were combined to get a short "climatology". Processed via idrisi software for input into ArcGIS.
Fishing Activity	CEFAS	Maps of relative densities of fishing vessels potentially impacting on the seabed were obtained from a CEFAS report and digitised.
Gas Presence	UKHO GEODB	Gridded gas type data extracted from Geolith and input into ArcGIS.
Bottom Contacts	UKHO RSDB	SBO and LBO details extracted from the RSDB. Processed in MS Excel for input into ArcGIS.
Vessel Traffic	NAVOCEANO	Annual shipping density for tankers and merchant vessels extracted from the database at a resolution of 10 minutes.

Table 2. Data included in the UKHO model (From Armishaw, 2005)

c. GIS Modeling

In order to determine the survey periodicity, a weighted suitability model was developed. This concept was used to simplify an extremely complex problem, input layers were weighted and combined as demonstrated by Figure 2.

Figure 2. GIS Weighted Suitability Model (From Armishaw, 2005)

In the UKHO model, each layer was re-classified to a scale of 0 to 9, with 0 representing a high degree of expected change and 9 representing little change. Each layer was then assigned a weighting value that represented the

assessed importance of that layer. Each layer value was then multiplied with the weighting value and added together for a particular location so that an assessment could be made to the re-survey interval routes. The weighting values used are shown in Figure 3. The route survey maintenance schedule was determined using the three layers: Burial Probability, given a weighting of 0.40, Burial Mechanisms, given a weighting of 0.40, and Change in Number of Bottom Contacts, given a weighting of 0.20. Each can be considered a sub-model.

The Burial Probability sub-model is comprised of bottom texture, weighting 0.30, seabed sediment type, weighting 0.30, total suspended sediment, weighting 0.10, fishing activity, weighting 0.20 and gas presence, weighting 0.10. The weightings in the sub-model represent the predicted importance of each factor within that sub-model.

The Burial Mechanism sub-model is comprised of bottom texture, weighting 0.45, seabed sediment type, weighting 0.45, and gas presence, weighting 0.10. All three of these parameters were also included in the Burial Probability sub-model, so it can be deduced that they are important in both processes. The importance of bottom texture and seabed sediment type are particularly relevant.

The Change in number of Bottom Contacts sub-model has two input factors. The existing contact density has a weighting of 0.35. Additional contacts from vessels, has a weighting of 0.65, this factor was devised by a further sub-model including merchant vessels and fishing vessels, both of which had a weighting of 0.50. The overall weighting of this sub-model is substantially lower than the other two, indicating it has a lower importance on the overall route survey maintenance schedule.

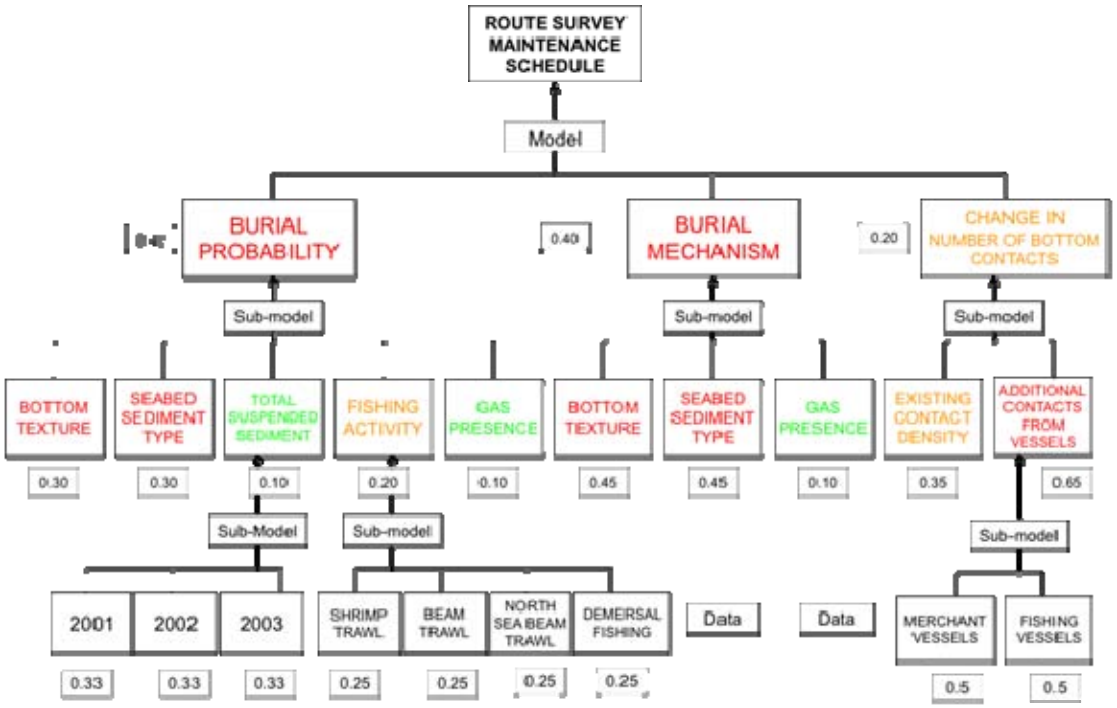

Figure 3. Relationship between model parameters, showing the weightings assigned to each layer (From Armishaw, 2005)

2. Model Interpretation

The model results were reclassified into four categories in order to assign survey periodicity, and the results were then further sub-divided in two priority groupings. The first, Priority 1, being areas of higher importance and the second, Priority 2, being areas of lower importance. The categories are shown in Table 3, each category corresponds to a seabed changeability, with two recommended survey intervals, depending on the priority of the region in question.

Category	Seabed Changeability	Priority 1 Survey Interval	Priority 2 Survey Interval
1	HIGH	3-5 yrs	10-12 yrs
2	MODERATE-HIGH	5-7 yrs	12-15 yrs
3	LOW-MODERATE	7-10 yrs	15-20 yrs
4	LOW	10-15 yrs	20 yrs

Table 3. Recommended re-survey intervals (From Armishaw, 2005)

The model output layer was then re-plotted into the assigned seabed changeability categories shown in Table 3, and from this a MCM Route survey-planning matrix was constructed for UK route surveys.

3. Model Limitations

Recommendations for areas of further study from the UKHO 2005 report included:

- Investigate the potential for the UKHO model to be used in other geographic locations.
- Determine if any additional environmental factors should be included in the model to refine the results.

The current iteration of the UKHO model is limited by the environmental parameters that have not yet been included. Important factors such as waves, tides and currents were not included.

The data included in the UKHO model, provides a good assessment for survey periodicity in the UK region. It cannot be used in other geographical locations due to the geographical boundaries of the input data. However, it could be used as a basis for route re-survey models in other regions. The quantity and quality of the data used to develop the UKHO model is extensive. Similar data for other geographical locations, has proved difficult to source, and due to time constraints of this study, a replica of the model for a different geographical location has not been achieved.

D. OVERVIEW OF THIS STUDY

The primary goal of this research is to determine the variability of temporal and spatial factors that will affect the survey periodicity of route surveys for Mine Warfare. Many of these factors have been addressed and included in the UKHO model. However, a significant omission is that of waves, tides, and currents. Waves, tides, and currents have a huge impact on sediment transport and

bedform formation, which in turn will have a large impact on mine burial. Therefore, these parameters are important in determining survey periodicity for route surveys.

In this study, sediment transport and bedform evolution are reviewed. San Francisco Bay is used as a case study. Experimental results from localized sediment grabs are used to determine changes in sediment type with time, and compared to the NAVOCEANO HFEVA sediment database. This allows the validity of the database to be assessed. The effect of waves, tides, and currents in the region are assessed. Theses results are then compared to multi-beam data gathered by the United States Geological Survey (USGS), collected to determine bedform evolution. The results from these two investigations are analyzed and an assessment for mine warfare survey periodicity for this region is determined.

From the San Francisco Bay results, the potential for additional layers including waves, tides, and currents for the inclusion in the UKHO model are reviewed and their values assessed.

THIS PAGE INTENTIONALLY LEFT BLANK

II. SEDIMENT DYNAMICS AND BEDFORM EVOLUTION

A. SEDIMENT TRANSPORT

Sediment transport is the movement of sediment; it is typically due to the gravity acting upon the sediment and the motion of the fluid in which the sediment is located. It is complex, however, it is an extremely important factor in determining the survey periodicity for route surveys. The sediment type will influence the probability of a mine burial. The sediment transport rate has a significant effect on the time period in which a mine will be buried or remain uncovered, and thus detected during a survey.

Sediment transport is dependent on a number of variables, which include: sediment size, shape and density of grains, settling velocity, sediment availability, flow depth, water density and viscosity, bed shear stress, bedform wavelength, height and steepness, maximum and residual tidal velocity and wave period and amplitude (Dyre, 1986).

Figure 4 shows a schematic of the dynamic interactions of sediment behavior. It shows a triad of three important factors: the sediment transport mechanisms—for example if the sediment will be transported in suspension or as bedload—the type of seabed, and the flow that influences the sediment in the form of waves and currents.

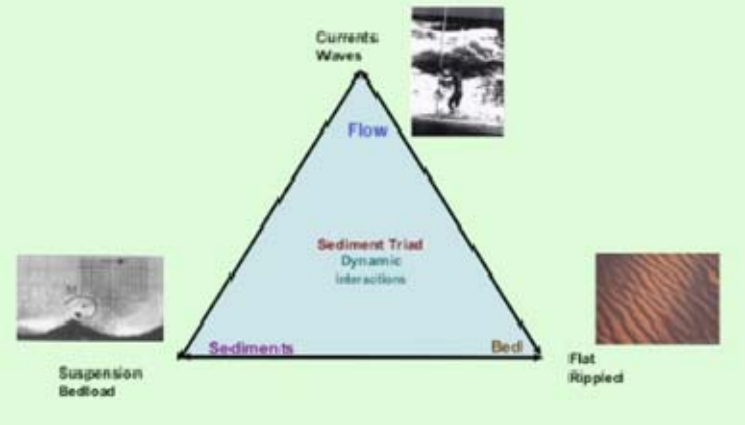

Figure 4. Sediment process triad (From Proudman, 2009)

In the last century, the mechanisms that influence sediment transport have been extensively studied. Sediment transport can be broken down into two categories: suspended sediment transport, and bedload transport. Suspended sediment transport includes finer particles that will travel with a fluid, they will tend to travel faster and further, and they can be estimated using satellite imagery.

Bedload transport involves particles that have settled and are found within a few grain diameters of the bed, they tend to travel slower than the surrounding fluid. Estimates of bedload transport are more difficult, however, due to recent improvements in multi-beam technology and data availability a number of studies to increase the understanding of bedload transport and bedform evolution are currently on going.

1. Sediment Type

Sediments tend to enter the coastal system through discharge from rivers; the volume of sediment discharged depends upon geology, topography, and the climate. It has been estimated that the annual worldwide discharge of sediment from rivers is 7×10^9 tons (Milliman and Meade, 1983). The sediment will sort itself in order of size, with larger sediment grains settling out first, while finer grains remain in suspension and generally travel further from the source.

a. The Wentworth Scale

Sediment grain size can be classified using the Udden-Wentworth scale, which utilizes a logarithmic scale. Sediment type is determined using:

$$\varphi = -log_2(X) \qquad (1)$$

where X is the grain size in mm. This is a very useful method in the analysis of sediment type. Mine burial is more likely to occur in areas classified as fine sand (φ = 2 to 3).

The Wentworth scale is summarized in Table 4—it relates the grain size in mm to phi units, and then assigns each sediment range a named classification. The grain size ranges from >256 mm to <0.0002 mm, when converted into phi the largest sediments are < -8 and the smallest sediments correspond to a phi value of >12. The sediment size ranges corresponding to each phi increment can be seen in Table 4.

Aggregate Name		Phi $\varphi = -log_2(mm)$	Grain Size (mm)
Boulder		< -8	> 256
Cobble		-6 to -8	64 to 256
Gravel	Very Coarse	-5 to -6	32 to 64
Gravel	Coarse	-4 to -5	16 to 32
Gravel	Medium	-3 to -4	8 to 16
Gravel	Fine	-2 to -3	4 to 8
Gravel	Very Fine	-1 to -2	2 to 4
Sand	Very Coarse	0 to -1	1 to 2
Sand	Coarse	0 to 1	1/2 to 1
Sand	Medium	1 to 2	1/4 to 1/2
Sand	Fine	2 to 3	1/8 to 1/4
Sand	Very Fine	3 to 4	1/16 to 1/8
Silt	Coarse	4 to 5	1/32 to 1/16
Silt	Medium	5 to 6	1/64 to 1/32
Silt	Fine	6 to 7	1/128 to 1/64
Silt	Very Fine	7 to 8	1/256 to 1/128
Clay	Coarse	8 to 9	1/512 to 1/256
Clay	Medium	9 to 10	1/1024 to 1/512
Clay	Fine	10 to 11	1/2048 to 1/1024
Clay	Very Fine	11 to 12	1/4096 to 1/2048
Colloid		> 12	<1/4096

Table 4. The Wentworth Scale. (From Dyre, 1986)

When a sediment sample is collected, it can then be analyzed using laboratory methods. It is assumed (Dyre, 1986) that within a given sample, a Normal Distribution of sediments will occur, and the sediment can be classified

by calculating the percentage of each sample within each range, then calculating the mean grain size for that sample and converting this to phi units. Statistical analysis can then be carried out utilizing the following calculations:

Percentage of Sample: % of each sub-sample (2)

Mean Grain Size: $$X_{\varphi} = \sum \left(Percentage \times GrainSize \right) \quad (3)$$

$$X_{\varphi} = \sum f\left(m_{\varphi}\right) \quad (4)$$

Standard Deviation: $$\sigma_{\varphi} = \sqrt{\sum f\left(m_{\varphi} - X_{\varphi}\right)^{2}} \quad (5)$$

Skewness: $$\alpha_{3\varphi} = \sum \frac{f\left(m_{\varphi} - X_{\varphi}\right)^{3}}{\sigma_{\varphi}^{\ 3}} \quad (6)$$

66% Confidence Interval: $$\pm 0.9542\left(\frac{\sigma_{\varphi}}{\sqrt{\text{No. of Samples}}}\right) \quad (7)$$

95% Confidence Interval: $$\pm 1.9600\left(\frac{\sigma_{\varphi}}{\sqrt{\text{No. of Samples}}}\right) \quad (8)$$

The percentage of each sub-sample within a sample must first be calculated. From this, the mean grain size can be calculated as shown in Equation 3. Equation 4 also shows the calculation for the mean grain size, with m_{φ} being equivalent to the percentage of each sub-sample multiplied by that samples grain size in mm. From this, the standard deviation and skewness can be calculated.

b. NAVOCEANO Database Data

NAVOCEANO uses a similar classification scheme to the Wentworth scale, although a larger number of categories are employed, this is shown in Table 5. Surface sediment type data provided by NAVOCEANO can be obtained at high and low spatial resolutions.

The databases include analysis of grabs and cores collected during surveys from multiple sources. Low resolution data is based on data for every five minutes of latitude and longitude. High resolution data is based on every six seconds of latitude and longitude. In certain areas, including San Francisco Bay, more detailed surveys have been compiled and the resolution is increased. In this investigation sediment samples are compared to the High Frequency Environmental Acoustics (HFEVA) dataset (NAVOCEANO, 2003).

HFEVA Standard Sediment Type	Phi $\phi = -\log_2(mm)$	Type ID
Rough Rock	-9	1
Rock	-7	2
Cobble	-3	3
Gravel		
Pebble		
Sandy Gravel	-1	4
Very Coarse Sand	-0.5	5
Muddy Sandy Gravel	0	6
Coarse Sand	0.5	7
Gravelly Sand		
Gravelly Muddy Sand	1	8
Sand	1.5	9
Medium Sand		
Muddy Gravel	2	10
Fine Sand	2.5	11
Silty Sand		
Muddy Sand	3	12
Very Fine Sand	3.5	13
Clayey Sand	4	14
Coarse Silt	4.5	15
Sandy Silt	5	16
Gravelly Mud		
Medium Silt	5.5	17
Sand-Silt-Clay		
Silt	6	18
Sandy Mud		
Fine Silt	6.5	19
Clayey Silt		
Sandy Clay	7	20
Very Fine Silt	7.5	21
Silty Clay	8	22
Clay	9	23

Table 5. NAVOCEANO HFEVA database sediment classification. (From NAVOCEANO, 2003)

2. Grain Size Distribution and Fluid Flow

Grain size distribution and fluid flow are important in calculating sediment transport. Sediment within a flow can be transported in three ways: along the bed as bedload, in suspension as suspended load, or along the air-water interface as wash-load. The location of the sediment is determined by the Rouse Number:

$$R_o = \frac{w_s}{\kappa u_s} \tag{9}$$

where w_s is the setting velocity; κ = 0.407, is the von Karman constant; and u_s is the shear velocity. The settling velocity of the sediment, w_s, is determined by the sediment density, ρ_s, and diameter, d of the sediment particle.

The required Rouse numbers for transport as bed load, suspended load, and wash load are summarized in Table 6.

Mode of Transport	Rouse Number
Bed load	>2.5
Suspended load: 50% Suspended	>1.2, <2.5
Suspended load: 100% Suspended	>0.8, <1.2
Wash load	<0.8

Table 6. Mode of transport related to Rouse numbers (From Wikipedia, 2009)

The shape of the grains also influences the settling velocity, and therefore the distribution of grains, as shown in Figure 5. As the size of the grains increase, the settling velocity also increases, indicating that larger grains can settle in regions with increased fluid flow, where as finer grains will settle in regions with a lower fluid flow.

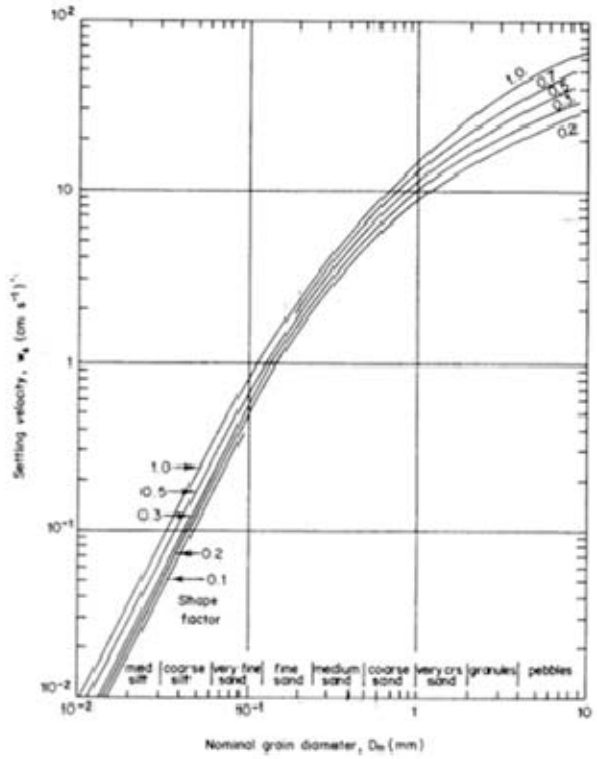

Figure 5. Settling velocities of grains in water at 20°C as a function of grain diameter and shape factor (From Komar and Reimers, 1978)

In this study, bedload transport is determined to be the most important factor. The magnitude of bedload transport is extremely difficult to quantify. There are a number of theories and studies that have been carried out, however, there is no generic solution to this problem. Therefore, in order to determine survey periodicity for mine warfare route surveys, a qualitative approach is necessary at this stage.

3. Threshold of Sediment Movement

The seabed is composed of individual sediment grains. The forces acting upon each grain are summarized in Figure 6.

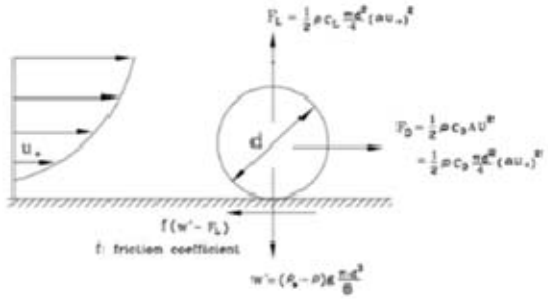

Figure 6. Forces acting on a grain resting on the seabed (From Liu, 2001)

The flow drag force on the grain is the driving factor, this is defined as:

$$F_D = \frac{1}{2}\rho C_D \frac{\pi d^2}{4}(\alpha u_*)^2 \tag{10}$$

where the friction velocity u_* is the flow velocity close to the seabed, α is a coefficient used to modify the friction velocity, in turn αu_* is the characteristic flow velocity past the grain. The grain will start to move at critical friction velocity , this can be denoted as u_{*c}. This is the point at which the grain is about to move, and occurs when the drag force is equal to the friction force that is parameterized as the net vertical force (gravity—lift) multiplied by an empirical friction factor, *f*.

$$\frac{1}{2}\rho C_D \frac{\pi d^2}{4}(\alpha u_{*,c})^2 = f\left((\rho_s - \rho)g\frac{\pi d^3}{6} - \frac{1}{2}\rho C_L \frac{\pi d^2}{4}(\alpha u_{*,c})^2\right) \tag{11}$$

This equation is then rearranged:

$$\frac{u_{*,C}^2}{(s-1)gd} = \frac{f}{\alpha^2 C_D + f\alpha^2 C_L}\frac{4}{3\alpha^2} \tag{12}$$

The left-hand side of the rearranged equation gives us the critical Shields parameter, θ_c, in turn the Shields parameter, θ can be defined as:

$$\theta = \frac{u_*^2}{(s-1)gd} \tag{13}$$

Movement will occur if the Shields parameter is greater than the critical Shields parameter. Figure 7 shows the thresholds of Shields parameter as delineating suspended and bedload sediment as a function of grain size according to Bagnold (1956) with a coefficient of 0.4 and McCave (1971) with a coefficient of 0.19. The actual figures are still disputed.

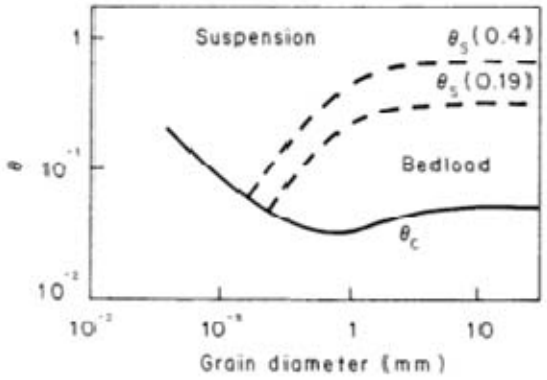

Figure 7. Shields diagram showing the threshold of suspension (From Dyre, 1986)

B. BEDFORM FORMATION

When sediment begins to move bedforms will begin to form. A flat bottom can become deformed, with a series of undulations. As water flow increases, drag will be increased, and this increases in the shear stress available at the bed to create grain movement (Dyre, 1986). In laboratory investigations, the sequence of bedforms with increasing flow intensity is: Flat bed, Ripples, Dunes, High Stage Plane Bed, followed by Antidunes. Terminology varies in different studies. A diagrammatic representation of the flow over bedforms and their movement is shown in Figure 8.

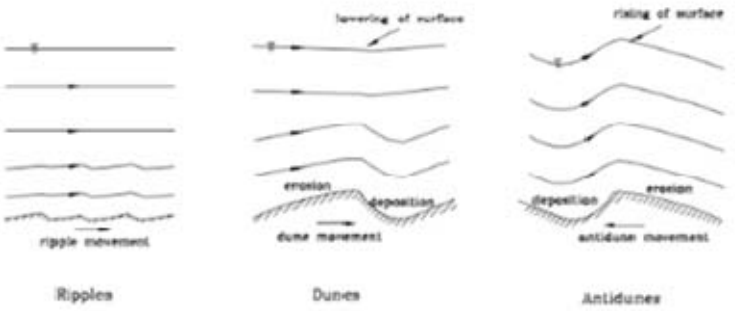

Figure 8. Flow over Ripples, Dunes and Antidunes (From Liu, 2001)

If the average current velocity, water depth and sediment size are known factors, then the expected bedforms can be predicted by empirical diagrams, as shown in Figure 9. The sediment size is represented by the settling velocity. In this example, the ripple speed is also given so that the figure can be used to estimate the bed-load transport, (Liu, 2001).

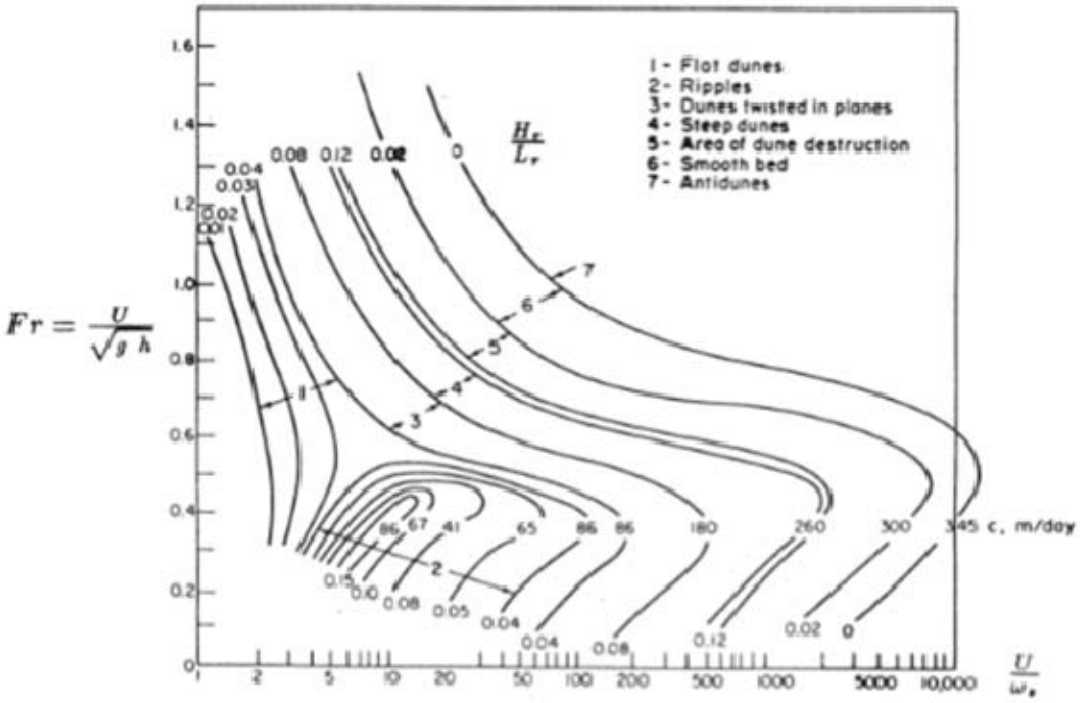

Figure 9. Bedform prediction diagram (From Liu, 2001)

1. Ripples

Ripples are formed at relatively weak flow intensity; the mean grain diameter for ripple formation is less than 0.7 mm (Liu, 2001). From observations, it is estimated that the average height and length of ripples are controlled by grain size, they are typically; $H_r = 100 d_{50}$ and $L_r = 1000 d_{50}$.

2. Dunes

Dunes, also known as Sand Waves, have a very similar shape to ripples, but are larger in size. The size of dunes is typically controlled by flow depth. Dunes are formed by coarser sediments, with mean grain size greater than 0.6 mm (Liu, 2001). As flow intensity increases, the dunes will increase in size, reducing the water depth at the crest of the dunes. The high velocity over the crest can cause the dunes to become washed out forming a flat plane bed.

3. Antidunes

Antidunes are formed when the Froude number exceeds unity. The wave height on the water surface is of the same order as the antidune height, this causes instability in the surface wave, which can grow and break in an upstream direction, causing the antidune to move upstream (Liu, 2001).

C. INFLUENCE OF CURRENTS AND WAVES ON BEDFORMS

Both currents and waves will influence the formation of bedforms, and they will affect the type of bedform, its size, and its shape. The magnitude of sediment transport due to currents and waves has been extensively studied, however, no single solution exists due to the complexity of the problem and the number of variables associated with it. Bedload transport formula have been put forward by Meyer-Peter (1948), Kalinske-Frijlink (1952), Einstein-Brown (1950), Bagnold (1946), and Bijker (1971). These methods are all complex and do not provide a general solution, however all provide solutions within the same order of magnitude. This study will therefore be qualitative rather than quantitative.

1. Currents

The typical pattern of bedform formation in a steady current is illustrated in Figure 10, showing typical bedforms related to increased flow. The starting point is a typical ripple pattern (A), in a steady current this will develop into dunes with ripples superposed (B) as the current continues to flow dunes will form (C), they will then become washed out dunes or in a transition phase (D). Following this, still under the influence of a steady current, a plane bed will form (E). If the flow continues to strengthen, antidunes may be formed.

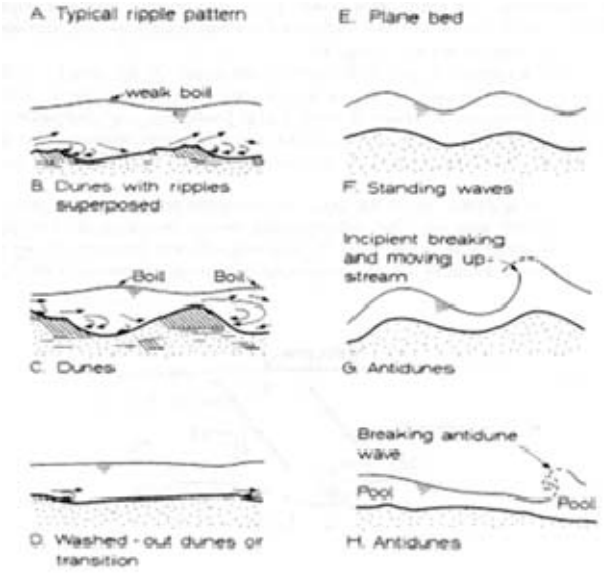

Figure 10. Typical bedforms in order of increased stream power (From Deigaard, 1992)

In a steady current, at the point where sediment transport will begin to occur, the bed becomes unstable. Fine sediments will form ripples usually with a length of less than 0.6 m and a height of less than 60 mm, ripple size is generally independent of water depth in this case, (Deigaard, 1992). As current velocity increases, total bed shear stress increases and the type of bedform will follow the pattern shown in Figure 11. Bed shear stress, τ_b, is shown as the vertical axis,

which is plotted against velocity, *V*, on the horizontal axis. As τ_b and *V* increase the progression of ripples, dunes, plane bed followed by anti-dunes at the higher τ_b and *V* values can be seen.

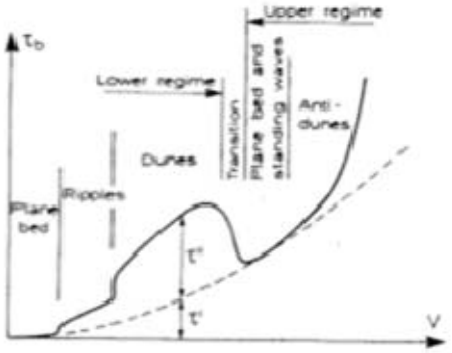

Figure 11. Relationship between total bed shear stress and flow velocity for different bedforms (From Deigaard, 1992)

If the current is oscillatory in nature the shape of the bedforms will be amended; this is shown in Figure 12. The bedform shape in oscillatory flow is shown in the upper part of the diagram, which can be compared with the bedform shape in steady flow in the lower part. It can clearly be seen that in oscillatory flow, the bedform will have more defined peaks, whereas in steady flow, the peaks will appear much smoother.

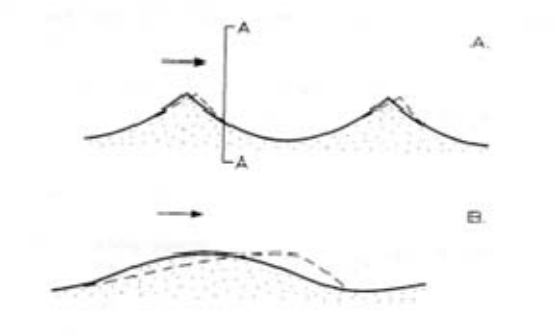

Figure 12. A) Bedform shape in oscillatory flow, B) Bedform shape in steady flow (From Deigaard, 1992)

2. Waves

Waves are oscillatory in nature, which amends the shape of the bedform as shown above. Ripples generated by waves, are generally less than 15 cm in height, and can be split into two main groups, rolling grain ripples and vortex ripples (Bagnold, 1946). Figure 13 shows the progression from rolling grain ripples (A) to vortex ripples (D). Rolling grain ripples are formed at a low Shields number, not much larger than twice the critical Shields number. Vortex ripples are formed at a higher Shields number, and the vortex is able to move an increased amount of sediment away from the seabed, thus increasing the amount of sediment in suspension.

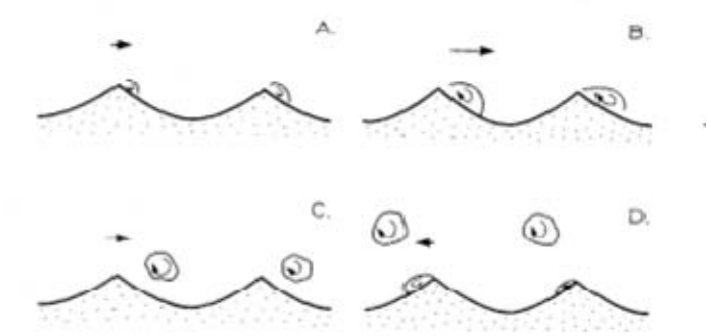

Figure 13. Sketch of vortices formed over a vortex ripple (From Deigaard, 1992)

Wave generated ripples are influenced by depth. Linear wave theory dictates the orbital motion of particles with depth. As depth increases, the orbital motion of a particle will decrease. This, in turn, will influence the bottom shear stress of the sea bed. This is demonstrated by Figure 14.

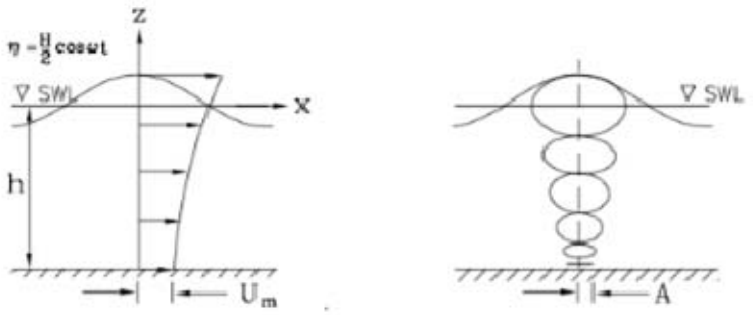

Figure 14. Horizontal velocity profile and water particle orbit as predicted by linear wave theory (From Liu, 2001)

3. Combined Current and Wave Interaction

The general principle of sediment transport in the coastal or littoral region is that waves stir up the sediment and currents, then in turn, transport the sediment. When both waves and currents are present, wave induced velocity will dominate the situation near to the bottom, even if the current velocity is much larger. Because of the oscillatory motion of the waves, current will generally be the main transport mechanism of sediment, except in breaking wave situations. The comparison of current and wave velocity profiles is shown in Figure 15. The velocity profile indicated by the solid line is that of wave induced velocity, the dashed line indicates tidal current velocity. On the left, the differences throughout the water column can be seen, with the tidal current velocity tending to be the larger. On the right, the diagram shows an enlargement of the region at the seabed, where it can be seen that wave induced velocity is dominant.

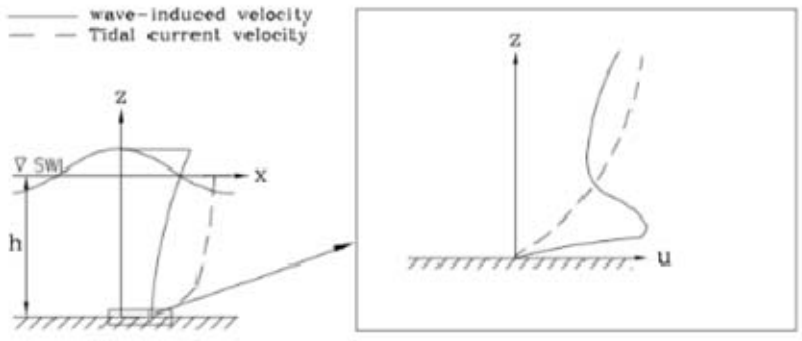

Figure 15. Comparison of current and wave velocity profiles (From Liu, 2001)

D. MODELING WAVE GENERATED RIPPLES

A number of numerical models have been developed to predict the ripple characteristics due to wind generated waves. In this study, the Wiberg and Harris model is utilized (Wiberg and Harris, 1994). This model uses linear wave theory to estimate the height, wavelength, and steepness of ripples.

A series of sediment transport applets developed by Woods Hole Oceanographic Institute are used for the calculations in this study (Sherwood, 2009). The theory outlined here is used. Using the inputs, wave height, H, wave period, T, and water depth, h, the wave number and angular frequency can be calculated from first principle linear wave theory. The dispersion relationship for gravity waves defines a unique relationship between the angular frequency, ω, and wavenumber, k.

$$\omega^2 = gk\tan(kh) \tag{14}$$

This implicit equation can be solved iteratively, but to simplify this an approximate direct solution of the wave dispersion equation (Hunt, 1979) can be used. This solution uses the Taylor expansion, and the resulting equation (shown below) gives an approximate solution for wave speed, *c*, with an accuracy of 0.1%.

$$\frac{c^2}{gh} = \left[y + \left(1 + 0.6522y + 0.4622y^2 + 0.0864y^4 + 0.0675y^5\right)^{-1} \right]^{-1} \quad (15)$$

$$y = \frac{\omega^2 h}{g} \quad (16)$$

$$c = \frac{\omega}{k} \quad (17)$$

From this relation, the near bed orbital diameter d_0, and the near bottom orbital velocity, U_{orb} can be calculated:

$$d_0 = \frac{H}{\sinh(2\pi h/L)} \quad (18)$$

$$U_{orb} = \frac{\pi d_0}{T} \quad (19)$$

Using these results and the sediment grain size (mm), the ripple height, ripple wavelength, ripple steepness, and classification can be determined as detailed in Wiberg and Harris (1994).

Ripples are divided into three categories, which was determined by analysis of ripple wavelengths. The ratio of near bed orbital diameter d_0 and mean grain diameter *D*, are examined. At small ratio values, ripple wavelength or spacing is proportional to d_0; these are referred to as orbital ripples (Clifton, 1976). At large ratio values, ripple wavelength appears to be independent of d_0, but is roughly a constant multiple of the grain size (~500*D*), which is referred to as anorbital ripples (Clifton, 1976). In the intermediate range the ripples are termed suborbital.

Wiberg and Harris examined experimental results from many previous studies, and relationships determined. It was found that for orbital ripples a simple linear relationship existed for ripple wavelength and steepness.

$$\lambda_{orb} = 0.62 d_0 \quad (20)$$

$$\left(\eta/\lambda\right)_{orb} = 0.17 \tag{21}$$

For anorbital ripples the relationship was more complex:

$$\lambda_{ano} = 535D \tag{22}$$

$$\left(\eta/\lambda\right)_{ano} = \exp\left[-0.095\left(\ln\frac{d_0}{\eta}\right)^2 + 0.442\ln\frac{d_0}{\eta} - 2.28\right] \tag{23}$$

For suborbital ripples a weighted geometric average bounded by the wavelengths of anorbital and orbital ripples was determined giving:

$$\lambda_{sub} = \exp\left[\left(\frac{\ln(d_0/\eta_{ano}) - \ln 100}{\ln 20 - \ln 100}\right)\left(\ln\lambda_{orb} - \ln\lambda_{ano}\right) + \ln\lambda_{ano}\right] \tag{24}$$

Wiberg and Harris, guided by previous studies, argued that the most important difference between orbital and anorbital ripples is the ratio of wave boundary layer thickness to ripple height, which can be approximated by the ratio d_0/η. Using this criteria:

d_0/η < 20 orbital ripples (25)

d_0/η > 100 anorbital ripples (26)

20 < d_0/η < 100 suborbital ripples (27)

Using this theory from three simple inputs, the ripple characteristics can be approximated, however, the ripple geometries are limited, with one of the main factors being depth. The calculations are limited to sand sized sediments, which also suggests that there may be no transport if the near bottom orbital velocity is less than 0.13 cm/s. Figures 16 and 17 show the results obtained by this model.

Figure 16 shows the near bottom orbital velocity for different wave heights and different wave periods plotted against depth. It can be seen that as wave height increases, so does the near bottom orbital velocity. The same is true for an increased wave period, which also increases the near bottom orbital velocity. It can also be seen that, in each case, the near bottom orbital velocity increases initially with an increase in depth. A maximum is reached at depths between 10 m and 15 m, the near bottom orbital velocity then steadily decreases with depth, in all cases at depths greater than 60 m the near bottom orbital velocity had reduced to 0.2 m/s or less.

Figure 17 shows the wave generated ripple heights for a 1 m wave. The ripple height is plotted against depth for different wave periods and three different sediment sizes, with phi 2.5, corresponding to fine sand, phi 1.5, corresponding to medium sand, and phi 0.5, corresponding to coarse sand. It can be seen that the ripple heights are larger for the coarse sand and reduced as the sand becomes finer. As wave period increases the ripple heights also increase. Peak ripple heights are found at approximately 10 m to 15 m depth, which corresponds to the maximum near bottom orbital velocities.

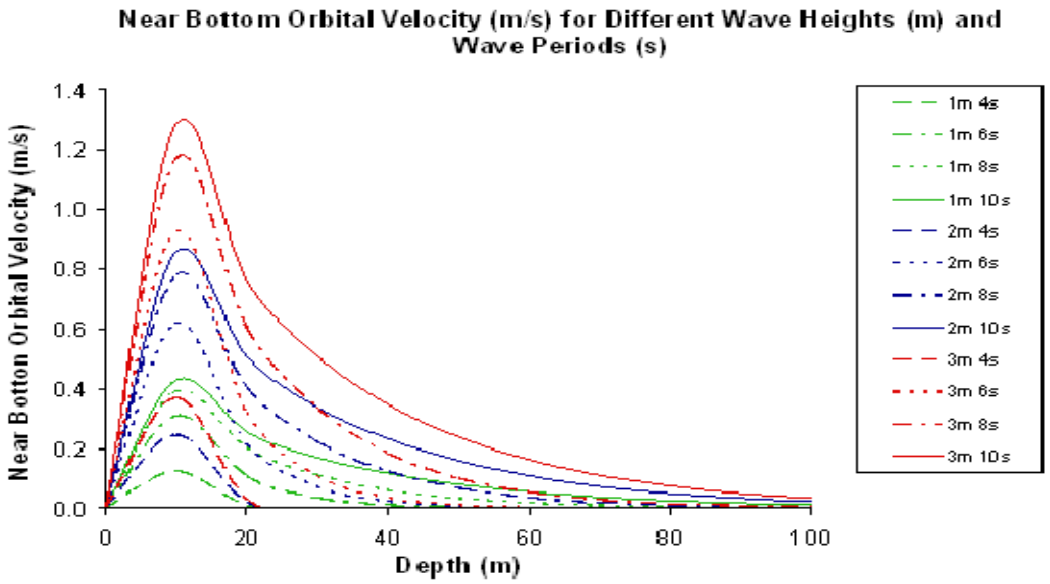

Figure 16. Differences in near bottom orbital velocity for different wave heights and wave periods, for a sediment size of 2.5phi, results obtained using the Wiberg and Harris model

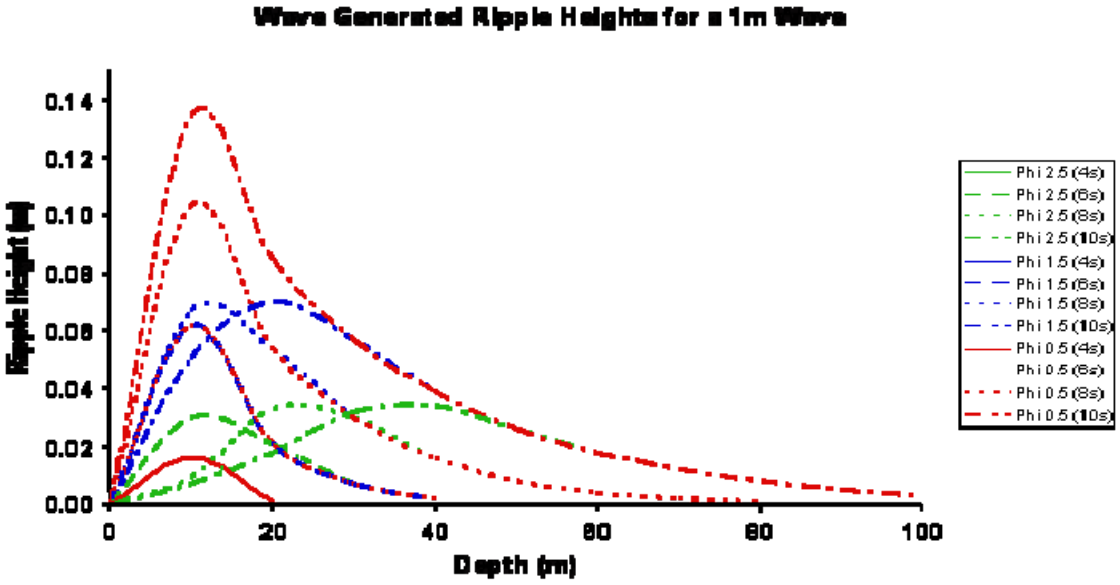

Figure 17. Differences in wave generated ripple heights for different wave periods and sediment size, for a wave with a height of 1 m, results obtained using the Wiberg and Harris model

III. CASE STUDY: SAN FRANCISCO BAY

A. INTRODUCTION

San Francisco Bay is a large, shallow, dynamic estuary located in California, on the west coast of the U.S. It is a major international shipping port, with large container facilities, which makes it a significant, economically important, port. It is an extremely busy waterway used by both commercial and recreational vessels. San Francisco Bay is thought to have been formed by a down-warping of the Earth's crust between the San Andreas Fault to the west and the Hayward Fault to the east.

The area has been subject to major changes in topography through the years. In the nineteenth century, the area was subjected to hydraulic mining, which released massive amounts of sediment that settled in areas of the bay with little or no currents. In the twentieth century, the Army Corp of Engineers began to carry out dredging operations, which have continued. Also aggregate mining has occurred in this region. These activities have all had an impact on the area, although the impact has not been quantified (Army Corp of Engineers, 1996; Friends of the Estuary, 1997).

Approximately 40% of water drainage from the central coast rivers enters the Pacific Ocean through the Golden Gate channel. This represents a mean high freshwater discharge rate of approximately 800 m^3/s (California Department of Water Resources, 2007). This is a huge amount of fresh water entering the estuarine system, which has the potential to carry a significant amount of sediment into the area.

The San Francisco Bay area is subject to a complex semi-diurnal tidal regime, this leads to temporally and spatially variable currents that can exceed

2.5 m/s. This leads to a diverse and complex pattern of bedform formations, which were first mapped using side-scan sonar in the late 1970s, and are now mapped using high resolution multi-beam surveys. (Barnard et al., 2007).

In this chapter, the Golden Gate region is investigated in detail. A comparison study of localized sediment grab data in the same positions for a three-year period is assessed and analyzed. This data is then compared to the NAVOCEANO HFEVA sediment database, and an assessment of the validity of this database is made. Multi-beam data, obtained by the USGS is examined and the impact of these findings on the mine warfare route survey periodicity assessed.

B. SEDIMENT ANALYSIS: COMPARISON OF LOCALIZED SAMPLE DATA AND DATABASE DATA

In February 2009, sediment samples were collected in the vicinity of the Golden Gate region of San Francisco Bay. Previous sediment studies had been carried out in the winters of 2007 and 2008. The intent of this investigation is to: 1) re-visit the previously sampled sites and determine statistically if there has been a change in the sediment properties, and 2) compare the latest sediment samples to the NAVOCEANO HFEVA database to determine if the database remains valid.

1. Data and Methods

Sediment samples were collected during a student cruise in the winter of 2009 (OC3570 Operational Oceanography course). The cruise took place from 29 January until 4 February 2009, onboard the R/V Point Sur. Four sediment samples were collected in San Francisco Bay. The sample locations were the same as those that had been previously sampled during the Winter 2007/2008 cruises.

a. Sediment Sample Collection

The samples were all collected using a double trap Van Veen sediment grab, deployed off the stern of the ship using a crane. The Van Veen grab is a light weight stainless steel sampler designed to take samples of soft bottom sediment. Water is able to flow through the grab as it is lowered. When it hits the seabed, the doors of the grab close due to tension on the cable, they remain closed while the grab is raised and recovered on deck.

Figure 18. Van Veen grab on board R/V Point Sur

Upon recovery of the grab, a representative sample of the sediment was collected in a quart mason jar. The jar was then sealed, labeled and stored, for laboratory processing.

b. Sediment Sample Analysis.

The sediment sample analysis was conducted in the oceanographic laboratory at the Naval Postgraduate School. Laboratory analysis can be broken down into phases.

The first phase involved emptying the contents of each jar into a standard plastic Rubbermaid basin; the sample was rinsed with fresh water while being agitated. The sample was then left to settle—the time this took depended

on the consistency of the sample, with silt samples taking much longer. The samples were generally left overnight; this allowed all the sediment to return to the bottom, leaving clear water on top. Following the settling period, any particulates or biologic material floating on the water was removed. The fresh water was then decanted out, being careful not to pour out any sediment. If necessary, this process was repeated.

The rinsed sediment was then transferred into a pre-weighed 8 x 8 inch, Pyrex casserole dish. Sediment was transferred by pouring, scraping using a spoon, and rinsing by squeezing a fine stream of water into the bowl. Once transferred, the sample was placed in the laboratory oven overnight to dry. The oven was set at approximately 90^{o} C. Once the sample was completely dry, it was weighed and prepared for the sieving process.

The dried sample was broken up, in some cases this could be achieved by using a spoon. However it was necessary to use a hammer to break up some of the more difficult samples. These tended to be the finer samples that had become like baked clay. The broken up sample was then placed in a pre-weighed plastic bag. The bagged sample was weighed and the result recorded.

The next phase, the sieving phase was achieved by using a Ro-Tap automated sieve. A 100 ml glass beaker was weighed, a quantity of the sample was added to the beaker and it was re-weighed, both weights were recorded. This was the part of the sample to be analyzed. The Ro-Tap sieve used in this experiment utilized 14 sieves ranging from 2.00 mm to 0.070 mm in mesh diameter.

The sample was poured into the top sieve (2.00 mm), and then sieved through the column of sieves for 15 minutes. The sample collected in each sieve was carefully collected, by pouring it onto a sheet of card and removing any residue from the sieve with a wire brush. Next, it was transferred

into a pre-weighed plastic bag. The bag and sample were then weighed, and the results recorded. A loss of less than 1% of the sediment weight had to be achieved, if the result was to be deemed accurate.

c. Localized Sample Data

The samples collected were compared to samples collected on the 2007/2008 cruises. The previous results were re-formatted for comparison.

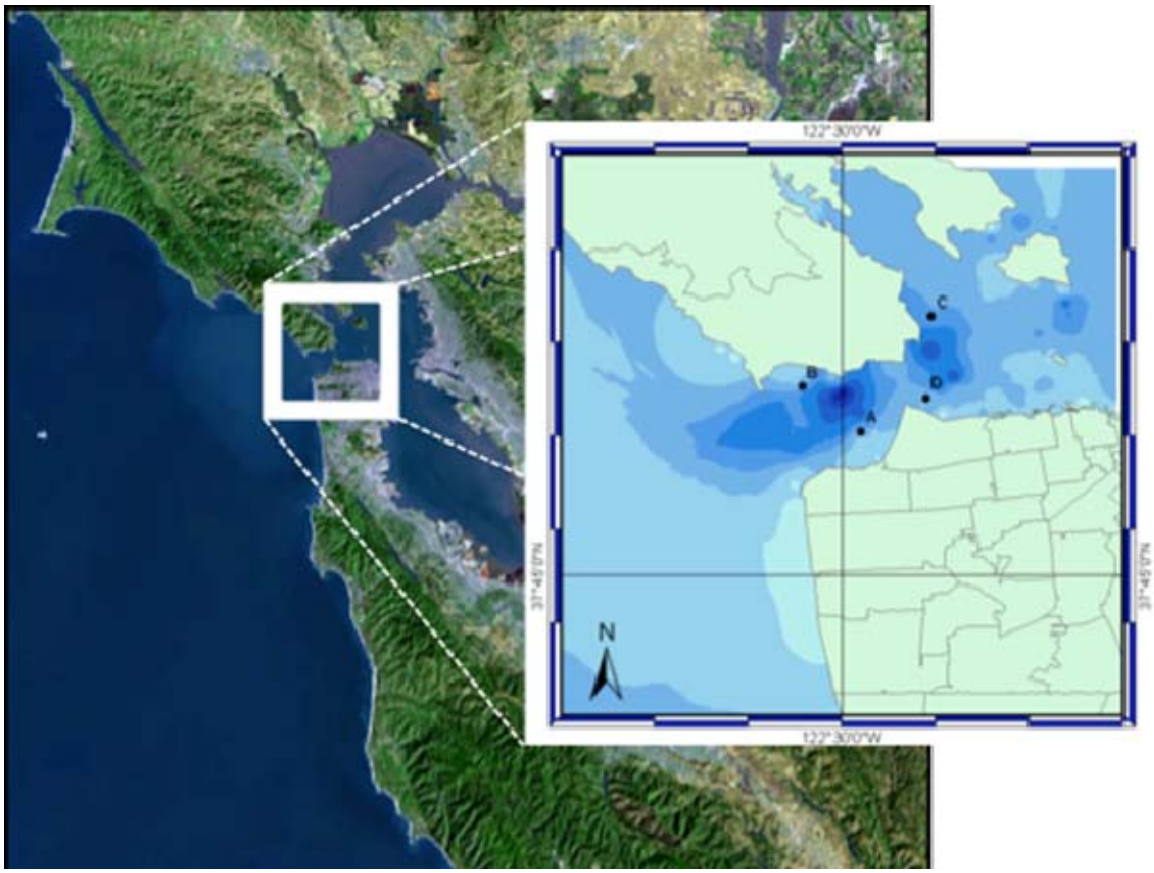

Figure 19. Locations of the localized samples used for comparison

Statistical analysis was carried out, and the results for each sample were first normalized to allow comparison to take place. Analysis, as described in Chapter II, was used (Dyre, 1986) to estimate the mean grain size, and classify the sediment sample according to the Wentworth scale.

2. Results and Analysis

The phi value was used in conjunction with the Wentworth scale in order to classify the sediment samples. Bar graphs showing the break down of each sample for each comparable year were plotted. X-Y plots showing 95% confidence interval error bars for 2009 were also plotted. The results were analyzed in order to determine if any changes of sediment properties had occurred at any of the positions with time. Following this, climatological data and linear wave theory, as described in Chapter II, were utilized in order to determine predicted ripple heights for the four positions. This allowed comparisons to be made between the samples and an assessment of the importance of wind generated ripple height for the mine warfare problem in this area.

a. Localized Sample Data Comparison.

Bar graphs, showing the sample sediment size distributions (positions A–D) broken down by sieves, are shown in Figure 20. Using the Wentworth Scale, the sediments were classified. Table 7 shows a summary of the results. The Phi values were calculated for each position for each year. Although phi values did fluctuate, the classification for each position throughout the three-year period remained the same.

	2007	2008	2009
A	2.48 Fine Sand	2.52 Fine Sand	2.51 Fine Sand
B	2.31 Fine Sand	2.29 Fine Sand	2.11 Fine Sand
C	1.47 Medium Sand	1.75 Medium Sand	1.90 Medium Sand
D	2.25 Fine Sand	2.17 Fine Sand	2.20 Fine Sand

Table 7. Sediment Classification based on Phi values for Positions A–D.

Figure 20 shows the breakdown of percentage sample mass for each position and each year. The largest grain size is shown on the left, and the smallest on the right. Each column represents the percentage of sample mass recovered from each of the 14 sieves and the bottom pan. The actual sediment sizes are shown in Figure 21, where a more detailed statistical analysis was carried out. Each bar graph shows that the sieve with the highest percentage of sample mass for each position remained the same in each year. These results would indicate that the sediment characteristics for all positions have changed little, and sediment classification remains unchanged for the 2007 to 2009 period.

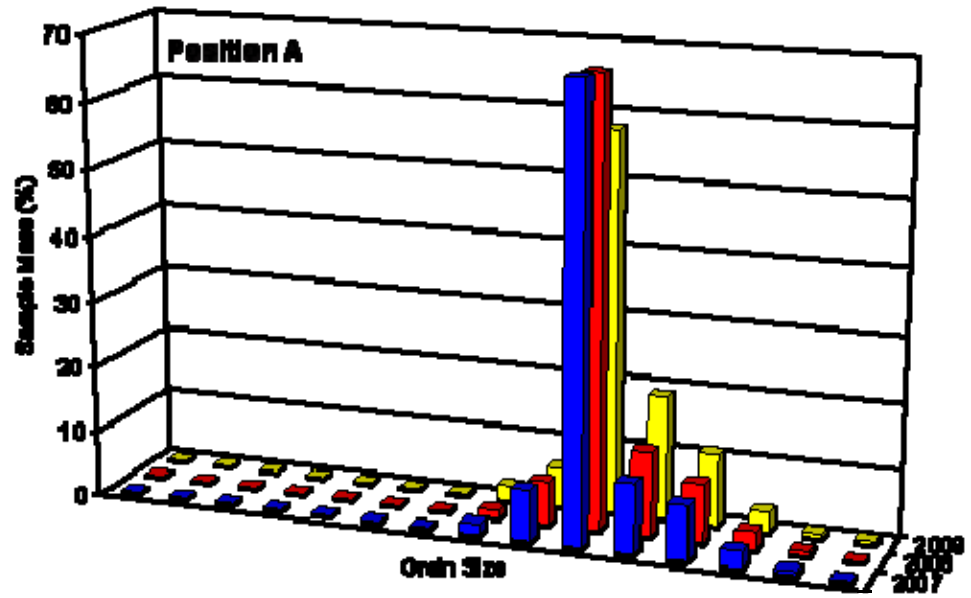
Position A
70
60
50
40
30
20
10
0
Sample Mass (%)
Grain Size
2008
2006
2007

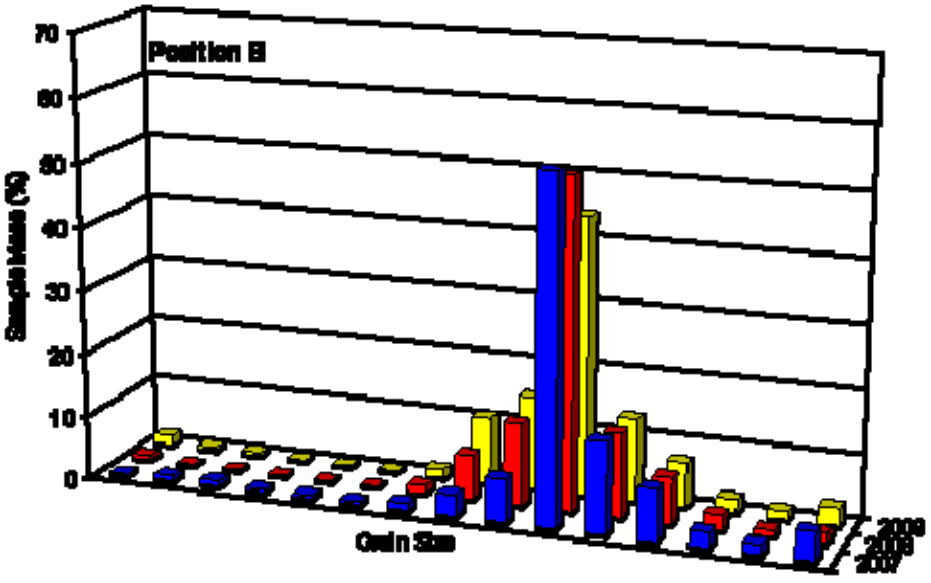
Position B
70
60
50
40
30
20
10
0
Sample Mass (%)
Grain Size
2008
2006
2007

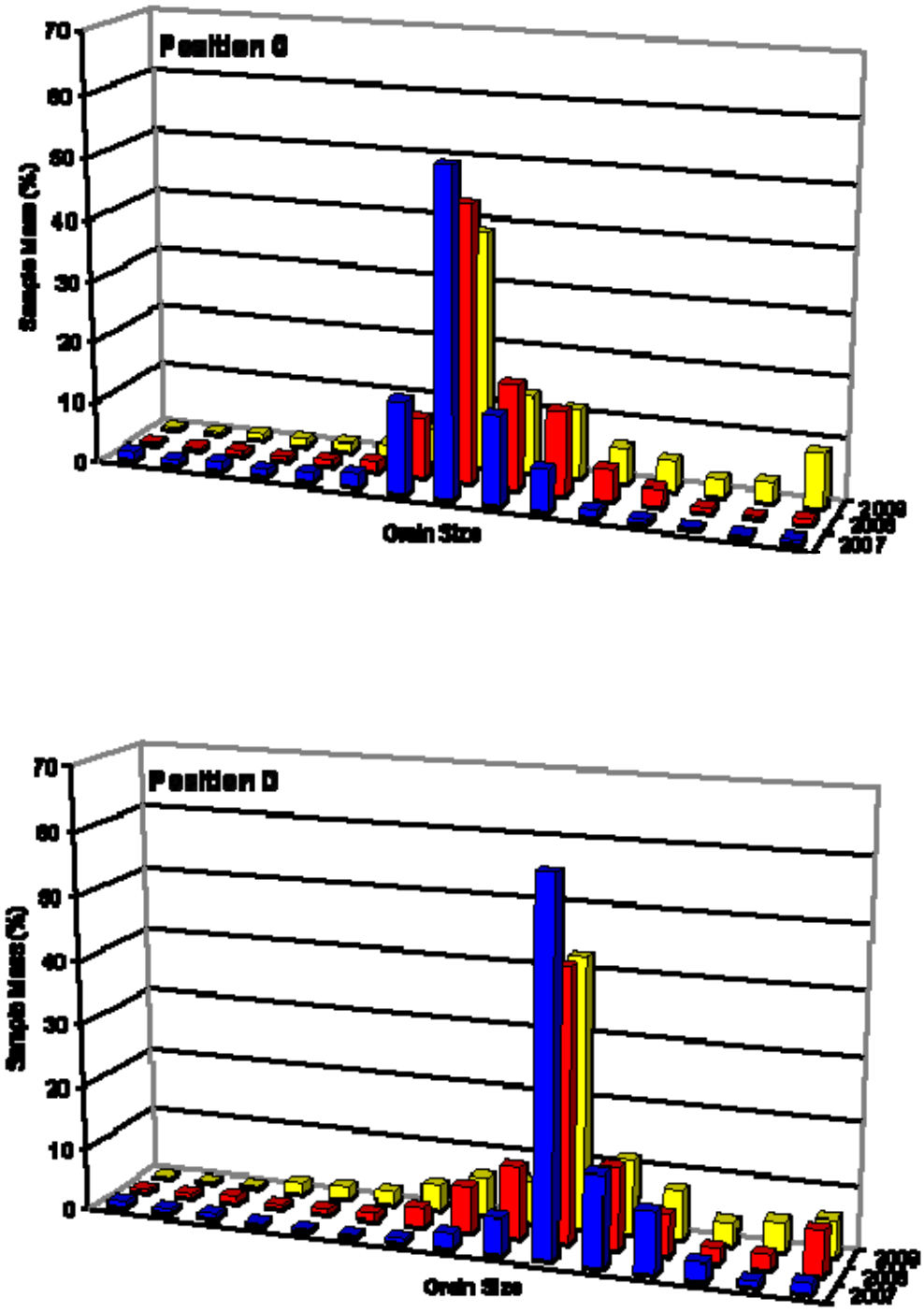

Figure 20. Column Graphs for positions A–D, showing sample breakdown, per year, from largest grain size (left) to smallest grain size (right)

Figure 21 shows the same breakdown of sediment samples by grain size, with 95% confidence intervals. Although there are differences between the distributions for each year these variations are not significant at a 95% confidence level. Thus, the main conclusion is that the sediment characteristics have not changed considerably within the three-year period.

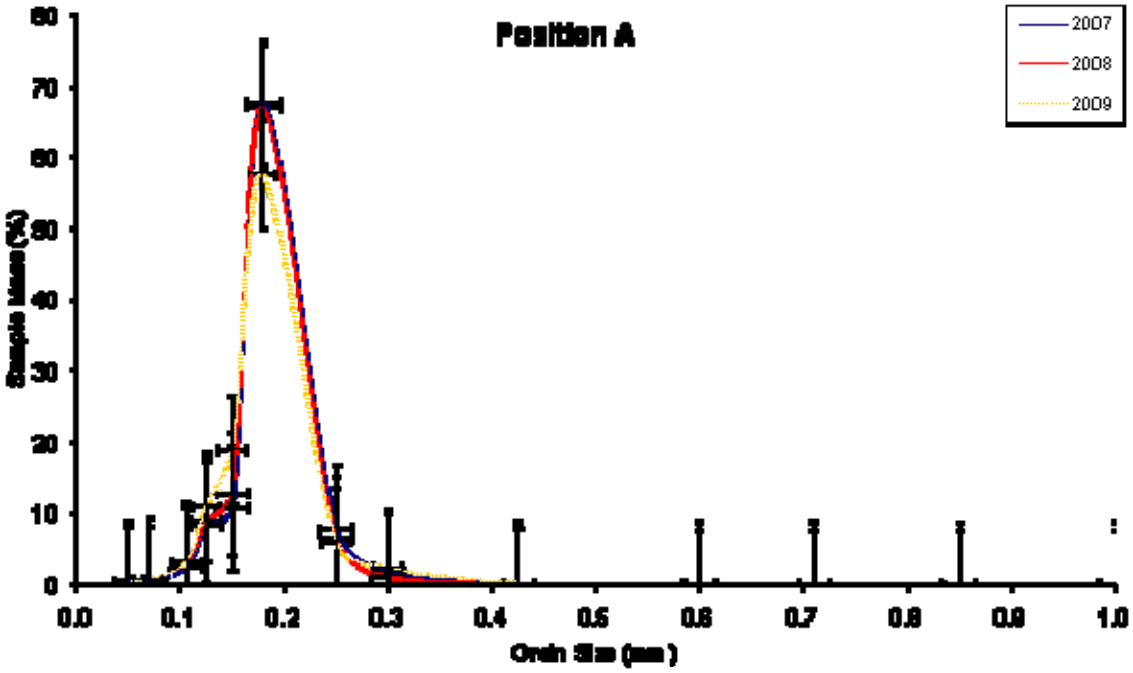

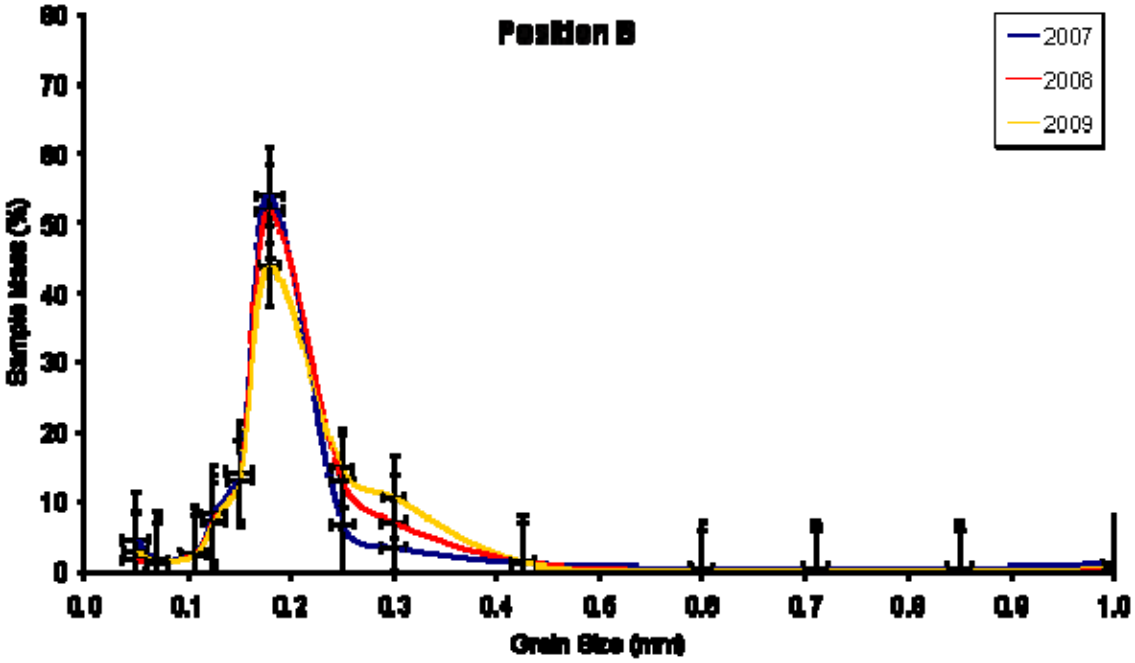
Position B
2007
2008
2009
Sample Mass (%)
Grain Size (mm)

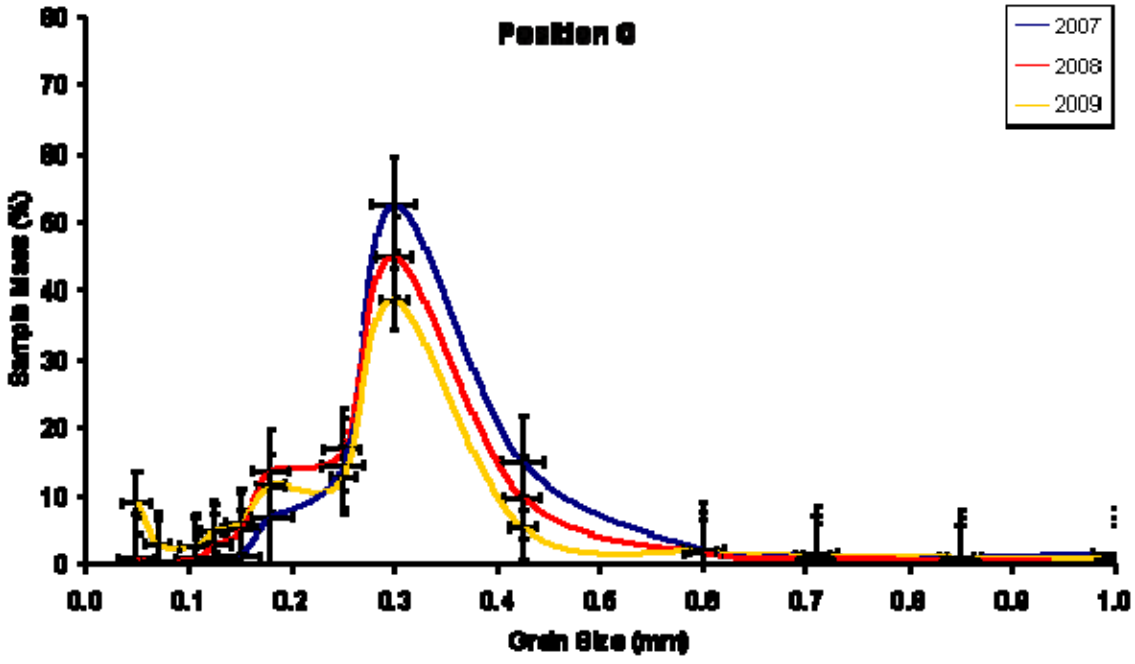
Position C
2007
2008
2009
Sample Mass (%)
Grain Size (mm)

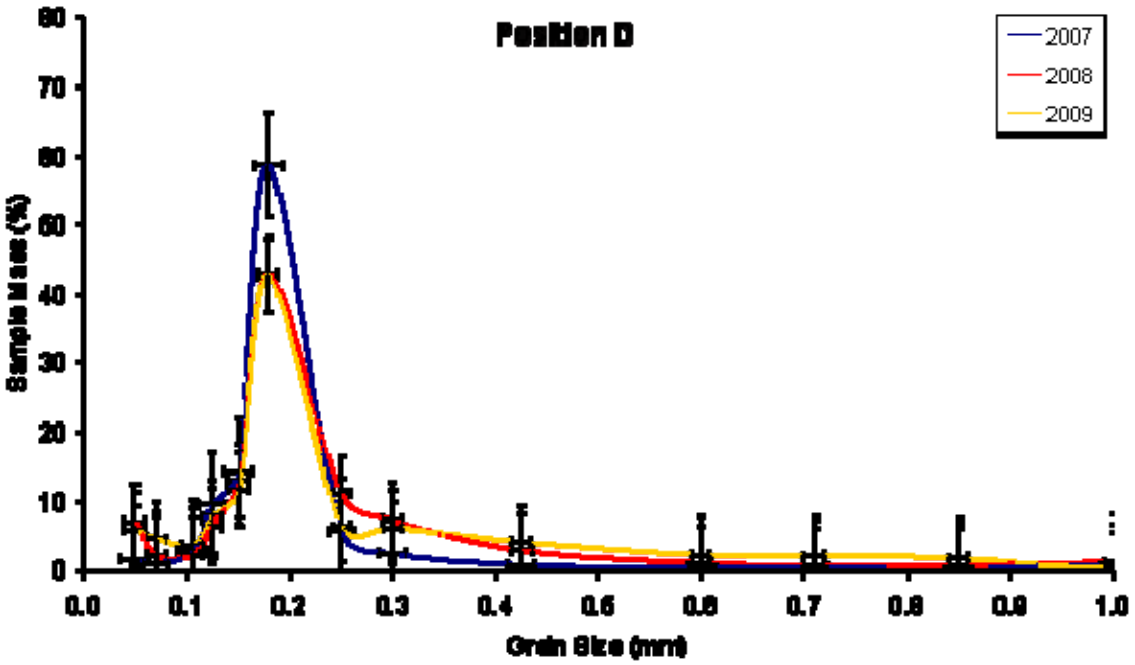

Figure 21. Sample mass (%) vs. grain size (mm) for positions A to D. Error Bars indicate the 95% Confidence Interval in both dimensions

b. Comparison of Ripple Heights

Table 8 shows the estimated ripple heights from waves and characteristics for positions A to D. The wave conditions were obtained from marine gridded climatology data provided by Fleet Numerical METOC Detachment in Ashville. Values were calculated by re-analysis of data from 1857 to 1997.

Position A results show all the ripples classed as orbital. The ripple height varies from 0.3 cm to 0.4 cm, which indicates a limited amount of variability at position A over the time period.

Position B results also show the ripples are classified as orbital in all cases. The ripple heights vary from 2.5 cm to 3.1 cm. Although this position has more variability, it remains at less than 1 cm, so cannot be deemed significant.

Position C results, again, classify the ripples as orbital, while the ripple height varies from 1.9 cm to 3.1 cm. Although the variability is slightly larger than the other two positions, the range of ripple heights remains relatively small and inconsequential.

Position D shows the largest variability. All ripples remain orbital, but heights range from 1.4 cm to 3.4 cm. The range of phi values is from 2.17 to 2.25, which is not a large range, however the depth at which the grab samples were obtained is more variable for this position, which could explain the variability in results. The difference of 2 cm ripple height over a three-year period is not large enough to be a significant problem.

From these results, it can be seen that the ripple heights for each position show a degree of variability, although not on a large scale. The variation for each position is in the order of centimeters, the estimated ripple heights from waves are all relatively small and would be inconsequential for mine burial at these positions. However, this does not take into account the currents in this region.

Although the ripple height is assessed as too small to bury a mine, it still remains an important issue in the mine warfare survey periodicity problem. Smaller ripples in the order of centimeters can cause a significant problem in mine detection due to scattering of acoustic rays.

		2007	2008	2009	Mean	SD
A	Phi	2.48	2.52	2.51	2.50	0.02
	Depth (m)	60	63	63	62	1.73
	Orbital Diameter (mm)	0.019	0.015	0.015	0.016	0.0023
	Orbital Velocity (m/s)	0.017	0.013	0.013	0.014	0.0023
	Ripple Height (cm)	0.4	0.3	0.3	0.33	0.0577
	Ripple Classification	Orbital	Orbital	Orbital		
B	Phi	2.31	2.29	2.11	2.23	0.11
	Depth (m)	37	35	38	36.6	1.52
	Orbital Diameter (mm)	0.128	0.151	0.118	0.132	0.0169
	Orbital Velocity (m/s)	0.115	0.135	0.106	0.119	0.0148
	Ripple Height (cm)	2.7	3.1	2.5	2.77	0.3055
	Ripple Classification	Orbital	Orbital	Orbital		
C	Phi	1.47	1.75	1.90	1.71	0.21
	Depth (m)	38	41	35	38	3.00
	Orbital Diameter (mm)	0.118	0.093	0.151	0.120	0.0291
	Orbital Velocity (m/s)	0.106	0.083	0.135	0.108	0.0261
	Ripple Height (cm)	2.5	1.9	3.1	2.5	0.6
	Ripple Classification	Orbital	Orbital	Orbital		
D	Phi	2.25	2.17	2.20	2.21	0.04
	Depth (m)	40	45	34	39.67	5.508
	Orbital Diameter (mm)	0.101	0.067	0.164	0.116	0.0492
	Orbital Velocity (m/s)	0.090	0.060	0.147	0.099	0.0442
	Ripple Height (cm)	2.1	1.4	3.4	2.3	1.01
	Ripple Classification	Orbital	Orbital	Orbital		

Table 8. Ripple Characteristics for positions A–D.

c. NAVOCEANO Database Comparison

The four samples were compared to the NAVOCEANO HFEVA database. Results are summarized in Table 9.

	Phi	Wentworth Sediment Classification	HFEVA Database
A	2.51	Fine Sand	Fine Sand
B	2.11	Fine Sand	Fine Sand
C	1.90	Medium Sand	Medium Sand
D	2.20	Fine Sand	Fine Sand

Table 9. 2009 sediments samples compared to NAVOCEANO Database Data.

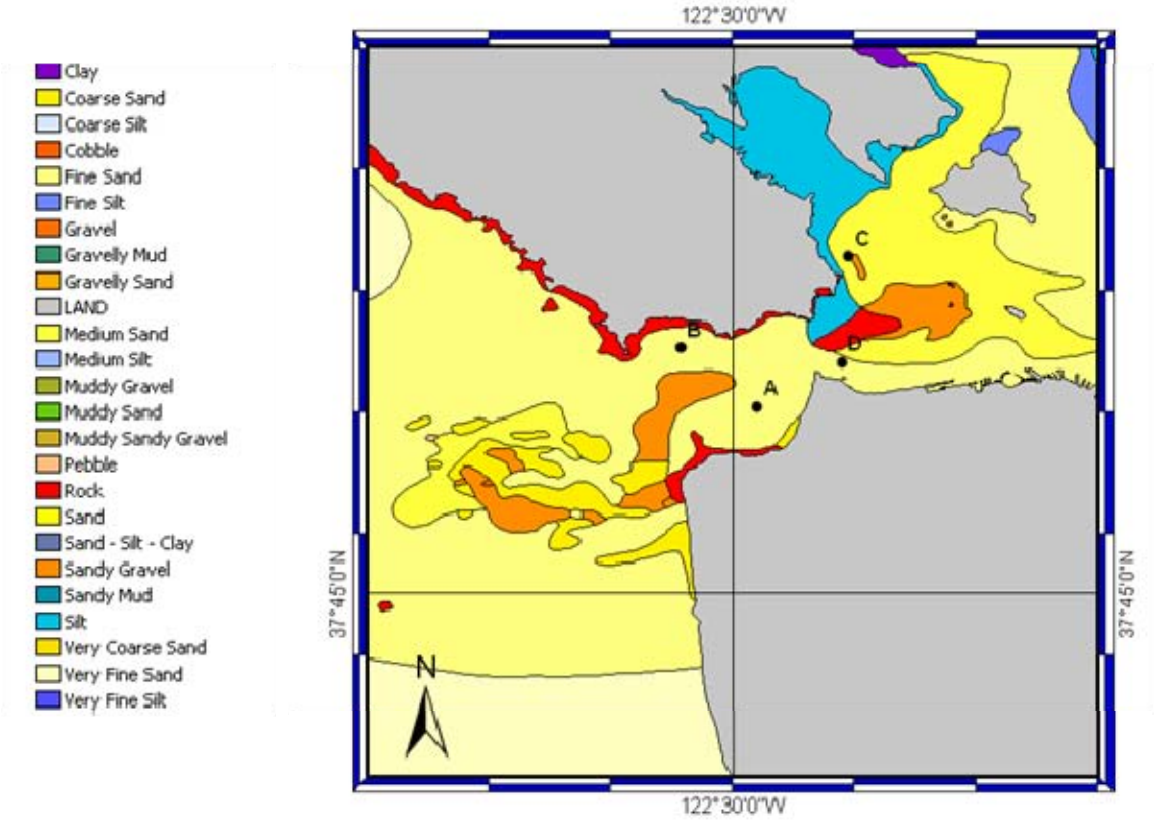

Figure 22. Positions A–D, overlaid on the NAVOCEANO HFEVA Dataset

Table 9 shows that the classifications of each of the four positions are the same as the NAVOCEANO database data. Figure 22 shows the NAVOCEANO HFEVA dataset plotted geographically; each color represents a different sediment type as shown in the key on the left of the figure. Figure 22 also shows that the experimental results compare well with the database data. The experimental results all fall within the same sediment categories that the database predicts. This would suggest that this is a valid database. Positions A, B and D all fall within the fine sand category geographically, and position C falls within the (medium) sand category.

d. Accuracy and Errors

There are issues involving the accuracy and errors associated with this investigation. Although, during the collection and laboratory processing, as much care as possible was taken to limit or eliminate errors.

During the collection phase, the bridge of the R/V Point Sur was given the positions of previously collected samples, the ship aimed to stay in station at these locations as accurately as possible during the deployment and retrieval of the grab. However, from comparing the positions over the three years, it can be noted that although the positions are extremely similar, they are not exactly the same. This is reflected in the depths used in calculating ripple height and is the main reason for the variation in the ripple height.

In order to gain a better representation of sediment type, it would be preferable to take a selection of samples at each position, so that the average result could be used, rather that relying on one sample. This would allow erroneous sediment samples to be excluded, or have a minimal effect on the results used for comparison. The results, used for comparison from previous studies, were assumed to be correct, as the sediment samples were not available for re-analysis.

The laboratory procedure for sediment analysis was carried out in a manner that minimized error. In order to be deemed a valid result, less than 1% sample loss could occur during the sieving process. There were problems that occurred that could introduce error. Finer samples proved problematic after the baking phase. The aim was to break up these samples as much as possible, however, this proved difficult at times, and could have caused a skew in results indicating a sample was coarser than it actually was. Every care was taken to avoid this.

During the sieving phase, care had to be taken to ensure that all of the sediment sample was removed from each sieve—at times this could be difficult, and was achieved by using a wire brush or a sharp pencil to poke any remaining sediment grains from the sieve.

The sieves available for the Ro-Tap sieve ranged from 2.00 mm to 0.070 mm. This limited the sediment classification range, from fine gravel to very fine sand, in the case of these sediment samples this range appeared adequate.

C. USGS MULTI-BEAM SURVEY DATA

The USGS has an ongoing investigation in the San Francisco Bay area, this includes analyzing bedforms mapped using multi-beam sonar to determine the regional bedload sediment transport patterns in the San Francisco Bay coastal system. This study has yielded some valuable results that can be used in assessing the mine warfare route survey periodicy problem in this region.

A series of high resolution multi-beam surveys were conducted in the San Francisco Bay area. The length, height, depth, and asymmetry of 3386 individual bedforms were derived. This allowed quantitative information regarding the bedforms to be derived, and a better understanding of coastal sediment transport gained.

Selections of USGS survey results are shown in this section (with permission, Barnard, 2007/2009), the effect of these findings on the survey periodicity problem are discussed. The results are also used as a quality control measure in determining a survey periodicity model for this area and are discussed in Chapter IV.

1. Bed Patterns in San Francisco Bay

Figures 23 and 24 show detailed multi-beam images of the San Francisco Bay region. The complexity and variety of the bedforms in this region can clearly be seen in these images.

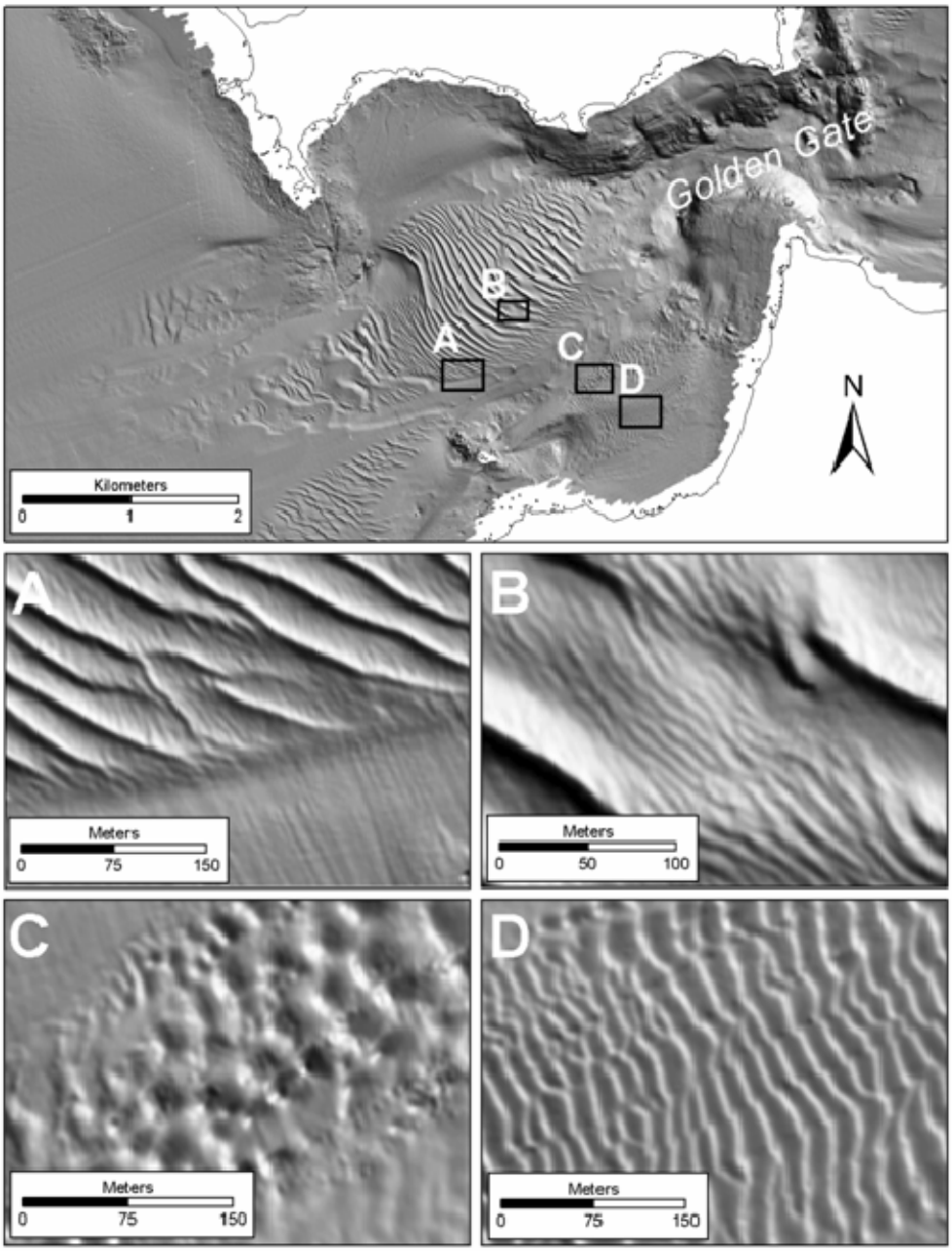

Figure 23. Bedforms in the inlet throat of San Francisco Bay (with permission, from Barnard et al., 2007)

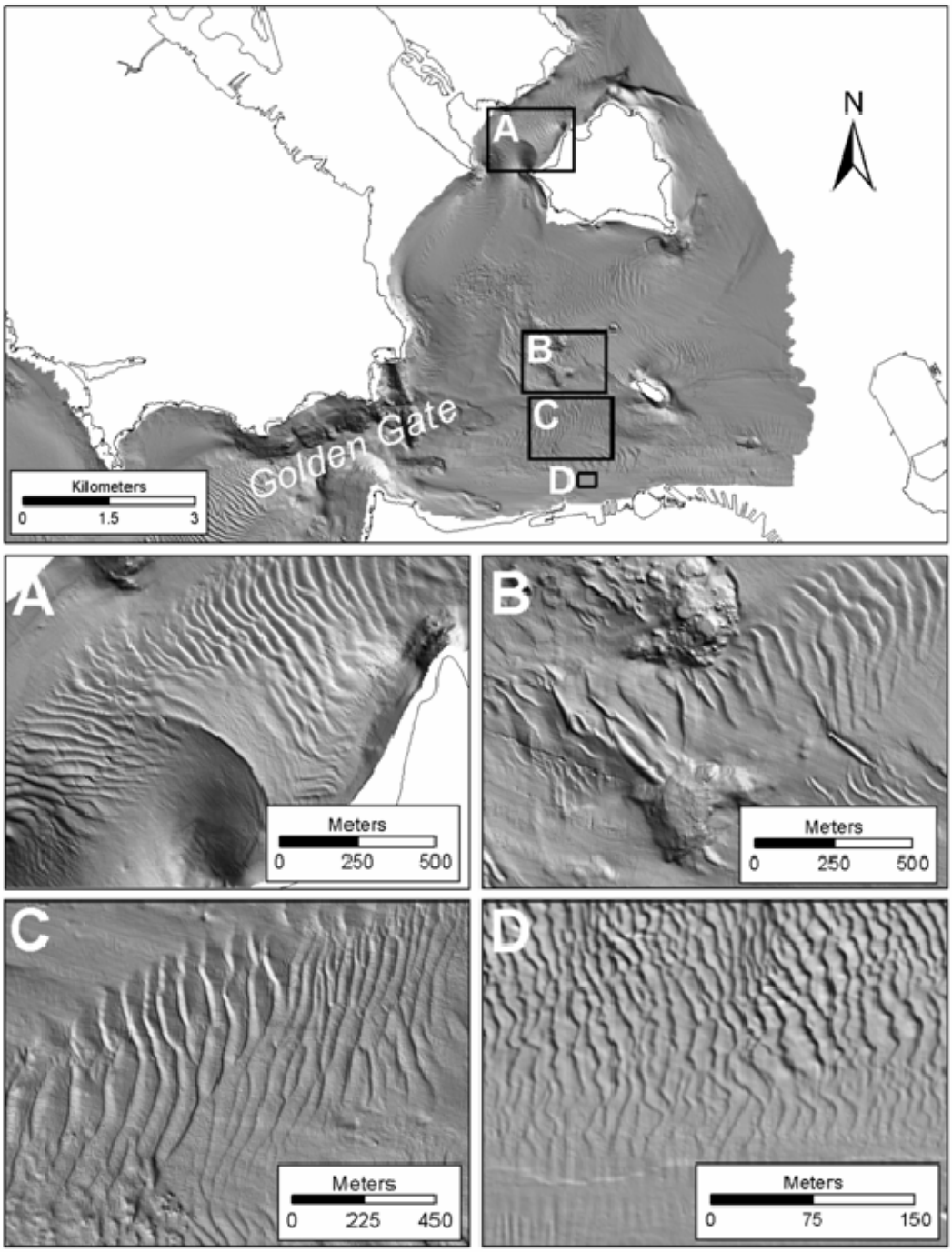

Figure 24. Bedforms inside San Francisco Bay (with permission, from Barnard et al., 2007)

2. Temporal Variation in Bedform Morphology

In the region of the larger bedforms, a number of surveys were conducted. The time scale of these surveys ranged from a few hours to more than ten years. Transects through these areas were analyzed to determine if bedform size and shape varied significantly, and on what time scales these variations occur. The USGS concluded that the bedform fields, as a whole, maintained relative symmetry, and that asymmetry values have not changed markedly with time (Barnard et al., 2007).

Figure 25 shows two transects. The first, in the mouth of San Francisco Bay (Transect B), was repeatedly surveyed in a 5.5 hour period in September 2005. It shows sand wave heights of approximately 5 m. These are large bedforms compared with for example the size of a MANTA mine (height approximately 0.5 m), and understanding their evolution is of great importance to the mine warfare community The second transect, (Transect C) the Alcatraz Shoal region, was surveyed from time scales of two weeks to eleven years, again it can be seen that although the height of the sand wave peaks do not vary considerably, their location does.

Figures 26 and 27 show the results from April and November 2008, in the region between Alcatraz and Angel Island. Again, it can be seen in the depth profile A-B, that the heights of the sand wave peaks do not vary considerably, but their location does. This area is further complicated by the fact that smaller bedforms are superimposed on the larger ones, which can be seen more clearly in transect C-D. The super imposed bedforms were only identified in the later survey with use of higher resolution multi-beam technology, and represent an additional change in height of 0.4 m.

From the transects, it can be seen that the height of the sand wave peaks does not vary considerably with time, however, the location of the peak does move with time. This is significant for the mine warfare route survey periodicity

problem. The movement of the sand waves would cause a mine to be buried, and hence not be detected during a survey, these regions should therefore be subject to a higher survey periodicity.

.

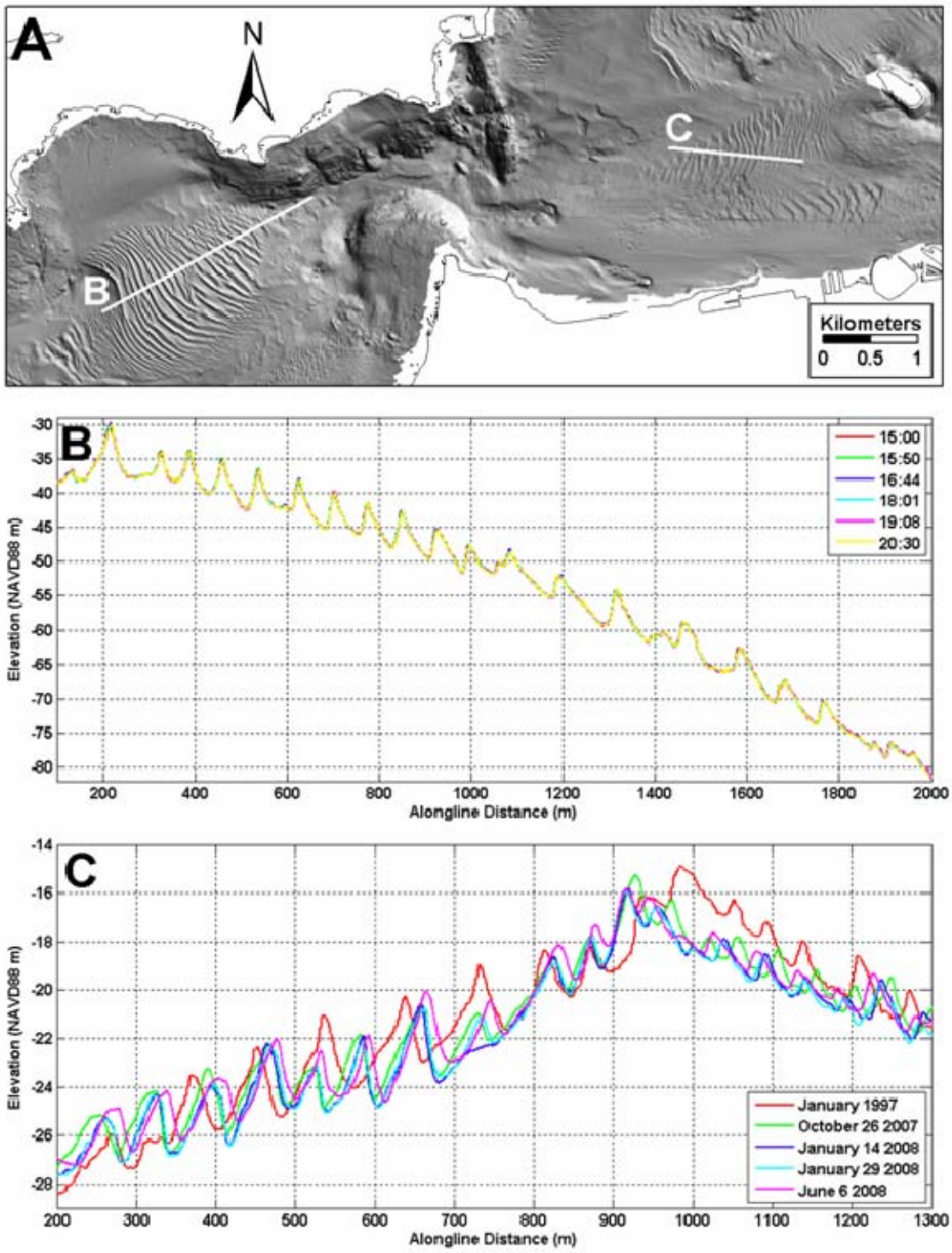

Figure 25. A) Location of sand wave transects. B) Transect from mouth of San Francisco Bay. C) Transect in vicinity of Alcatraz Shoals. (with permission, from Barnard et al., 2007)

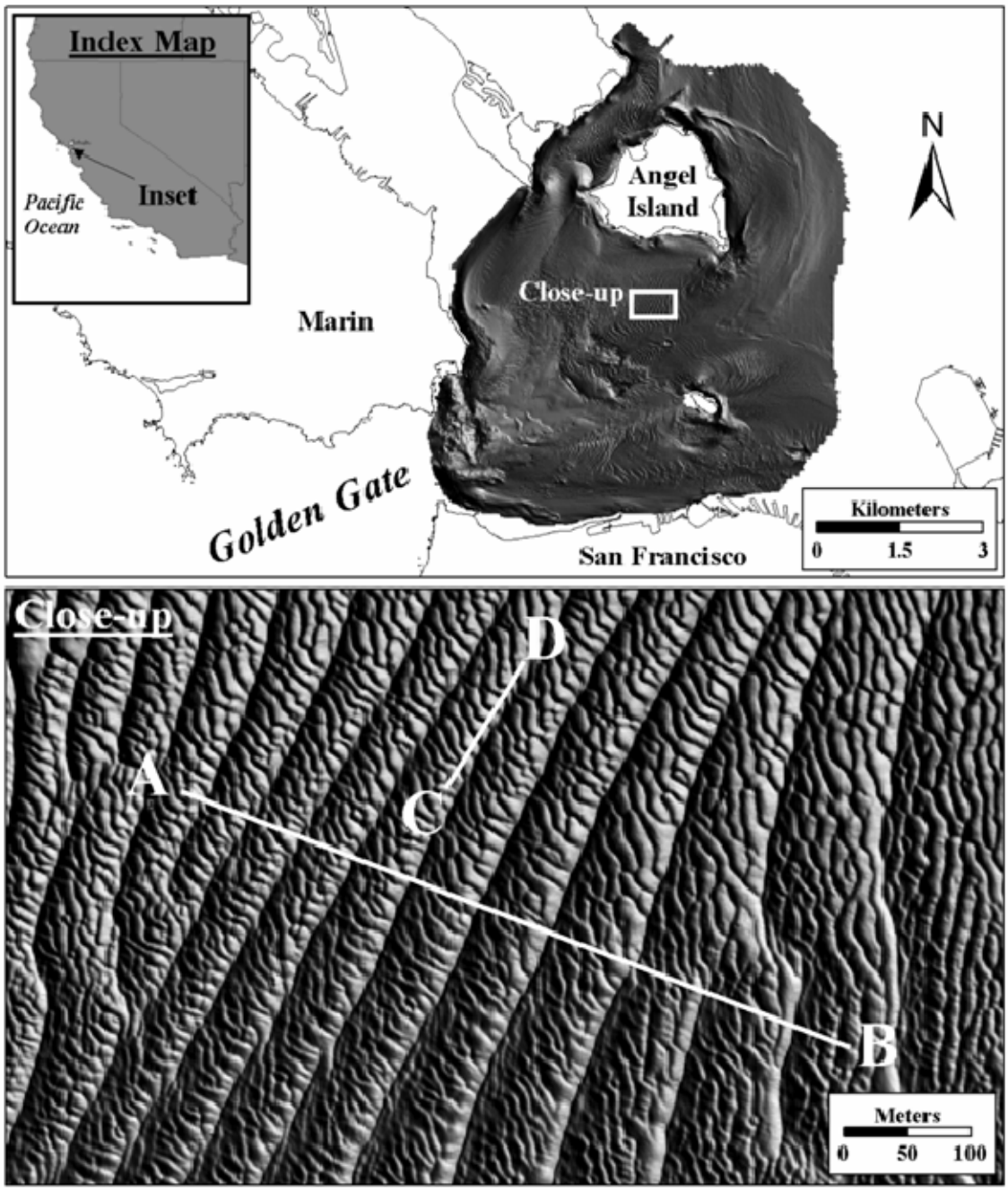

Figure 26. Region of study between Alcatraz and Angel Island (with permission, from Barnard et al., In Press, 2009)

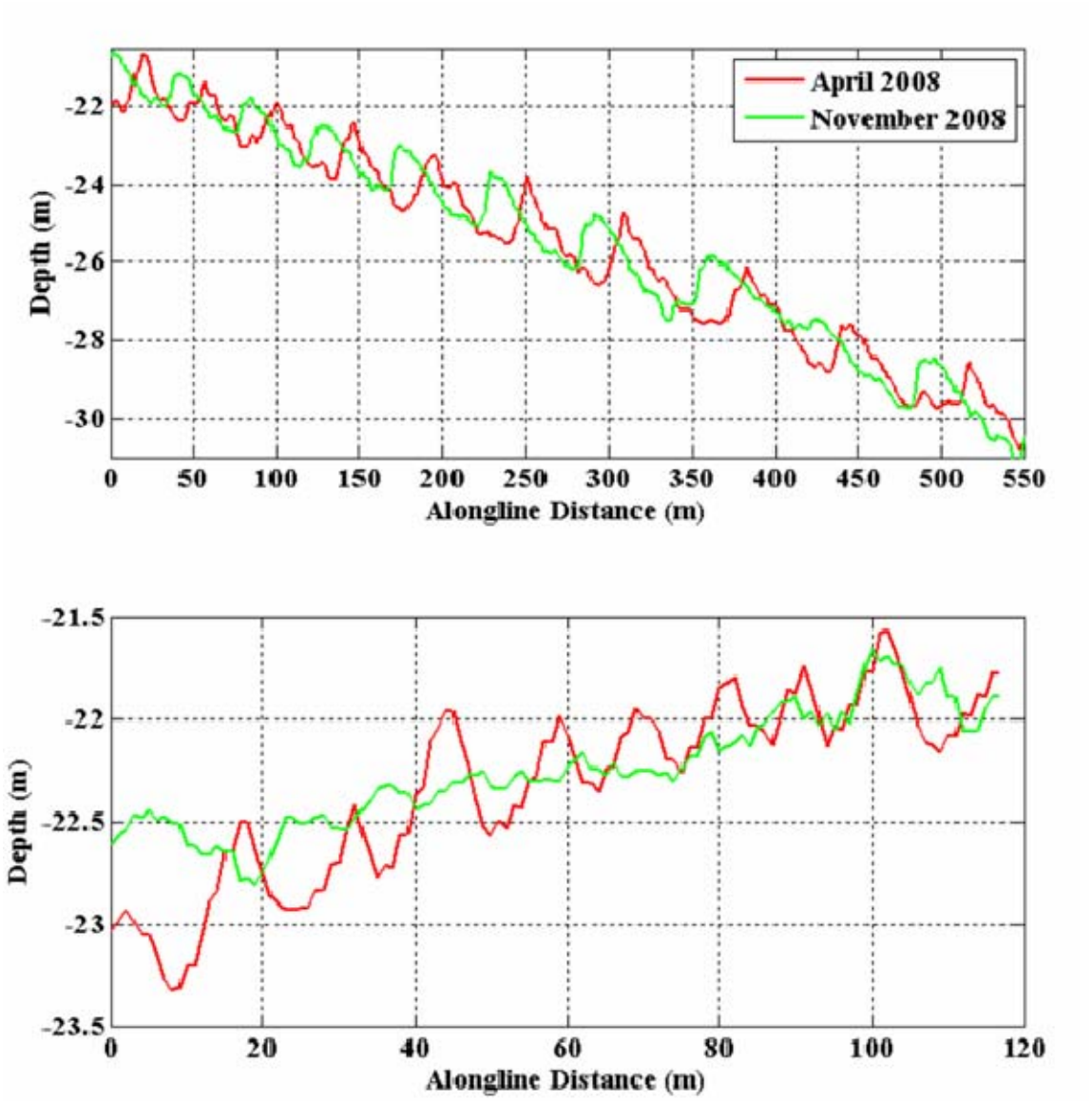

Figure 27. Transects from Figure 26. A) Transect A-B. B) Transect C-D. (with permission, from Barnard et al., In Press, 2009)

3. Bedform Asymmetry and Sediment Transport Patterns

Detailed high resolution multi-beam data surveys have enabled an assessment to be made of the relationship between bedform patterns and dominant tidal transport directions. This can be seen in Figure 28, the intersecting bedform patterns occur a) where a flood channel cuts obliquely across alongshore migrating ebb-orientated bedforms and b) in a large region of onshore directed bedform migration.

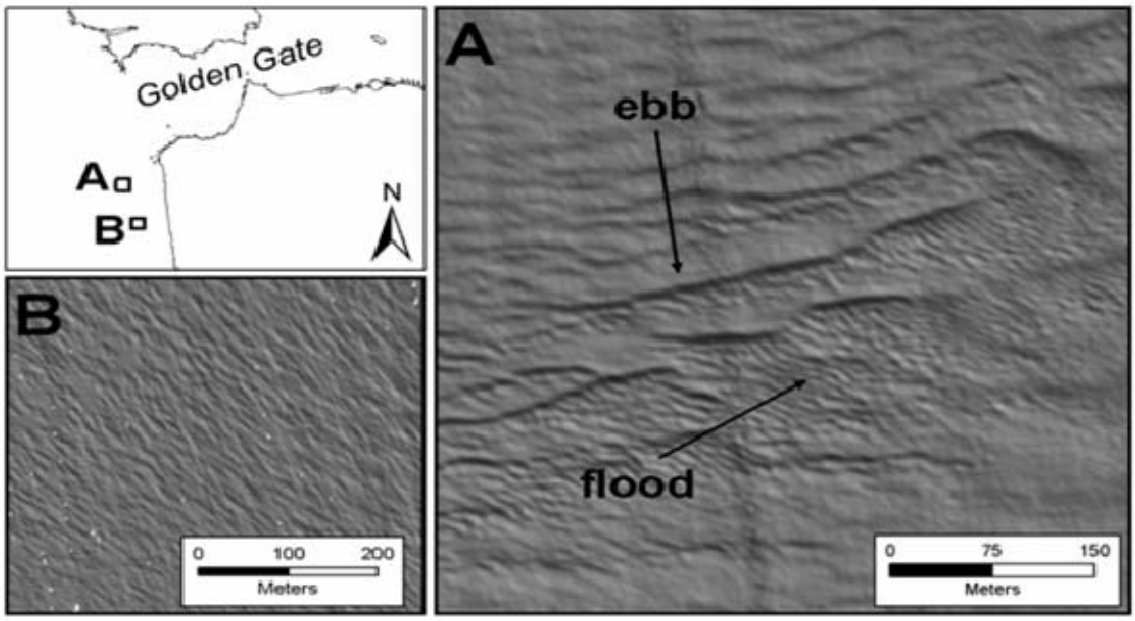

Figure 28. Complex current patterns offshore of Ocean Beach (with permission, from Barnard et al., 2007)

The asymmetry of bedforms in the region of the Golden Gate has been assessed. As shown in Figure 29, the southern region of the bedforms are flood dominated, and in the northern region bedforms are ebb dominated. From this the inferred net bedload sediment transport directions can be determined, as shown in Figure 30. The USGS used this information, coupled with tidal information to develop a hydrodynamically calibrated numerical model to predict total mean sediment transport, instantaneous water discharge and sediment transport through the Golden Gate.

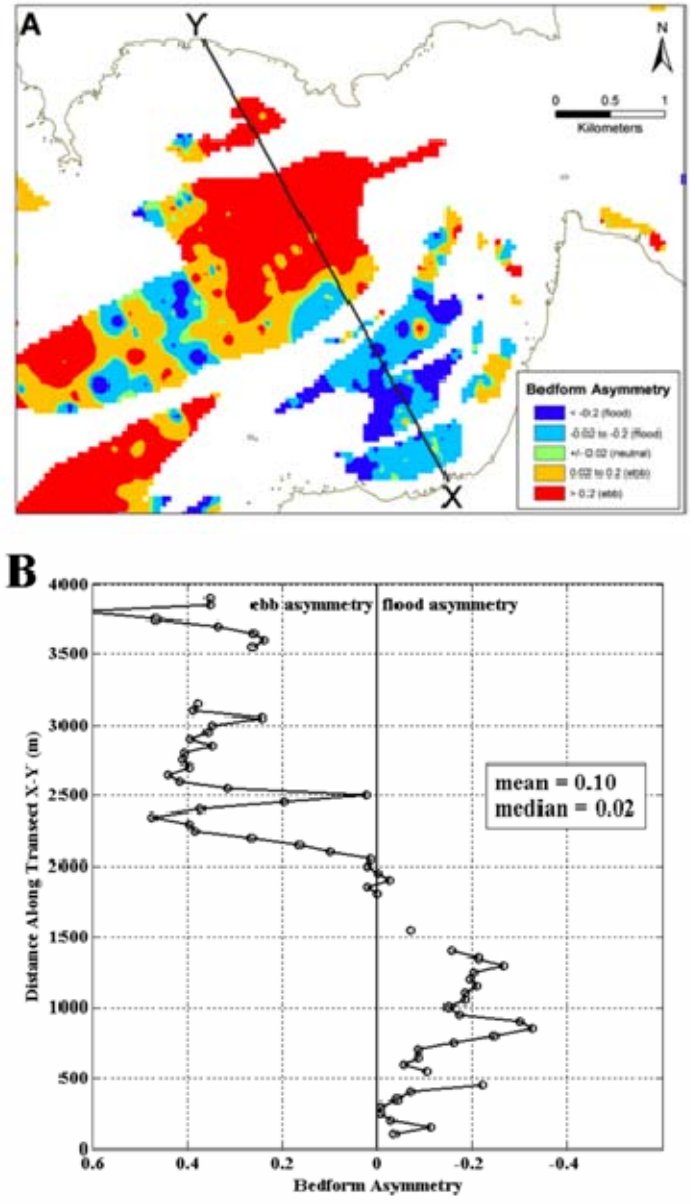

Figure 29. Asymmetry values across the Golden Gate (with permission from Barnard et al., 2007)

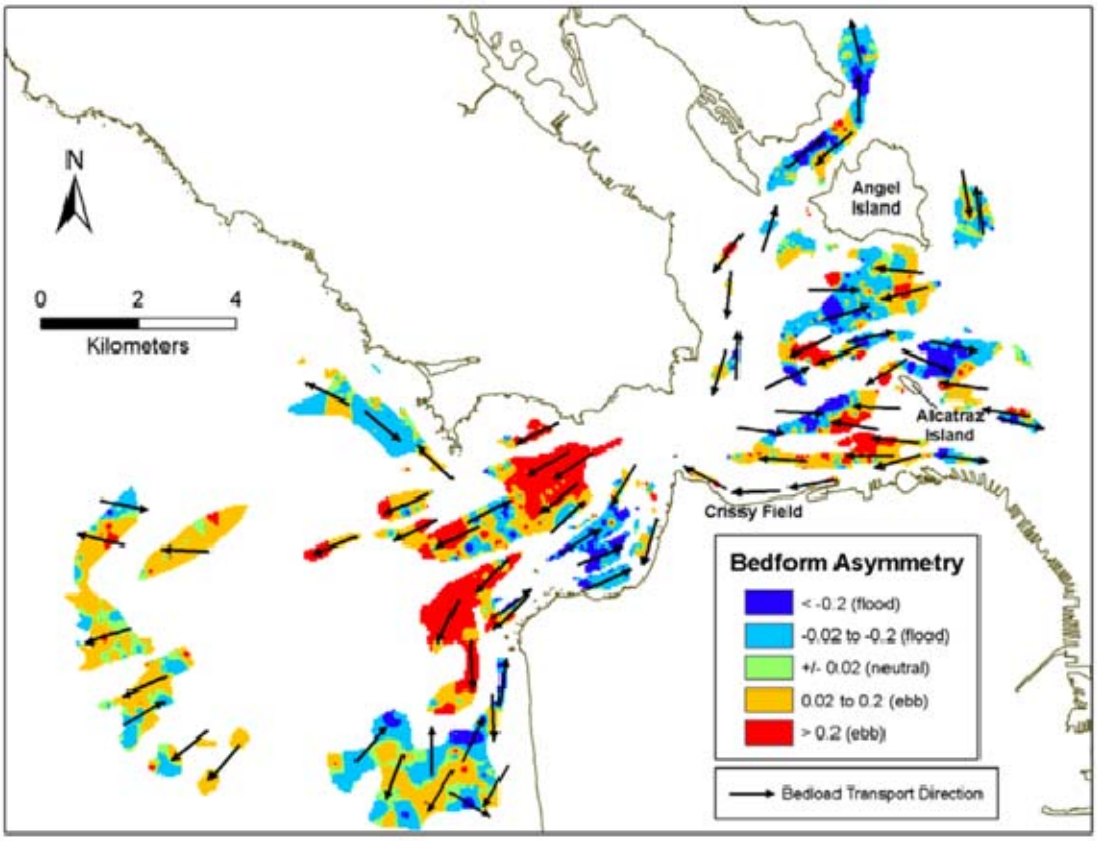

Figure 30. Inferred net bedload sediment transport directions based on asymmetry values, arrows indicated direction only, not magnitude (with permission, from Barnard et al., 2007)

IV. DETERMINING ROUTE SURVEY PERIODICITY FOR SAN FRANCISCO BAY

A. INTRODUCTION

In order to determine the mine warfare route survey periodicity for San Francisco Bay, a weighted suitability GIS model, utilizing a similar methodology to the UKHO model, was developed. From the background theory in Chapter II, and the findings based on information in Chapter III, it is hypothesized that waves, tides, currents, and sediment size will influence bedform formation and sediment processes; this in turn will affect the survey periodicity requirement.

Tidal data, from NAVOCEANO predictions is examined, and the variability in this region is shown. Historical current data, provided by NAVOCEANO is analyzed. Using linear wave theory and climatological data, the estimated wave generated ripple heights are calculated. Sediment data obtained from grab samples provided by USGS is utilized. This data is weighted and combined, and a model for survey periodicity is obtained.

This chapter details the process used to develop the survey periodicity model for the San Francisco Bay region, and provides the input layers used and the weighting schemes employed. A number of different options based on various weightings are reviewed, and the most representative one chosen based on the actual conditions found from the high resolution multi-beam data collected by USGS.

B. THE MODELING CONCEPT

The concept of the weighted suitability model used here is summarized in Figure 31. It utilizes three main input layers; predicted bedform type (green), predicted bottom current (blue), and predicted wave generated ripple height

(red). Each of these layers can be thought of as a sub-model, similar to those used in the UKHO model. The details of each layer is described in the following section.

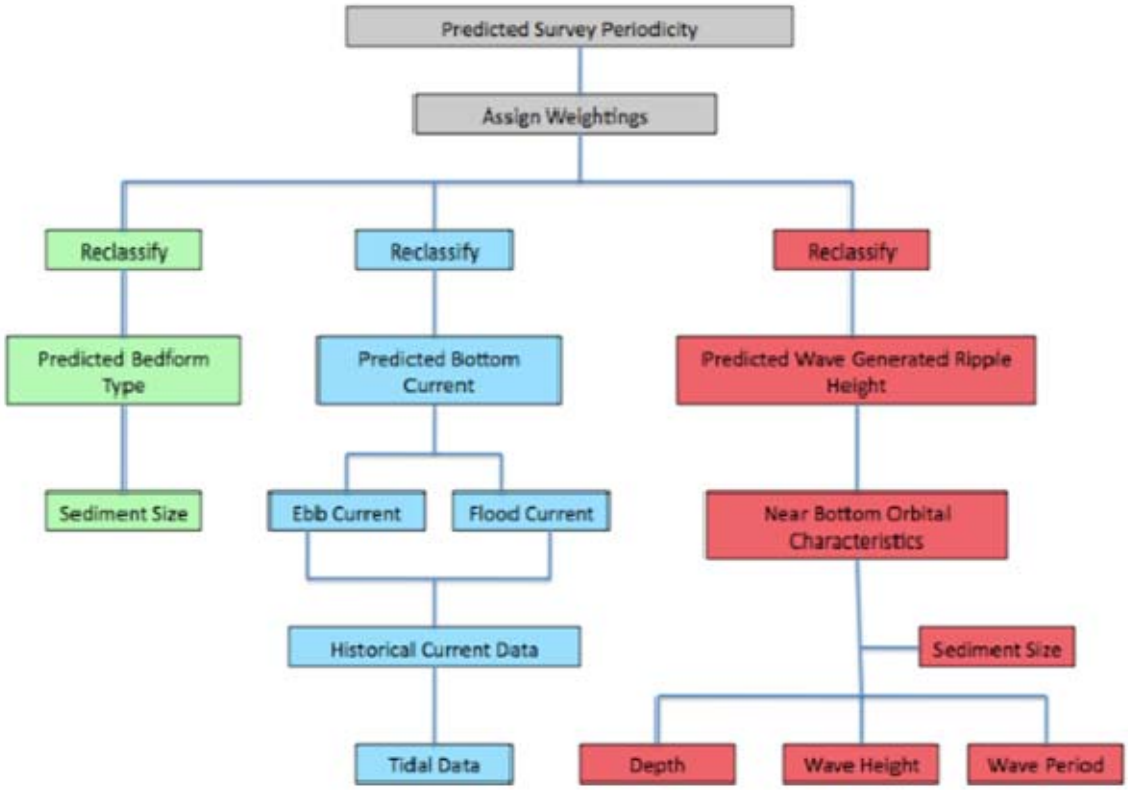

Figure 31. Flow chart showing the three layers used to predict survey periodicity

1. The Input Layers

a. Predicted Bedform Type

In order to predict the bedform type, 174 grab samples were obtained from the USGS. The grab samples were taken during surveys dated between 2004 and 2008. In addition, the grab samples detailed in Chapter III were also included. The data included latitude, longitude, depth, and sediment grain size. The dataset was compiled in excel and entered into the GIS software

program ArcMap. The data points were interpolated into a raster dataset and classified using the Wentworth scale. The interpolated sediment classifications are shown in Figure 32, with the positions of the grabs samples overlaid. A graduated color scale is used with red representing the coarsest sediments and blue representing the finest. It can be seen that the coarsest sediment can be found in the mouth of the Golden Gate region.

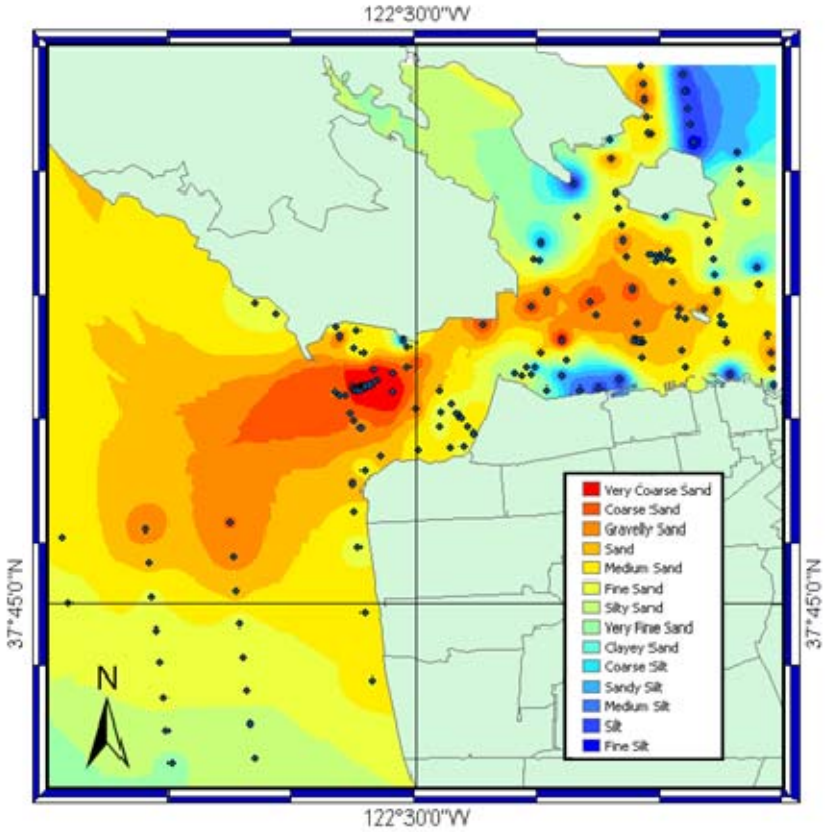

Figure 32. Sediment type calculated from grab samples, locations of the grab samples are overlaid

From background theory discussed in Chapter II, it is assessed that ripples will be generated if the sediment grain size is less than 0.7 mm, these are generally formed by wave motion. If the sediment size is greater than 0.6 mm sand waves are more likely to form, these are generally due to current motions. Taking this into account the grain size in mm was calculated and re-plotted, the

results are shown in Figure 33. Potential areas of wave generated ripples is shown in green, this indicates a sediment size of less than 0.6 mm, potential areas of current induced sand waves are shown in red, indicating a sediment size greater than 0.7 mm. An intermediate zone between 0.6 mm and 0.7 mm is shown in yellow.

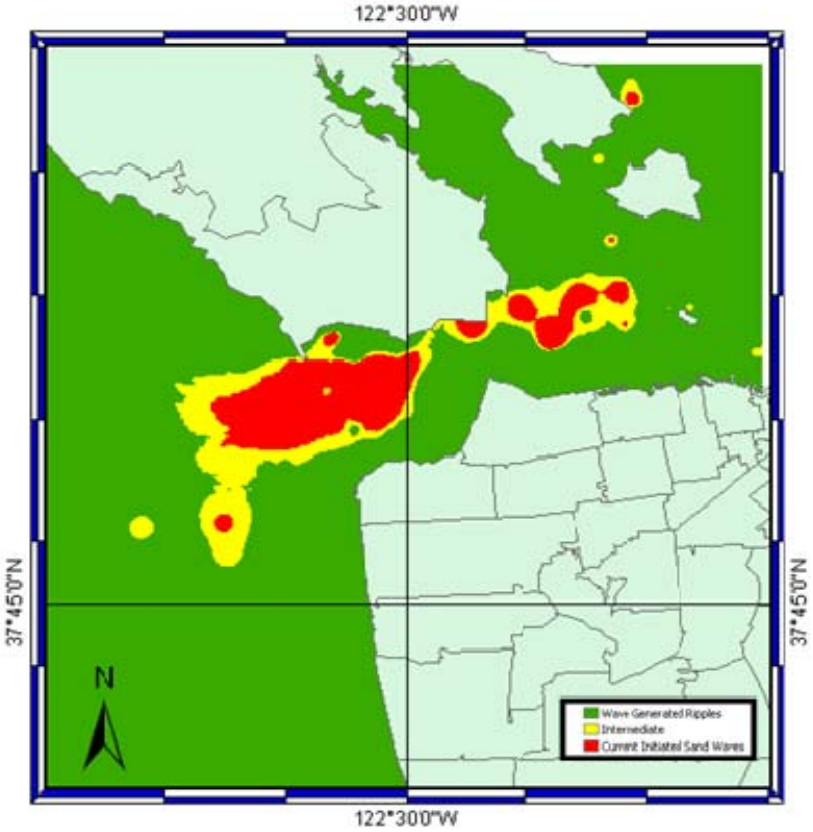

Figure 33. Potential bedform areas

When Figure 33 is compared to the multi-beam data shown in Figures 23 and 24, similarities can be easily identified. The regions identified as current initiated sand waves tie in well with the sand wave fields observed in the multi-beam surveys. This indicates that the theoretical assessment, that sediment grain size is an important factor in the generation of bedforms, is correct.

b. Predicted Bottom Currents

In order to obtain the predicted bottom currents, a number of data sources were examined. The tidal regime in the San Francisco Bay area is primarily semi-diurnal, however, it is extremely complex. Tidal prediction data was obtained from NAVOCEANO. In order to predict the tidal heights in this region, NAVOCEANO had split it into a number of different zones and the tide in each zone is predicted separately due to the variability of tidal height in the region. Tidal curves were plotted from the data provided, the tidal height is relative to Mean Sea Level and the times were referenced to GMT. Figure 34 shows the zones in the region of study and Figure 35 shows a selection of the plotted tidal curves. The tidal curves demonstrate the variability of tidal height in this region. Six tidal curves are shown, the first is located at the mouth of the Golden Gate, zone 37, and then proceed Northeast inshore to zone 12.

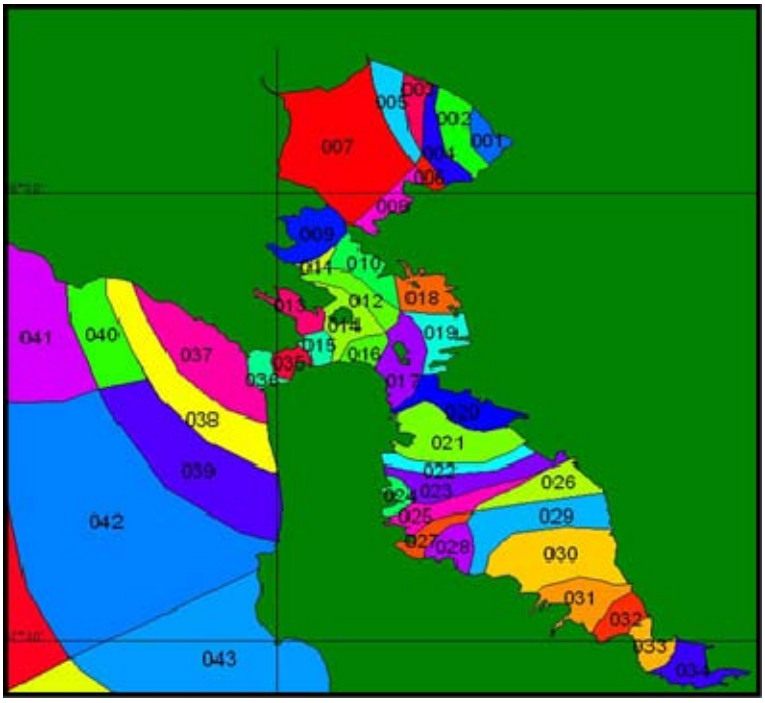

Figure 34. Tidal Zones in the San Francisco Bay region. (From NAVOCEANO, 2009)

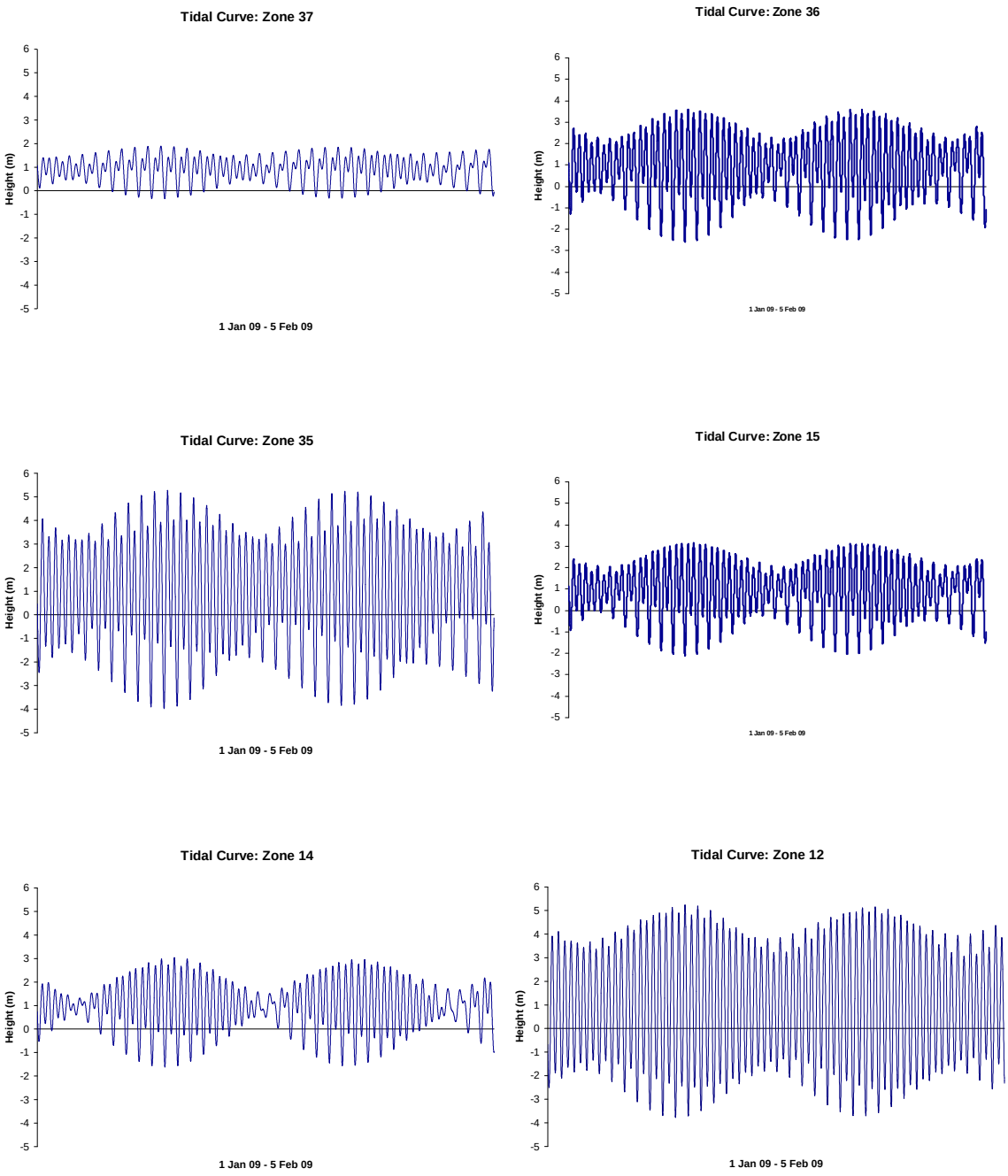

Figure 35. Tidal Curves in the San Francisco Bay Region

The complexity of the tidal regime leads to a complex system of tidal currents. It was decided, that in this study, tidal height would not be a suitable parameter to use. However, the tidal data is taken into account by the historical current data for this region. In this model data from NOAA has been utilized. Over 50 current stations were analyzed, the data included latitude, longitude, depth and mean annual ebb and flood currents for each station. This data includes the currents due to tides. The data was imported into MS Excel and then directly imported into ArcMap. The data was separated into surface currents and bottom currents. Locations of the current stations are shown in Figure 36.

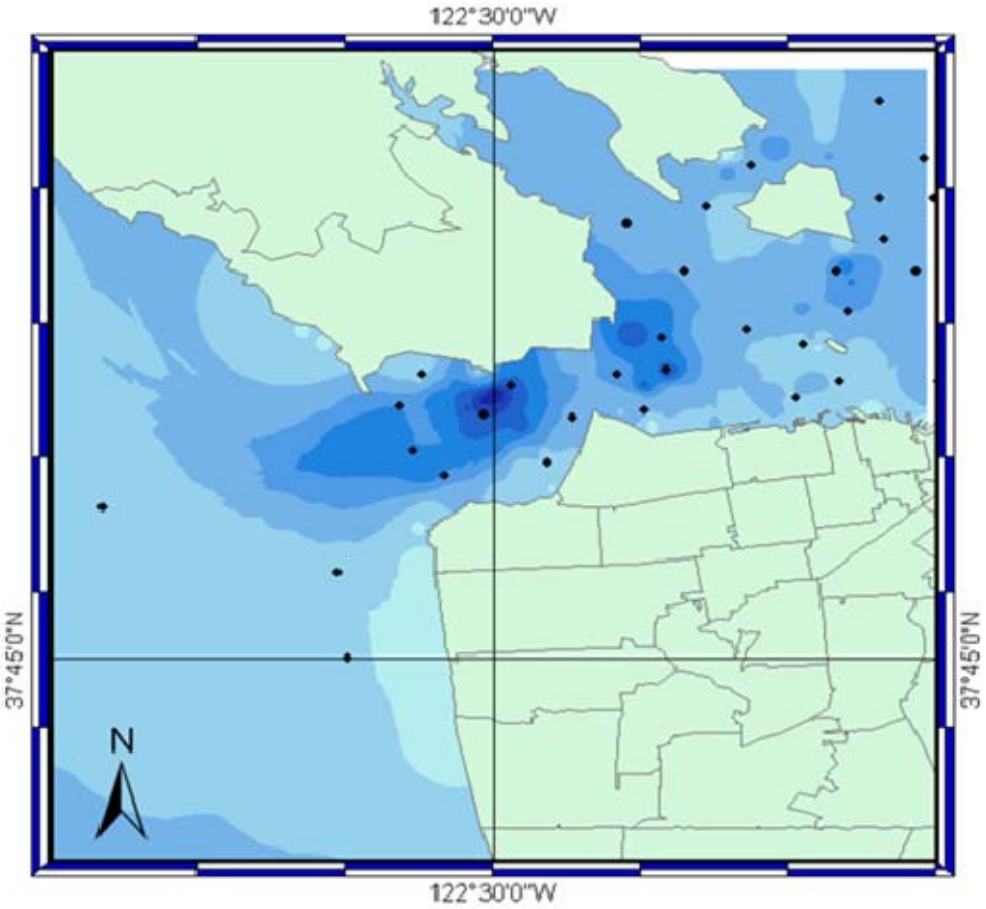

Figure 36. The locations of the current station data used

Both the mean ebb and mean flood surface current data was plotted with the arrows indicating the magnitude and direction of the current at the station location. Red arrows indicate ebb currents and green arrows indicate flood currents. The bottom currents were plotted in the same manner. The results are shown in Figure 37 (surface currents) and Figure 38 (bottom currents).

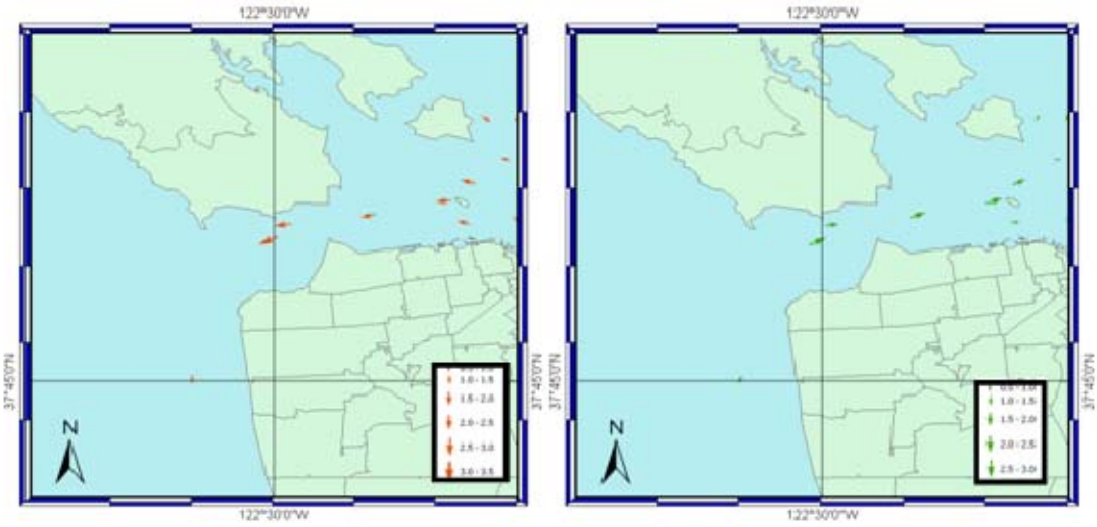

Figure 37. Surface currents, arrows indicate the magnitude and direction of the current, red indicates ebb currents, green indicates flood currents

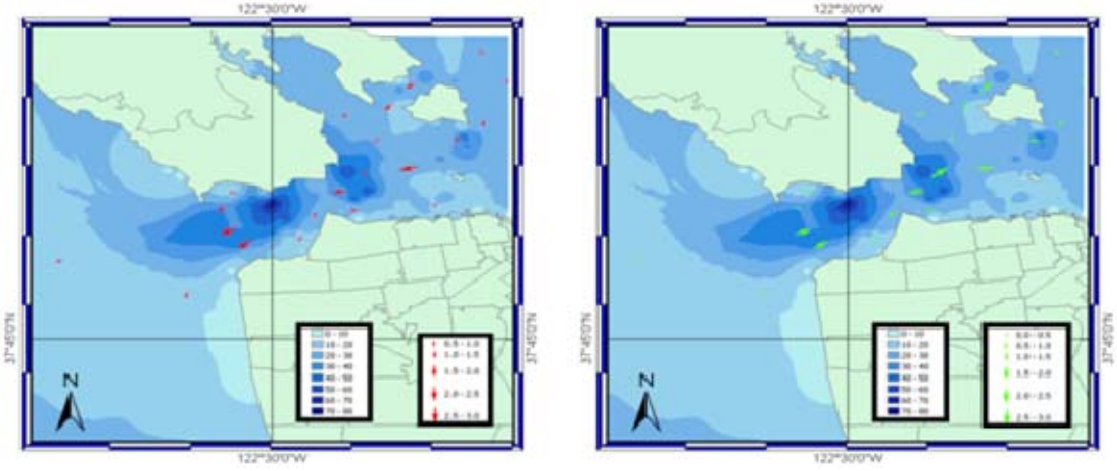

Figure 38. Bottom currents, arrows indicate the magnitude and direction of the current, red indicates ebb currents, green indicates flood currents. Graduated depth scale shown in meters

Due to the importance of flood and ebb dominated currents in bedform formation, further interpolation of this data was conducted. The currents were interpolated into a raster dataset and separated into ebb dominated and flood dominated regions. Ebb currents were assigned a negative value, and flood currents were assigned a positive value and the residual differences between the two calculated. The results of this interpolation are shown in Figure 39. Ebb dominated regions are indicated in red and flood dominated regions are shown in green. The contours indicate current speed, and are plotted at 0.1 m/s intervals, with the interface between the ebb and flood regions being 0.

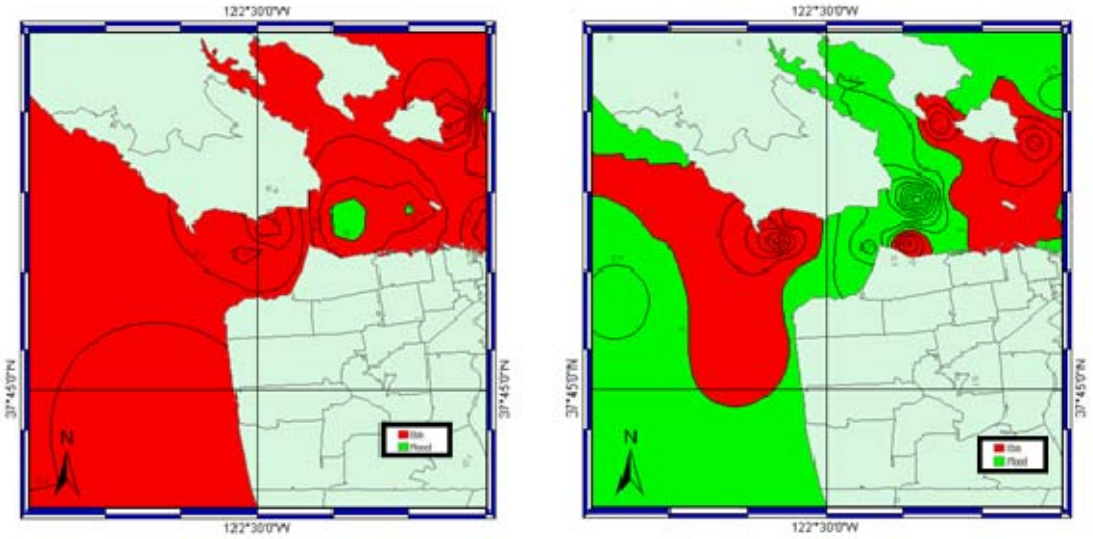

Figure 39. Ebb and flood dominated regions, surface currents (left), bottom currents (right)

From Figure 39, a good insight into the circulation patterns of San Francisco Bay can be gained. The general circulation pattern is similar to that in the Straits of Gibraltar, with an influx of saline water at the bottom and an out flow of fresh water at the surface. Examination of the representation of bottom currents shows some interesting features. When compared with the asymmetry of bedforms generated by USGS (Figure 29), extremely good correlation is noted. When compared with the multi-beam data, (Figures 23 and 24), it can be seen that where the boundary between ebb and flood dominated regions occur,

bedforms also occur. This is particularly noticeable to the north of Angel Island, in the region of the Alcatraz Shoal, and in the inlet throat of the Bay. This layer was therefore selected for use in the survey periodicity model.

c. Predicted Wave Generated Ripple Heights

To calculate the mean wave generated ripple heights, the theory described in Chapter II was utilized. The grab samples provided latitude, longitude, depth and sediment size data. This data was used in conjunction with marine gridded climatology data obtained from Fleet Numerical METOC Detachment in Ashville. The climatological data is calculated by re-analysis of data from 1857 to 1997. Example data for the months of January and July are shown in Table 10.

	January	July
Sea Surface Temp (^{o}C)	10–12	14–16
Salinity (psu)	32	32
Wind Speed (m/s)	7–8	4–5
Wind Direction (deg)	020	080
Wave Direction (deg)	270	270
Wave Height (m)	2.74–3.66	0.91–1.83
Wave Period (s)	7	5
Significant Wave Height (m)	1.83–2.74	0.91–1.83
Swell Direction (deg)	270	270
Swell Height (m)	1.83–2.74	0.91–1.83
Swell Period (s)	6–9	6–9

Table 10. Climatological data used in this study.

Using linear wave theory, the depth, mean wave height and mean wave period, the near bottom orbital velocity, and near bottom orbital diameter, were calculated. Applying the Wiberg and Harris model, and including the sediment grain size data, the predicted ripple height was calculated. This data was collated in MS Excel and then imported into ArcMap. The data was

interpolated into a raster data set. Layers were generated for the monthly mean data, and were then combined in order to generate an annual mean wave generated ripple height layer. Examples of the layers generated for January, July, and the mean wave generated ripple heights, are shown in Figure 40. The smaller ripple heights are shown in pink, with the greatest ripple heights shown in orange and brown, according to the color scale shown. It can be seen that the greatest ripple heights occurred seaward of the San Francisco Bay region in January, which coincided with the larger wave heights.

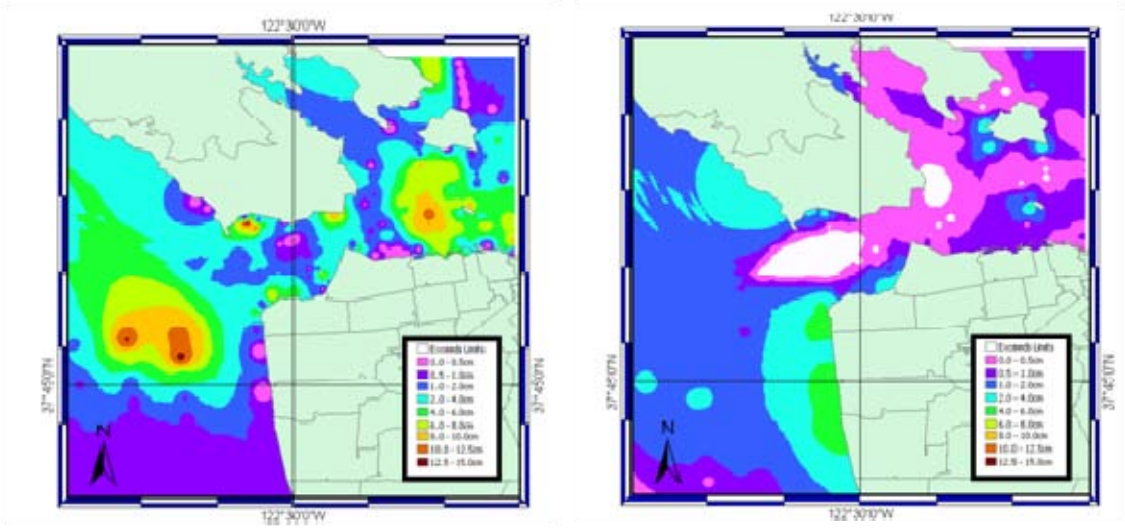

Figure 40. Mean wave generated ripple heights in cm, for January (left) and July (right)

In certain regions, under specific circumstances, for example where the waves are too small in deep channels, there are no ripples generated from the waves, as the near bed orbital velocity and near bed orbital diameter are not large enough to generate ripples. In cases where this occurred, the value was classified as 'Exceeds Limits', which is shown in white, and can be seen in the Golden Gate region in July. When this occurred, a value of -0.1cm was assigned to that data point, and was then classified as exceeding limits in the resulting layers. Figure 41 shows a mean ripple heights layer that was selected for use in the survey periodicity model. This layer is a composite of the monthly layers

generated, and each monthly layer was given an equal weighting. The larger ripple heights can be seen in the yellow/green region offshore and the Alcatraz Shoal region.

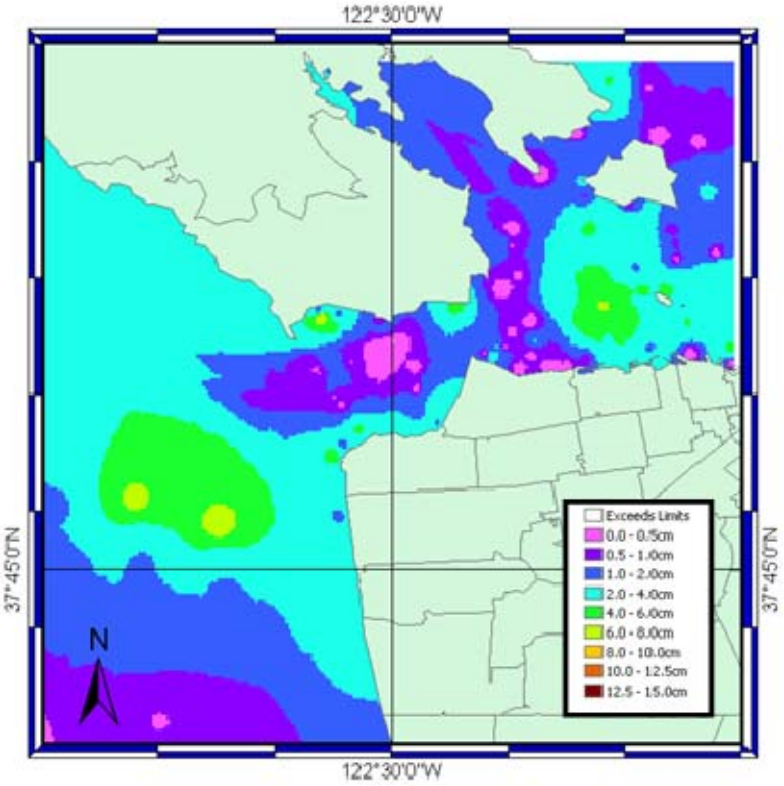

Figure 41. Predicted wave generated ripple height layer

2. Layer Classification

Before the three layers could be combined, a common classification scheme had to be determined. The UKHO classification scheme was utilized, and a scale of 0 to 9 was employed, with 0 representing the highest degree of importance, shown in red, and 9 representing the lowest, shown in blue. Each layer was reclassified using the reclassification tool within the spatial analysis application in ArcMap.

a. Predicted Bedform Type

It is assessed that large bedforms will occur when sediment sizes are larger; these are likely to be current induced bedforms. Larger sediment sizes were assigned a higher weighting and the weighting reduced with reducing sediment size. The weighting scheme is detailed in Table 11 and the resulting layer shown in Figure 42. Figure 42 shows the largest sediment sizes in red, in accordance to the colored weighting scheme shown. The largest sediments occur in the Golden Gate region and the Alcatraz Shoal region, which also corresponds to deeper water and strong currents.

Sediment Size (mm)	Weighting
>0.7	0
0.6 – 0.7	1
0.5 – 0.6	2
0.4 – 0.5	3
0.3 – 0.4	4
0.2 – 0.3	5
0.1 – 0.2	6
0.05 – 0.1	7
0.01 – 0.05	8
<0.01	9

Table 11. Weighting scheme for sediment size.

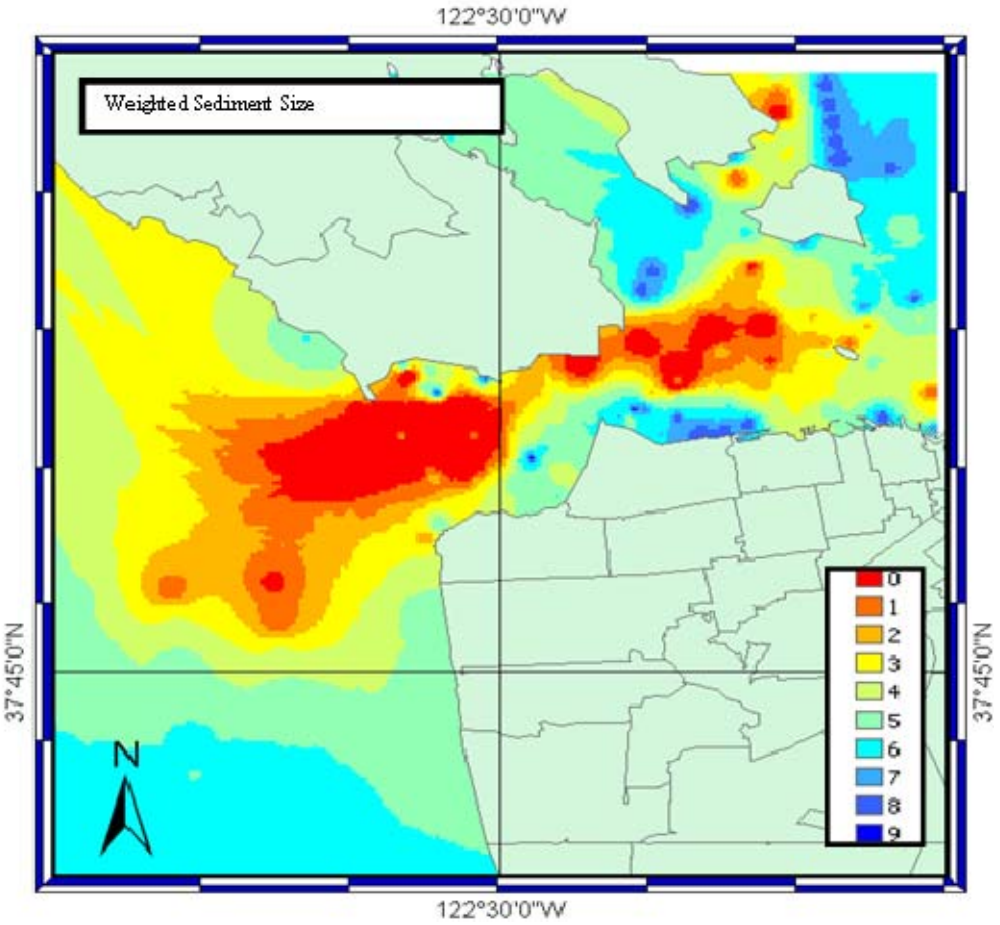

Figure 42. Weighted sediment size layer

b. Predicted Bottom Currents

From background theory it was assessed that larger currents will give rise to increased sediment transport, the regions with higher currents have therefore been assigned the highest weighting and the weighting reduced with reduction in the magnitude of the current. The currents were separated into ebb and flood constituents, and the same weighting criteria applied to both. The weighting scheme is detailed in Table 12, and the resulting layer shown in Figure 43. It can be seen that the highest currents occur in the region of the channel, inshore of the Golden Gate, which is indicated in red. Further inshore the current decreases.

Bottom Currents (m/s)	Weighting
> ±0.6	0
±0.5 – ±0.6	1
±0.4 – ±0.5	2
±0.3 – ±0.4	3
±0.2 – ±0.3	4
±0.1 – ±0.2	5
±0.05 – ±0.1	6
±0.02 – ±0.05	7
±0.01 – ±0.02	8
-0.01 – 0.01	9

Table 12. Weighting scheme for bottom currents.

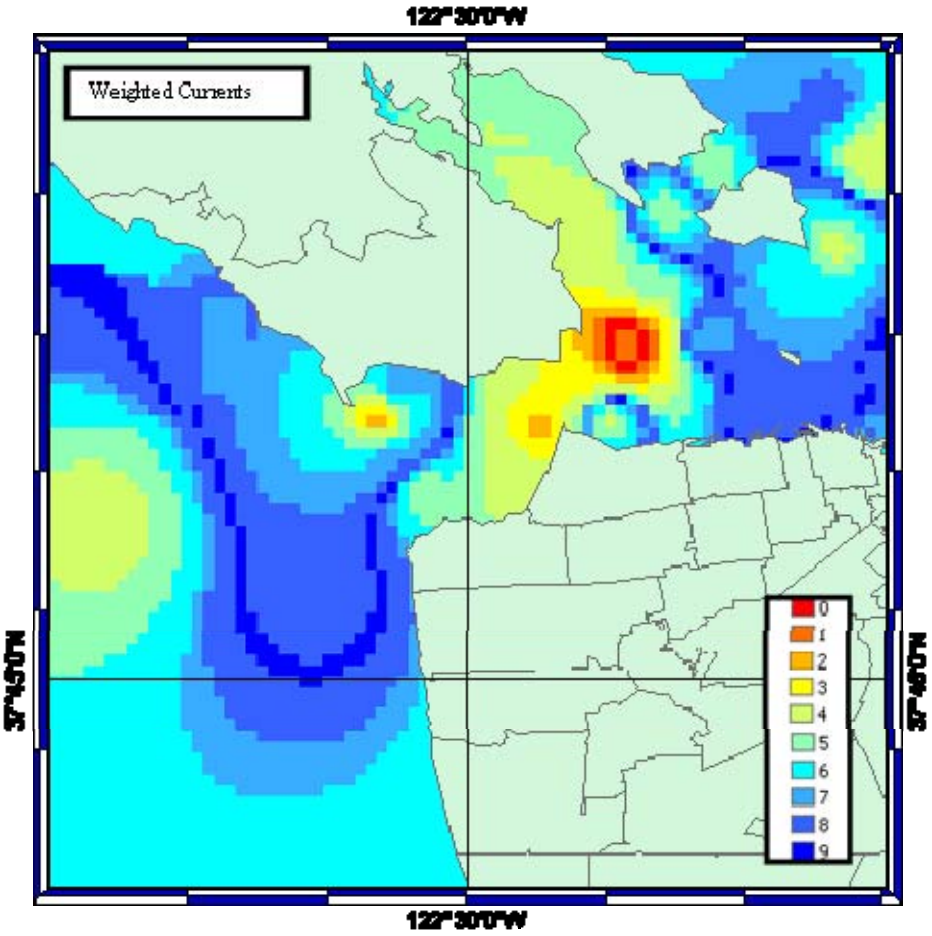

Figure 43. Weighted bottom currents layer

c. Predicted Wave Generated Ripple Heights

It is assessed that the larger ripple heights will have a higher effect on the survey periodicity. The larger ripple heights have therefore been assigned a higher weighting, and the weighting reduces with reducing ripple height. The weighting scheme is detailed in Table 13, and the resulting layer shown in Figure 44. The higher ripple heights occur in the Alcatraz Shoal and offshore. The lower ripple heights occur in the deeper water located in the channel.

Ripple Height (cm)	Weighting
12.5 – 15.0	0
10.0 – 12.5	1
8 .0 – 10.0	2
6.0 – 8.0	3
4.0 – 6.0	4
2.0 – 4.0	5
1.0 – 2.0	6
0.5 – 1.0	7
0.0 – 0.5	8
Exceeds Limits	9

Table 13. Weighting scheme for wave generated ripples.

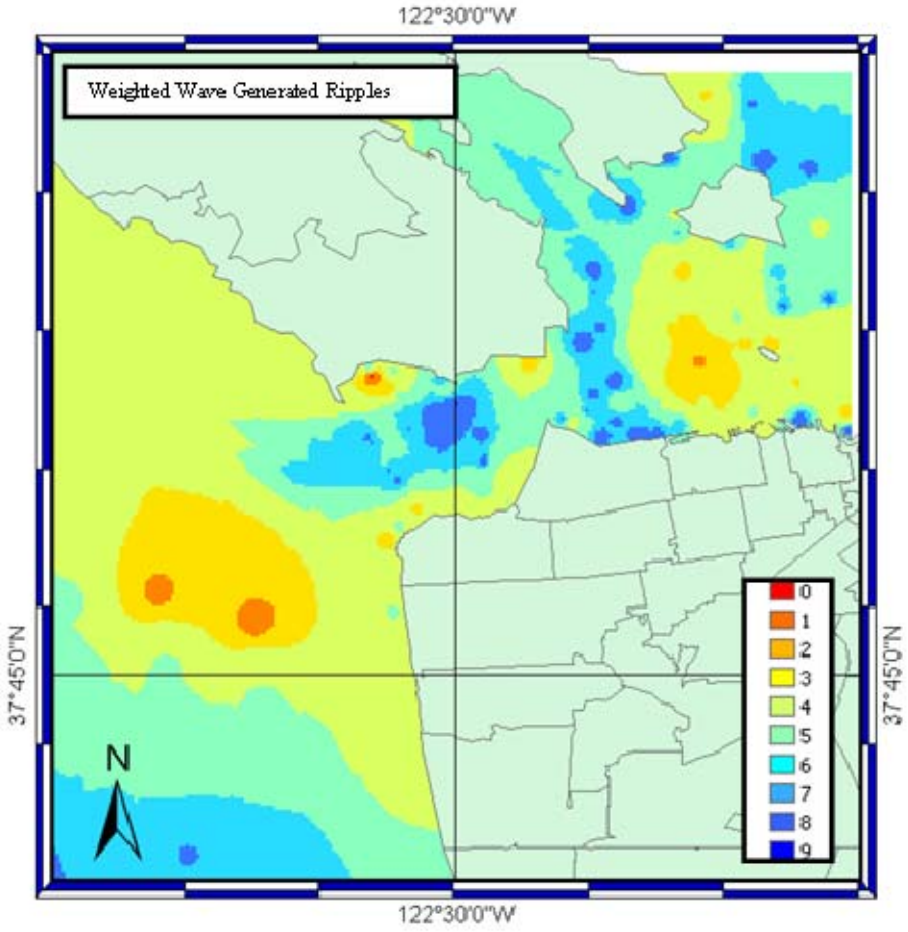

Figure 44. Weighted wave generated ripple layer

C. ASSIGNING LAYER WEIGHTING

Each layer is important in the formation of bedforms, and hence survey periodicity. A number of different weighting options were investigated before choosing the most appropriate one, based on comparison with the multi-beam data and the findings of the USGS and localized sample data investigation detailed in Chapter III. Background theory of sediment transport mechanisms was also taken into account in the assessment of the most suitable weighting option prior to survey periodicity being determined.

The layers were combined using the raster calculator tool, within the spatial analyst application within ArcMap.

1. Option 1

Figure 45 shows the first option with the following weighting scheme: weighted sediment size, 50%, weighted currents, 25% and weighted wave generated ripples, 25%.

Higher combined weightings occur throughout the region of the Golden Gate Channel, particularly in deeper water, the higher weightings extend offshore from the channel. The region to the Northeast of the Golden Gate and the West of the Alcatraz Shoal has the highest weighting. In this region, the sediment size was large, the currents were strong, and the wave generated ripples were also large.

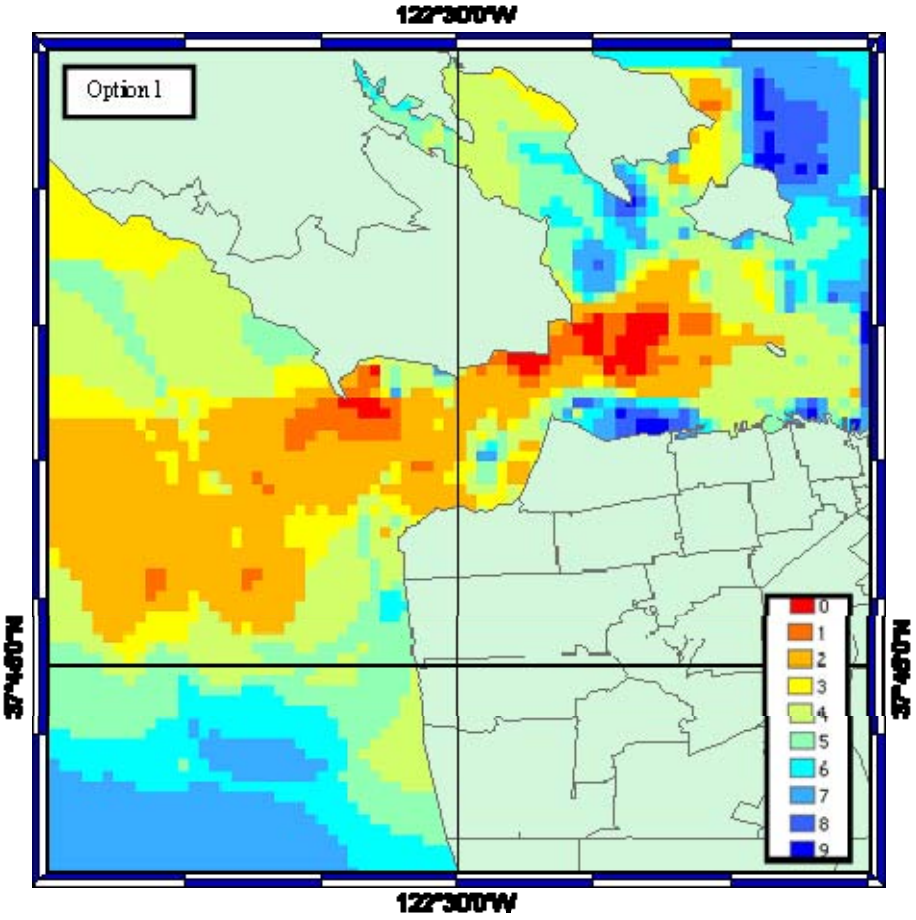

Figure 45. Combined weighted layers, Option 1

2. Option 2

Figure 46 shows the second option, with equal weights employed: weighted sediment size, 33%, weighted currents, 33% and weighted wave generated ripples, 33%.

Again the higher weightings occur to the Northeast of the Golden Gate and the West of the Alcatraz Shoal. In this region, the sediment size was large, the currents were strong, and the wave generated ripples were also large. There is quite a high weighting offshore, and also on the Northwest side of the channel. This option has many regions with a low weighting, indicated by blue.

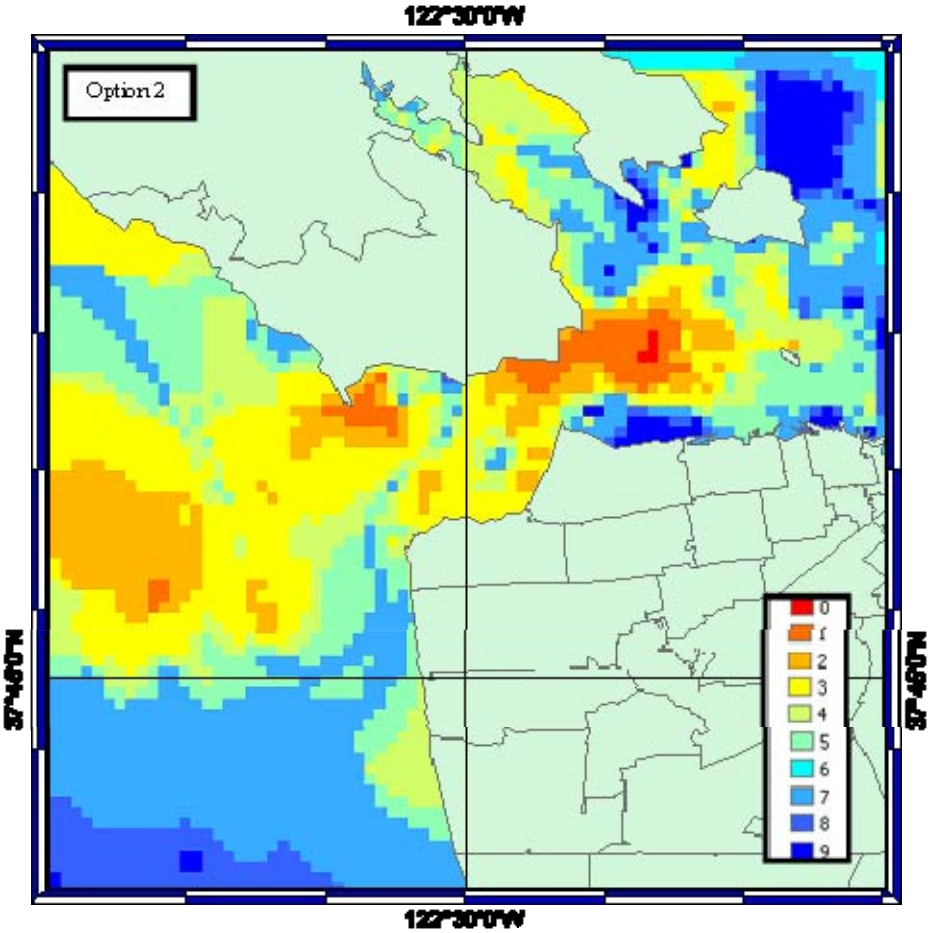

Figure 46. Combined weighted layers, Option 2

3. Option 3

Figure 47 shows the third weighting option, using the following weighting; weighted sediment size, 25%, weighted currents, 50% and weighted wave generated ripples, 25%.

In this option, higher priority is assigned to regions with strong current, resulting in lower weightings over the majority of the area. Only the region to the Northeast of the Golden Gate, and the West of the Alcatraz Shoal, would be frequently surveyed. This would not capture all the dominant sand wave movements.

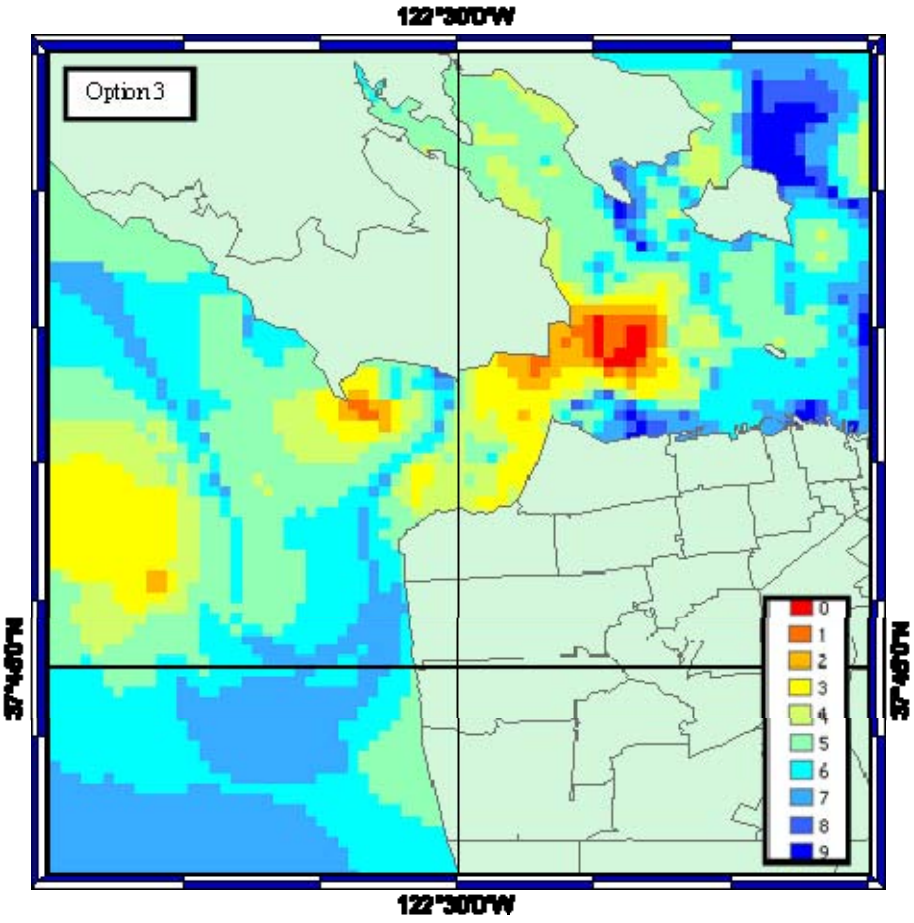

Figure 47. Combined weighted layers, Option 3

4. Option 4

Figure 48 shows the fourth weighting option, the following weighting was employed; weighted sediment size, 25%, weighted currents, 25% and weighted wave generated ripples, 50%.

From Figure 48, it can be seen that a large percentage of the region has a weighting of 3. This indicates a relatively high changeability throughout the area. Again the region to the Northeast of the Golden Gate and the West of the Alcatraz Shoal stands out, as having the highest changeability. However, as the magnitude of wave generated ripples appears to be much smaller than the effect of sediment size and currents, this option should be immediately discounted.

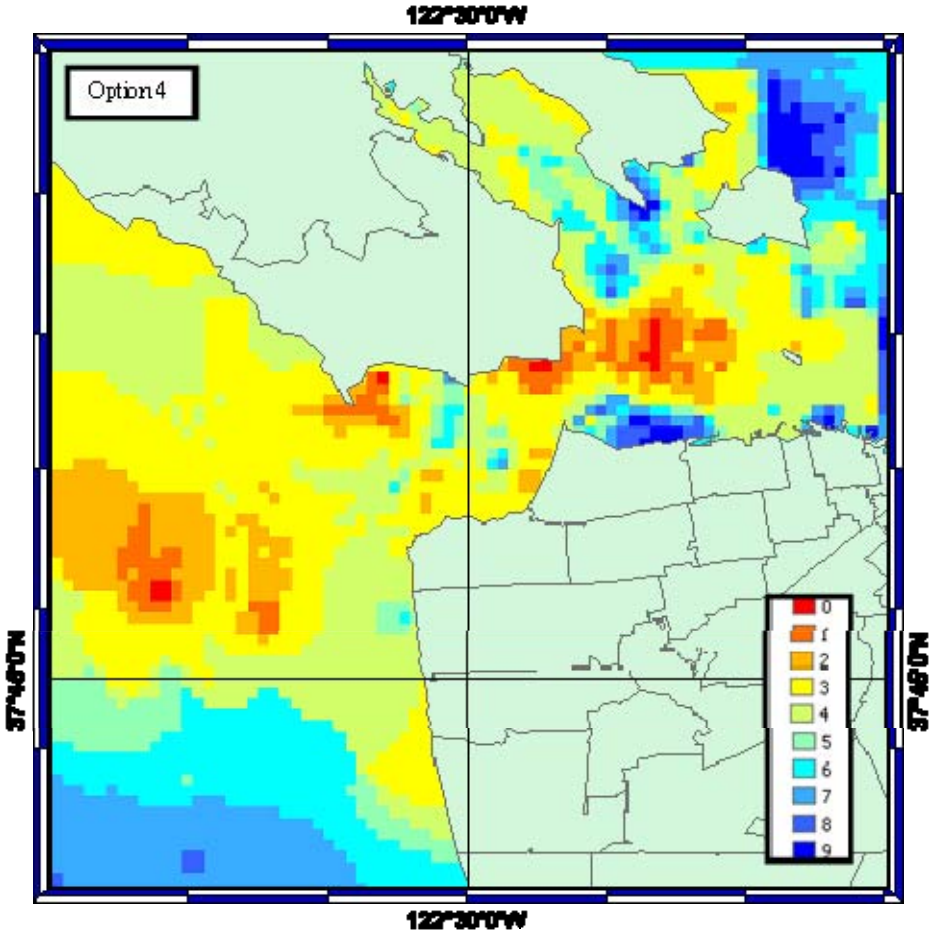

Figure 48. Combined weighted layers, Option 4

5. Option 5

Figure 49 shows the fifth weighting option, this option reduces the importance of wave generated ripples and assigns a higher weighting to currents, with the highest weighting being assigned to sediment size; weighted sediment size, 45%, weighted currents, 35% and weighted wave generated ripples, 20%.

From Figure 49, it can be seen that the higher weightings occur throughout the region of the Golden Gate Channel, although the weightings to the seaward extent of the channel are highly variable. The higher weightings extend offshore from the channel. The region to the Northeast of the Golden Gate and the West of the Alcatraz Shoal, has the highest weighting.

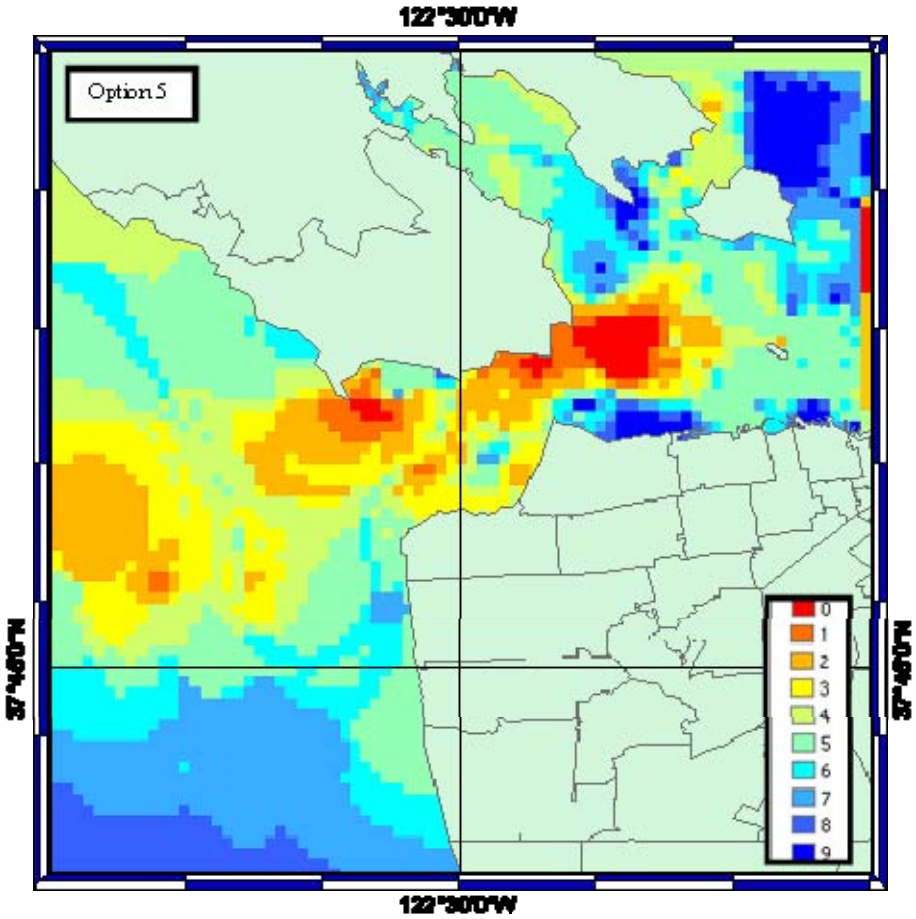

Figure 49. Combined weighted layers, Option 5

D. DETERMINING SURVEY PERIODICITY

In order to determine the recommended survey periodicity, the weighted option layers were reclassified, using the UKHO recommended re-survey intervals (Table 3). This was achieved by reclassifying the layer into the four survey categories. With category 1, indicating a high level of changeability and therefore a low survey re-interval, shown in red. The lowest changeability, category 4, was shown in blue.

From the detailed study of the five weighting options put forward in the previous section, it was determined that Option 5 provided the best representation of both the multi-beam data and the background theory.

Option 5 had 45% weighting for the sediment layer, from the background theory it was extremely apparent that sediment grain size was particularly important in sediment transport mechanisms and in bedform formation mechanisms. Currents were weighted at 35%, this demonstrates the importance of currents, in this case due to a particularly strong tidal regime, the importance of currents was also apparent from the background theory of sediment transport. Waves had a weighting of 20%, the lower weighting was due to the smaller magnitude of ripple heights due to wave motion, although the ripple height from wave motion cannot be discounted it is not of a large enough magnitude to cause mine burial.

Each option was carefully compared to the known patterns of San Francisco Bay from the high resolution USGS multi-beam data (Figures 23–27). Options 1 and 5 both showed a high correlation with this data. Options 2, 3 and 4, showed some correlation but it was significantly less than the other two options. It was decided that Option 5 was the most representative; it captured the majority of features shown on the multi-beam data.

The red regions of Figure 50, located throughout the Golden Gate Channel and the Alcatraz Shoal, show the regions of highest seabed changeability, those that should be surveyed most often. Following the UKHO

recommended re-survey intervals (Table 3), this region should be assessed as Priority 1, this is due to its significant economic and commercial importance, so these regions should be surveyed every 3–5 years. The yellow regions should be re-surveyed every 5–7 years, the light blue regions every 7–10 years and the dark blue every 10–15 years.

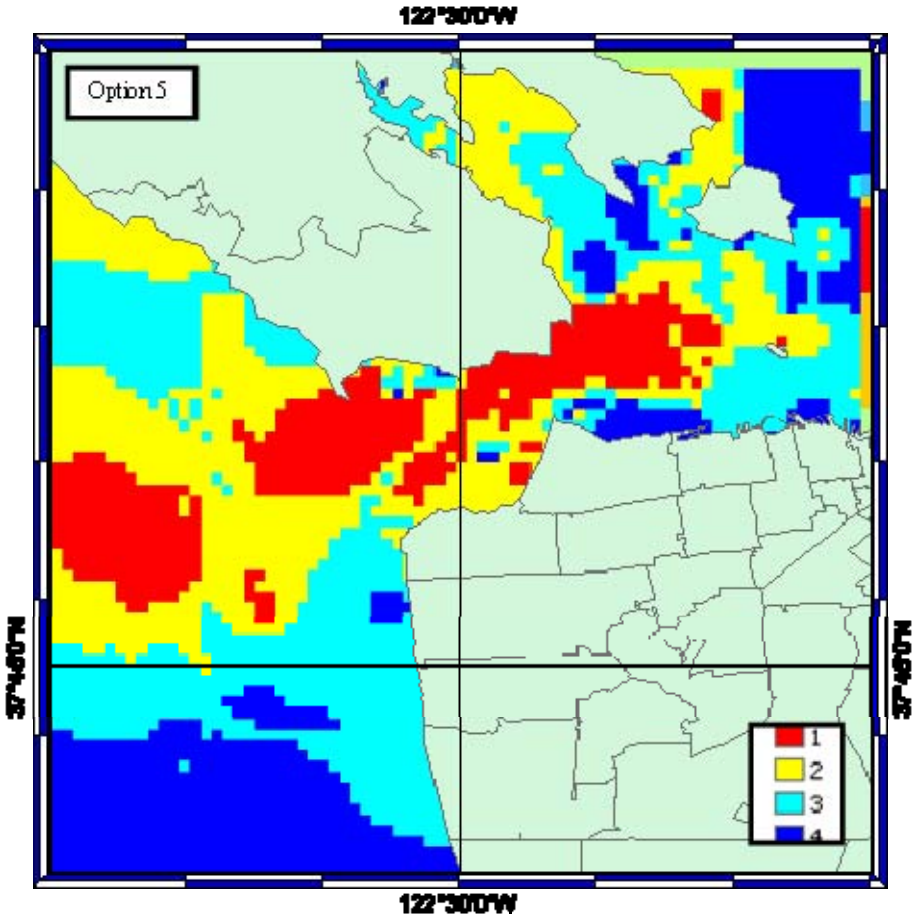

Figure 50. Recommended survey periodicity for San Francisco Bay

From Figure 50, it can be seen that the areas identified as significant in the USGS multi-beam survey data in Chapter III, all fall within the high changeability category and should therefore be surveyed at the lowest possible interval. The model results and the high-resolution multi-beam results compare well.

THIS PAGE INTENTIONALLY LEFT BLANK

V. CONCLUSIONS AND RECOMMENDATIONS

It is essential to maintain an up-to-date database of route surveys for mine warfare in order to maintain maritime security at home and abroad. Mine warfare routes often pass through strategic sea-lanes in order to gain access to ports and harbors, these routes traverse the littoral region, a complex oceanographic environment, in which a variety of mines could be laid. This study is primarily valid for VSW, SW and DW regions, not the surf zone as the sediment transport mechanisms and processes are much more complex in this region. The bathymetry in the regions of interest can be complex and often difficult to predict. Complex bathymetry patterns hinder the mine warfare problem due to increased clutter, scouring and burial of mines, unfortunately the impact of bathymetry, particularly bedforms is poorly understood, and little research of the impact has been conducted.

It is known that seabed type, sedimentation, and transport due to tides, currents and wave interaction are extremely important in sediment transport mechanisms and bedform formation. Sediment transport and bedform formation, in turn, are extremely important in the mine warfare route periodicity problem, when taking into account the size of a typical mine (height 0.5 m), a relatively small change in ripple height or bedform height in any location can easily cause the burial of a mine. By assessing the rate of change in a location an assessment of survey periodicity can be made. Due to the complex nature and number of mechanisms involved a qualitative rather than quantitative assessment has been made.

The UKHO GIS weighted suitability model, formed a qualitative assessment for the UK mine countermeasures route survey maintenance schedule in 2005. This model could not be used for the U.S. due to its geographic limitations, but the concepts used in its construction can. The U.S. currently has no such model for determining route survey periodicity.

A. SUMMARY OF RESULTS

1. Localized Sample Data and Database Comparison Results

San Francisco Bay was used as a case study; a sediment analysis investigation was carried out in February 2009. The investigation involved the comparison of grab samples taken over a three-year period, the aim of this was to determine if there had been any change with time in the sediment properties at the sites sampled and to compare the results to the NAVOCEANO HFEVA database, to assess if the database remained valid.

From the results, it can be concluded that at the sites sampled, there was no significant change in sediment properties with time. From the results and climatological data, the predicted ripple heights were calculated. These results concluded that the ripple heights showed variability of a few centimeters over the three-year period, which is not deemed significant.

When compared to the NAVOCEANO HFEVA database, the sediment type of each sample concurred with the database results, suggesting that this database remains a valid assessment of sediment type in this area. Every care was taken to assure the accuracy of this investigation as discussed in Chapter III.

2. USGS Multi-beam Survey Results

The comprehensive results using high resolution multi-beam survey techniques obtained by USGS, show that bedform fields, as a whole, maintained relative symmetry, and asymmetry values had not changed markedly with time (Barnard et al., 2007). From these results, the temporal variability of bedforms in the San Francisco Bay region was demonstrated.

The height of the bedforms was assessed as a significant factor in the determination of route survey periodicity, although the location of the bedform

fields did not change significantly with time, the location of the sand wave crests did. This has the potential to cause mine burial and was of significant interest during this study.

3. Modeling Results

The route survey periodicity model developed for San Francisco Bay was based on the concepts of the UKHO model. Although different input layers were used, the UKHO model included layers to depict the MCM environment and the maritime environment, but did not include waves, tides, or currents. Due to difficulties sourcing the data included in the UKHO model for the San Francisco Bay area, an alternate approach was necessary. From background theory and the experimental results, it was apparent that bedform size and mechanisms were an integral part of this problem. It was decided that sediment size, tides and currents, and ripples generated from wind waves, were critical in bedform formation and size. If this could be predicted, survey periodicity could be determined based on the bedform size and the known movement characteristics.

The San Francisco model was comprised of three layers. The sediment size layer was constructed from 174 grab samples, which were interpolated into a raster dataset, from this predicted bedform type could be determined. Tides and currents were accounted for by interpolating over 50 current stations. The predicted wave generated ripple heights were calculated from climatological data and the Wiberg and Harris model. Each layer was weighted, the weighting scheme was used, and each layer was re-classified with a scale of 0 to 9, with 0 representing a high degree of change, and 9 representing little change. As these layers had not been used before, the weighting schemes used were based primarily on background theoretical concepts.

The recommended re-survey intervals, used in the UKHO model (shown in Table 3) were used in this model. In order to determine the most

representative weighting of each layer, five options were examined. The resulting layers were compared to the high-resolution multi-beam data, in order to determine which weighting option was the most representative.

The fifth option had the predicted bedform type layer weighting of 45%, in all background theory literature sediment size was shown to be the most important factor in bedform type and hence size. The predicted bottom current layer had a weighting of 35%, indicating that currents, in this case due to the tidal regime had a greater importance than waves, which were given a weighting of 20%. A lower weighting was given to waves due to the fact that the ripple heights capable of being generated were much smaller than those generated by currents.

When compared to the high-resolution multi-beam data, this option was deemed to be the most representative. In regions where the seabed changeability was assessed to be high, a survey interval of 3–5 years was assigned. A number of these regions corresponded with comprehensive regions of study by the USGS (Figures 25–27). The temporal variability shown in these regions indicated that this survey interval would be the most suitable. Figure 23 and 24 show the bed patterns in San Francisco Bay. When compared to the model, the results are extremely encouraging.

B. RECOMMENDATIONS

This study has resulted in a number of recommendations. Potentially, this model could be used to determine the route re-survey interval for the U.S. Implementing the three layers discussed could do this. The NAVOCEANO HFEVA database could be used to form the basis of the predicted bedform layer. However, it is recommended that NAVOCEANO include the recent grab sample data obtained by USGS and other sources to improve the resolution of the HFEVA database. This can be demonstrated by examination of Figures 22 and

32. This model could be used in other worldwide regions of interest as all the input data can be gained from easily available open sources, although obviously the better the resolution of the input data, the better the results.

1. Recommendations for the UKHO Model

The San Francisco Bay model utilizes layers including; sediment size, waves, tides and currents. One of the recommendations for areas of further study in the UKHO 2005 report was to determine if any additional environmental factors should be included in the model to refine the results. This investigation has shown by using the three layers; sediment size, waves, tides and currents; predicted bedform regions can be obtained and a survey periodicity determined.

Although the UKHO model does not include waves, tides and currents, sediment type and bottom texture are included. Sediment size, waves, tides and currents are the inputs required to determine bedforms. Bedforms are already included in the UKHO model from sediment type and bottom texture. When UKHO results are compared to results from the SEAs reports, it can be seen that regions of bedforms, determined by the SEAs study, correspond to regions with a low re-survey interval determined by the UKHO model. It is therefore, recommended that inclusion of these extra environmental parameters is not necessary for the UKHO model.

2. Limitations

In San Francisco Bay coarse sediments are found in regions of strong tidal currents, this is where the larger bedforms occur. The same is true for regions around the UK, however, this may not be true in all cases. A further limitation could occur in regions of fine sediments, fine sediments would not cause large ripple heights or bedforms to occur, however, they do remain a region of interest for the mine warfare survey periodicity problem. In fine

sediment regions, a mine could potentially become buried by scour or suspended sediments being washed down a river. This model does not capture these effects.

3. Recommendations for Further Study

All results from this study indicate the San Francisco Bay model results are viable and the survey periodicity suggested is credible for this area. It is recommended that this study be replicated in a different regions, where high-resolution multi-beam data is available and the weighting scheme for the model verified by this.

Different regions should include regions with similar characteristics, for example sandy sediments and strong tidal currents. If deemed correct then this model could be implemented for use in the U.S. and other similar regions of interest. The model should also be replicated in regions of finer sediments to determine if additional layers or and alternate weighting scheme should be used in these regions.

From the results analyzed throughout this study, it has become apparent that one of the most important factors in determining the survey periodicity for mine warfare is sediment size, a further study could be conducted to determine if an assessment of survey periodicity could be made from this data alone, particularly in regions where little data is available.

LIST OF REFERENCES

Armishaw, J. E. (2005). *Route Resurvey Model (QRM): Use of GIS Modelling to Review the UK Route Survey Maintenance Schedule*. UKHO/MEIC TR/05/01, June 2005. Taunton, Somerset.

Armishaw, J. E. (2005). *Optimising MW Surveying by Modelling the Seabed Environment using GIS Techniques*. Adapted by DIJE from UKHO/MEIC TR/05/01, June 2005. Taunton, Somerset.

Bagnold, R. A. (1946). *Motion of Waves in Shallow Water: Interaction Between Waves and Sand Bottoms*. Proc. R. Soc. London Ser, **A187**, 1-15.

Bagnold, R. A. (1956). *Flow of Cohesionless Grains in Fluids*. Phil. Trans. Royal Society, London, **A249**, 235-297.

Barnard, P. L. *et al*. (2006). *Giant Sand Waves at the Mouth of San Francisco Bay.* EOS, Vol 87, **29**, 285-289.

Barnard, P. L. *et al*. (2006). *Massive Bedforms and their Movement Mapped at the Mouth of San Francisco Bay Using Multibeam Sonar*. American Geophysical Union, Fall Meeting 2006.

Barnard, P. L *et al*. (2007). *Coastal Processes Study at Ocean Beach, San Francisco, California; Summary of Data Collection 2004-2006*. U.S. Geological Survey Open File Report 2007-1217. Retrieved on 10 February 2009, from http://pubs.usgs.gov/of/2007/1217/

Barnard, P. L. *et al,* (In Press, 2009). *Analyzing Bedforms Mapped Using Multibeam Sonar to Determine Regional Bedload Sediment Transport Patterns in the San Francisco Bay Coastal System.* Sedimentology, In: Li, M., Sherwood, C., and Hill, P. (Eds.), International Association of Sedimentologist's Special Publication Book on Shelf Sedimentology, 33 pp.

Blondeaux, P. (2001). *Mechanics of Coastal Forms*. Annual Review Fluid Mechanics, 33, 339–370.

British Geological Survey, (2005). *DTI Strategic Enviromnetal Assessment Area 6, Irish Sea, Seabed and Surficial Geology and Processes*. Continental Shelf and Margins Commissioned Report CR/05/057.

British Geological Survey, (2007). *DTI Strategic Enviromnetal Assessment Area 8, Superficial Seabed Processes and Hydrocarbon Prospectivity*. Marine Coastal and Hydrocarbons Commissioned Report CR/07/075.

California Department of Water Resources, (2007). *Delta Outflow*. California Data Exchange Center, Retrieved on 5 May 2009, from http://cdec.water.ca.gov/

Clifton, H. E. (1976). *Wave-formed Sedimentary Structures: A Conceptual Model, in Beach and Nearshore Sedimentation*. Edited by R.A. Davis and R. L. Ethington, SEPM Special Publication, **24**, 126-148.

Dare, C; Craig, M and Torresan, M. (2006). *Grain-Size Analysis of sediments From San Francisco Bay: A Comparison of LISST and Sieve Analysis Methods.* American Geophsical Union, Fall Meeting 2006.

Davis, A. G. *et al.* (2002). *Intercomparision of Research and Practical Sand Transport Models*. Coastal Engineering, **46,** 1-23.

Deigaard, F. (1992). Mechanics of Coastal Sediment Transport. World Scientific, Singapore.

Dyre, K. R. (1986). *Coastal and Estuarine Sediment Dynamics*, John Wiley & Sons, Chichester.

Dyre, K. R. and Soulsby, R. L. (1988). *Sand Transport on the Continental Shelf. Annual Review Fluid Mechanics,* **20**, 295-324.

Fleet Numerical METOC Detachment, (2009). *Marine Gridded Climatological Data: 1857-1997*. Ashville. Retrieved on 22 April 2009, from http://niprnavy.ncdc.noaa.gov/webv7-servlet/jsps/marine/context/idx_smgc_graphic.jsp

Friends of the Estuary, (1997). Annual Report, 1996-1997.

Hudson, D. (2008). *Sediment Analysis: Statistical Variation of Localized Samples and Database Verification*. OC3570: Operational Oceanography Report, Naval Postgraduate School, Monterey, California.

Hunt, J. N. (1979) Direct solution of wave dispersion equation. *J. Waterways, Ports, Coastal Ocean Div., ASCE* **105**(WW4):457-459.

King, D. (2007). *Sediment Analysis and Database Verification Report*. OC3570: Operational Oceanography Report, Naval Postgraduate School, Monterey, California.

Komar, P. D. (1976). *Beach Processes and Sedimentation*. Prentice-Hall, Inc. New Jersey.

Komar, P. D. and Reimers, C. E. (1978). *Grain Shape Effects on Settling Rates.* Journal of Geology, **86**, 193-209.

Liu, Z. (2001). *Sediment Transport*. Laboratoriet for Hydraulik og Havnebygning, Aalorg Universitet. Retrieved on 7 January 2009, from http://lvov.weizmann.ac.il/lvov/Literature-Online/Literature/Books/2001_Sediment_Transport.pdf

MacVean, L. J. and Stacey, M. T. (2008). *Lateral Mixing Processes in a Estuary: San Francisco Bay and its Exchange With Perimeter Habitat*. American Geophysical Union, Fall Meeting 2008.

McCave, I. N. (1971a). *Wave effectivness at the Sea Bed and its Relationship to bedforms and Deposition of Mud.* Journal of Sedimentology and Petrolium, **41**, 89-96.

McCave, I. N. (1971b). *Sand waves of the North Sea off the Coast of Holland*. Marine Geology, **10**, 199-225.

McCoy, J. and Johnston, K. (2002). *Using ArcGIS Spatial Analyst*. ESRI. Redlands, USA.

Milliman, J. D. and Meade, R. H. (1983) *World wide delivery of River Sediment to the Oceans.* Journal of Geology, **91**, 1-21.

National Research Council (2000): *Oceanography and Mine Warfare*. Ocean Studies Board, Commission on Geosciences, Environment, and Resources. National Academy Press. Washington DC.

National Research Council (2001). *Naval Mine Warfare: Operational and Technical Challenges for Naval Forces.* Committee for Mine Warfare Assessment, Naval Studies Board, Retrieved on 10 October 2008, from www.nap.edu/catalog.php?record_id=10176

Parker, K. A. *et al*. (2003). *Sediment Distribution in Central San Francisco Bay in the Vicinity of Racoon Strait.* American Geophysical Union, Fall Meeting 2003.

Proudman Marine Laboratory (2009). *Sediment Process Triad.* Retrieved on 22 May 2009, from http://www.pol.ac.uk/home/research/theme3/wp33.php

Royal Navy (2004). *BR1806: British Maritime Doctrine*, 3rd Edition. Ministry of Defence, TSO (The Stationary Office). London.

Royal Navy (2009). *Naval Operations*. Retrieved on 17 November 2008, from www.royalnavy.mod.uk/operations-and-support/surface-fleet/mine-countermeasure

Schoellhamer, D. H. (1996). *Factors Affecting Suspended Solids Concentrations in South San Francisco Bay, California*. Journal of Geophysical Research, Vol 101, **C5**, 12087-12096.

Sherwood, C. (2007). *Demonstration Sediment Transport Applets*. Retrieved on 15 March 2009, from http://woodshole.er.usgs.gov/staffpages/csherwood/sedx_equations/sedxinfo.html

Stive, M. J. F. *et al*. (2002). *Variability of Shore and Shoreline Evolution*. Coastal Engineering, **47,** 211-235.

Soulsby, R. L. *et al*. (1983). *The Detailed Processes of Sediment Transport by Tidal Currents and by Surface Waves*, Institute of Marine Sciences, Natural Environment Research Council. Retrieved on 7 January 2009, from http://eprints.soton.ac.uk/14569/01/152.PDF

US Navy Marine Corps (2005). *Mine Warfare*. University Press of the Pacific, Honolulu, Hawaii.

United States Army Corp of Engineers, (1996). *Ocean Beach Storm Damage reduction Feasibility Study; Final Feasibility Study for the City and County of San Francisco.* San Francisco District.

United States Naval Oceanographic Office. (September 2003). *Database Description for Surface Sediment Type*, Stennis Space Center, Mississippi: Acoustics Division.

Weltmer, M. A. (2003). *Bedform Evolution and Sediment Transport Under Breaking Waves.* M.S. thesis, Naval Postgraduate School, Monterey, California.

Wiberg, P. L., and C. K. Harris (1994) *Ripple geometry in wave-dominated environments.* Journal of Geophysical Research, **99**(C1):775-789.

Wikipedia, (2009). *Naval Mine*. Retrieved on 17 November 2008, from http://en.wikipedia.org/wiki/Naval_mine

Wikipedia, (2009). *Sediment Transport.* Retrieved on 7 January 2009, from http://en.wikipedia.org/wiki/Sediment_transport

INITIAL DISTRIBUTION LIST

1. Defense Technical Information Center
   Ft. Belvoir, Virginia

2. Dudley Knox Library
   Naval Postgraduate School
   Monterey, California

3. Professor Peter Chu
   Department of Oceanography
   Naval Postgraduate School
   Monterey, California

4. Professor Thomas Herbers
   Department of Oceanography
   Naval Postgraduate School
   Monterey, California

5. Dr J E Armishaw
   Maritime Environment Information Centre
   Hydrographic Office
   Admiralty way
   Taunton
   Somerset
   United Kingdom

6. Dr Patrick Barnard
   Research Geologist
   USGS
   Pacific Science Center
   Natural Bridges Drive
   Santa Cruz, California

7. Lt Cdr C Chapple RN
   SO2 ENVIRON
   Maritime Warfare Centre
   Marlbourough Building
   HMS Collingwood
   Newgate Lane, Fareham
   Hampshire
   United Kingdom

8. Lt Cdr K Pullen RN
DI ICSP-JGI-HM1-SO2
DI ICSP
Old War Office
Whitehall
London
United Kingdom

9. Cdr M Jones RN
CDR HM
Defiance Building
HMNB Devonport
Plymouth
Devon

10. Cdr A V Swain RN
FOST HM
Fitzroy Building
Upper Battery Road
HMNB Devonport
Plymouth
Devon
United Kingdom

11. Cdr D Turner RN
British Embassy
Washington DC

12. RADM D W Titley USN
Oceanographer & Navigator of the Navy
Massachusetts Ave
Washington DC

13. RADM J W White USN
CNMOC, CO
Stennis Space Center, Mississippi

14. RADM Ellis G Winford USN, Ret.
Chair, Undersea Warfare & Director
Undersea Warfare Research Center
Wayne E. Meyer Institute of Systems Engineering
Monterey, California

15. RADM R Williams USN, Ret.
Chair of Mine Warfare
Wayne E. Meyer Institute of Systems Engineering
Monterey, California

16. Mr R Winokur
Technical Director
Oceanographer & Navigator of the Navy
Massachusetts Ave
Washington DC

17. Mr E C Gough, Jr
TD/CNMOC
Stennis Space Center, Mississippi

18. CAPT R E Kiser USN
CNMOC DOO
Stennis Space Center, Mississippi

19. CAPT Van Gurley USN
CNMOC DOO
Stennis Space Center, Mississippi

20. CAPT P Oosterling USN
CNMOC DOO
Stennis Space Center, Mississippi

21. Mr Ronald Betsch
MIW Program Manager
Naval Oceanographic Office
Balch Blvd,
Stennis Space Center, Mississippi